Climate-Specific Degradation Rate and Linearity Analysis of Photovoltaic Power Plants using Performance Ratio, Performance Index, and Raw kWh Methods

by

Christopher Raupp

A Thesis Presented in Partial Fulfillment
of the Requirements for the Degree
Master of Science

Approved April 2016 by the
Graduate Supervisory Committee:

Govindasamy Tamizhmani, Chair
Devarajan Srinivasan
Bradley Rogers

ARIZONA STATE UNIVERSITY

May 2016

ABSTRACT

In the past 10 to 15 years, there has been a tremendous increase in the amount of photovoltaic (PV) modules being both manufactured and installed in the field. Power plants in the hundreds of megawatts are continuously being turned online as the world turns toward greener and sustainable energy. Due to this fact and to calculate LCOE (levelized cost of energy), it is understandably becoming more important to comprehend the behavior of these systems as a whole by calculating two key data: the rate at which modules are degrading in the field; the trend (linear or nonlinear) in which the degradation is occurring. As opposed to periodical in field intrusive current-voltage (I-V) measurements, non-intrusive measurements are preferable to obtain these two key data since owners do not want to lose money by turning their systems off, as well as safety and breach of installer warranty terms. In order to understand the degradation behavior of PV systems, there is a need for highly accurate performance modeling. In this thesis 39 commercial PV power plants from the hot-dry climate of Arizona are analyzed to develop an understanding on the rate and trend of degradation seen by crystalline silicon PV modules. A total of three degradation rates were calculated for each power plant based on three methods: Performance Ratio (PR), Performance Index (PI), and raw kilowatt-hour. These methods were validated from in field I-V measurements obtained by Arizona State University Photovoltaic Reliability Lab (ASU-PRL). With the use of highly accurate performance models, the generated degradation rates may be used by the system owners to claim a warranty from PV module manufactures or other responsible parties.

To,
My parents, Richard Raupp and Pamela Habig, and other friends and family members
for their constant support and love

ACKNOWLEDGMENTS

I would like to first give my thanks and appreciation to Dr. Govindasamy Tamizhmani for accepting me into his lab and providing me all the amazing opportunities I've had and for his constant support throughout my thesis work. The work I have done in his lab has allowed for me to get hands-on-experience for almost all aspects of the PV systems and I consider myself very fortunate to have been able to learn under him, as well as from both current and past students in the lab. I would like to thank my fellow lab students for their support, and I would specifically like to thank Sai Tatapudi, our technical lab manager, Matthew Chicca and Sanjay Shrestha, former lab students, for their support and guidance. I would like to also thank all the other students that I have had the pleasure of working with at ASU-PRL. Finally, I would like to thank my committee members, Dr. Rogers and Dr. Srini, for their help and support along the way and for all of the valuable information that they shared.

TABLE OF CONTENTS

Page

CHAPTER PAGE

LIST OF TABLES

Table Page

Table Page

Table Page

LIST OF FIGURES

Figure Page

Figure Page

Figure Page

Figure Page

Figure Page

Figure Page

Figure Page

1.0 INTRODUCTION

1.1 Background

A large number of developed and developing countries have set milestones of reaching 20-30% of their energy demands by 2050 using clean energy. Solar photovoltaic (PV) is one the primary technologies being used to meet these goals and thus has seen tremendous growth in the amount of installation seen around the globe. Specifically within the U.S., solar has seen more and larger scale PV power plants being turned online due to cheaper module and system costs, as well as the renewable tax credit (RTC) that gives companies incentives to invest into these PV power plants. Because of the recent extension to the RTC, it is expected that a surge of large scale PV installations will be seen in the near future. This then leads to the need of having highly accurate modeling and energy predictions of how these power plants will generate energy.

Arizona State University has been one of first U.S. colleges to install a large amount of PV systems, having a total of 23 MW of installed PV from more than 70 PV systems. With all of these systems being located in the greater Phoenix-Metro area, the collected data from these systems can be used to understand the behavior of PV power plants that are installed in the hot-dry climate of Arizona. By understanding the behavior of the degradation rates of PV modules, and by extension PV power plants, more accurate energy predictions can be obtained which will in turn allow module manufactures to better understand the rate at which their modules are degrading in a specific climate, allow consumers to have a better idea of what to expect from there PV systems, and

allow a smarter grid management that is able to account for the losses which can be experienced when dealing with PV power plants.

1.2 Scope of Work

This thesis deals with the challenges of analyzing and implementing climate-specific models, for both irradiance and module temperature, in order to develop high accuracy performance ratio (PR) and performance index (PI) values for 38 commercial size PV power plants installed in a hot-dry climate of Arizona. Based on the PR, PI and filtered raw kWh data, the degradation rates were determined. These degradation rates are then analyzed to determine whether or not the degradation rates experienced by these systems are shown to be linear. All systems evaluated in this thesis are crystalline (monocrystalline and polycrystalline) silicon based PV systems (except one system which is composed of HIT modules). The ages of these power plants vary from 2 years to 16 years with the majority of the analyzed systems being less than 5 years of age.

2.0 LITERATURE REVIEW

2.1 Irradiance Models

It is well known that the two biggest factors that affect PV module performance is that of the amount of irradiance seen by the module (plane of array, POA, irradiance) and the temperature at which the module is operating. It is because of this there have been extensive studies into developing models that accurately predict the operating conditions of PV modules when there is lack of monitored POA irradiance and module temperature.

When analyzing the performance of PV system, it is critical to first know the irradiance hitting the POA being analyzed. Often only global horizontal irradiance (GHI)

is measured on the ground or calculated based on the satellite data instead of directly measuring POA irradiance. Because of this issue, there is ae need of converting GHI data into POA irradiance data using decomposition models and transposition models.

2.1.1 Decomposition Models

The use of decomposition models plays an important role in the overall effectiveness of modeling the POA irradiance due to the fact that they empirically determine the amount of direct and diffused irradiance hitting a horizontal plane. The more accurate a decomposition model is at predicting the beam and diffused components on the horizontal, the more accurate transposition models will be able to convert these data into POA irradiance.

2.1.2 Transposition Models

The decomposed diffuse and beam components of GHI are then transposed to POA using transposition models. Extensive studies have been undertaken by the industry to develop the most accurate transposition models. The POA irradiance that is empirically derived can then be used to model the performance, operating temperature, or many other parameters of a PV system.

2.1.3 Previous Irradiance Modeling Work

The use of decomposition and transposition models is often widely used. Lave *et al.* showed an extensive comparative analysis of 12 decomposition models and four transposition models, for multiple locations across the United States [1].

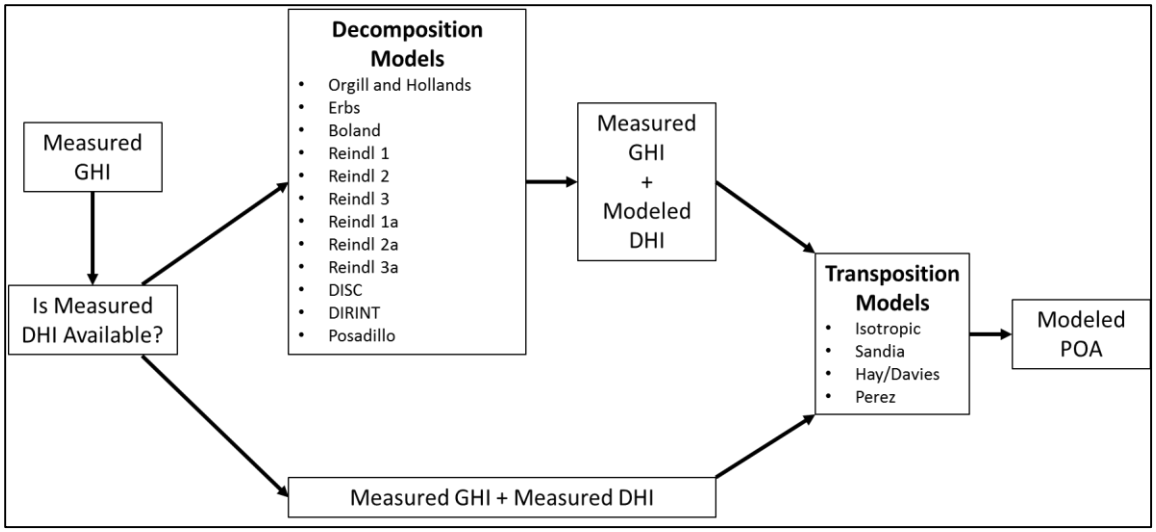

Fig. 1. Flowchart Showing How to Model POA Irradiance from Measured GHI [1].

Similar studies were also conducted by Wong and Chow which also showcases a different set of optimized decomposition and transposition models for Hong Kong [2]. Yang *et al.* [3] presented a reverse study of the best decomposition and transposition models to convert POA irradiance into GHI for Singapore.

2.2 Thermal Models

The second main effect on the performance of a PV module(s)/array is that of the temperature at which the model(s) is/are operating at (T_{mod}). Due to the fact direct measurements of PV module temperatures are not always available, there is a need for highly accurate PV module temperature models based on operating conditions of irradiance, ambient temperature (T_{amb}), and wind speed (WS).

2.2.1 Previous Thermal Modeling Works

A study done by Schwingshackl *et al.* evaluates the comparison of multiple PV temperature models with measured cell (backsheet) temperatures for a large PV power plant in Italy [4]. A similar study was also conducted by Olukan and Emziane comparing

thermal models to measured PV module temperatures in Abu Dhabi [5]. The results of both papers indicate that it is not only important to understand the effect of wind and other operating conditions on the operating temperature of PV modules, but also gives insight to the fact that there is not one conclusive model that works for all climates and regions.

2.3 Performance Models

The importance of correct irradiance and temperature modeling is seen when the performance of PV module(s)/arrays/systems is/are analyzed. Performance metrics such as PR and PI can be used to see the performance and relative health of the module(s)/arrays/systems that are being evaluated. Recent studies done by Shrestha *et al.* showed how accurate PR and PI degradation rates can be when compared to onsite field I-V evaluations for the degradation rates measured in the Phoenix-Metro area [6]. The metric of performance ratio is defined by the IEC 61724 standard in which the approach for analyzing a photovoltaic system is discussed [7]. As shown by Townsend *et al.*, by incorporating other system losses, such as temperature, soiling and inverter efficiency, a more accurate PR, now identified as PI, can be calculated [8]. Shrestha *et al.*, also showed, in his thesis work, a method of using filters for POA and T_{mod} in order to develop degradation rates based solely on metered kWh data [6]. In this thesis, a new method is devised using a statistical approach to accurately calculate degradation rates based solely on raw kWh data without having any measured or modeled operating conditions.

2.3.1 Performance Ratio (PR)

The performance ratio calculated for each evaluated system is done as per the IEC 61724 standard [7]. Performance ratio is defined as the ratio of the system yield, Y_f, and the reference yield, Y_r. As is the standard, the performance ratio is an indicator of how well a system is operating, after being corrected for only irradiance losses. Equations shown below are used to calculate the performance ratio of a PV system.

$$Y_f = \tau_R * \frac{\sum P_A}{P_O} * \eta_{load} \quad (1)$$

$$Y_r = \tau_R * \frac{\sum G_I}{G_{I,ref}} \quad (2)$$

$$PR = \frac{Y_f}{Y_r} \quad (3)$$

Where,

$\tau_R * \sum P_A =$ daily array energy of the system

$P_O =$ rated array power

$\eta_{load} =$ efficiency with which the energy from all sources is transmitted to the loads

$\tau_R * \sum G_I =$ daily energy incident on the system

$G_{I,ref} =$ reference irradiance, $1000 \frac{W}{m^2}$

2.3.2 Performance Index (PI)

As stated before, the performance index is nothing but a more accurate performance ratio that accounts for other losses such as temperature, wiring, module mismatch, balance of systems (BOS), and etc. The performance index is a dimensionless unit, just as PR, but gives a more accurate representation as to the actual losses being

seen in PV power plant [8]. The performance index is defined as the ratio of actual energy to that of the expected energy, adjusted for known losses, as shown in Equation 4.

$$\text{PI} = \frac{\text{Actual Energy}}{\text{Adjusted Energy}} \qquad (4)$$

Where,

Actual Energy = measured energy at any given time

Adjusted Energy = Rated Power x Loss Adjustments

When substituting in the actual loss factors that can be derived for PV systems, Equation 4 can be modified to that of Equation 5, as shown below.

$$\text{PI} = \frac{\text{Actual Energy} * \text{Rated Irradiance}}{\text{Rated Power} * \text{Actual Insolation} * \text{TA} * \text{DA} * \text{SA} * \text{BOSA}} \qquad (5)$$

Where,

Rated Irradiance = 1000 W/m^2 for flat plate modules

Rated Power = nameplate power of the array

Actual Insolation = total energy incident on the plane of array

TA = Temperature Adjustment

DA = Degradation Adjustment

SA = Soiling Adjustment

BOSA = Balance of System Adjustment

2.3.3 kilowatt-hour (kWh) Analysis

As was previously reported, Shrestha *et al.* looked into the use of only metered kWh analysis. This method, as outlined in the diagram below, requires the use of filtering data based on user defined manual filtration. While this method was shown to be accurate, it required for the user to individually evaluate whether or not a data point

should be considered an outlier [6]. A newer statistical method is presented later on in the current thesis that allows processing that can be done quicker and ensuring that the same degradation rate can be calculated independent of user's expertise in identifying the correct outliers.

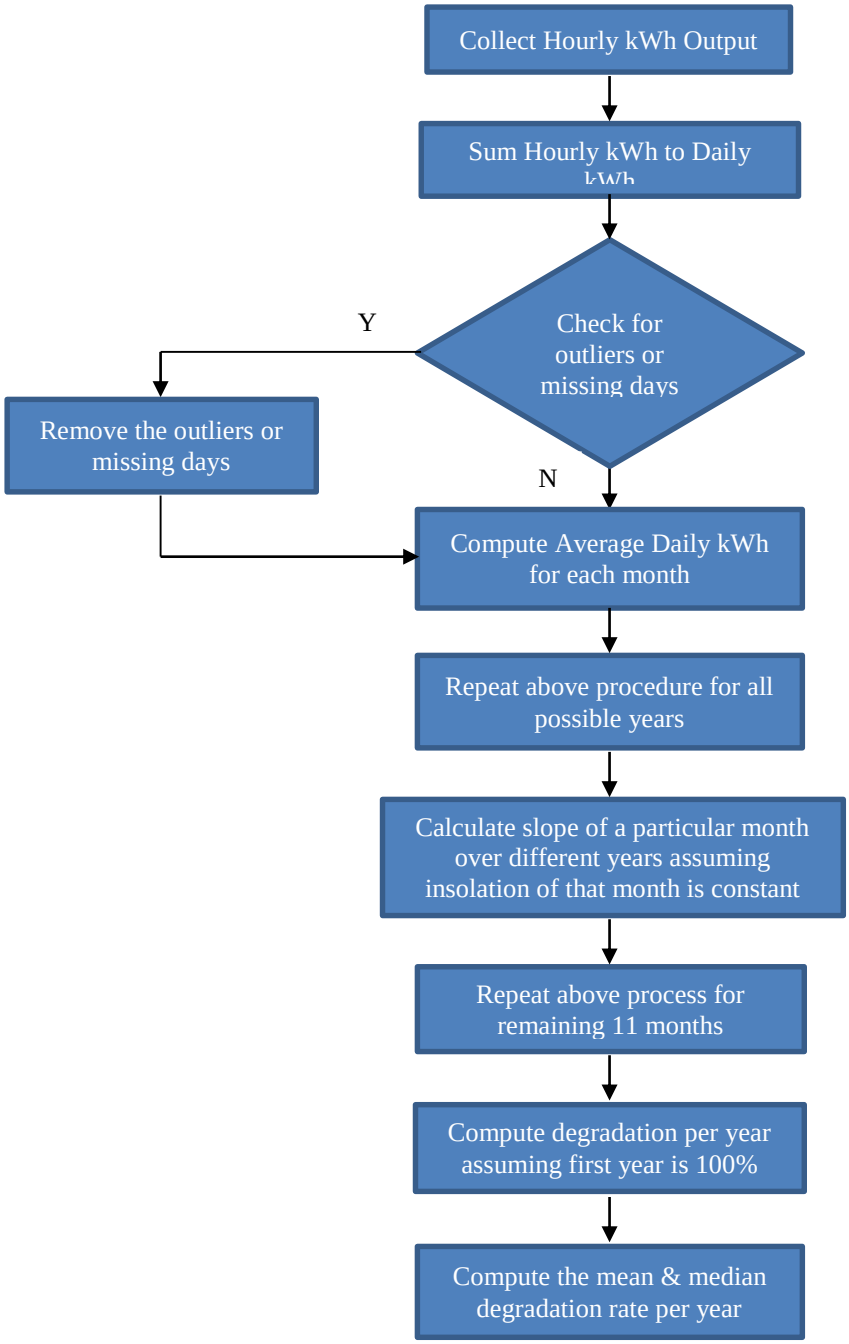

Fig. 2. Calculation of Degradation Rate per Year Using Only Raw (Manually Filtered) Metered kWh Data [6].

3.0 METHODOLOGY

The optimization of irradiance and temperature models was the first step in the analysis of the 38 PV systems that were evaluated in this thesis. Due to the fact that all PV temperature models require POA irradiance as an input, it was critical that the best combination of decomposition and transposition model would be found first. The flow chart below gives an overview of the measurement, analysis, and validation steps that were completed and implemented.

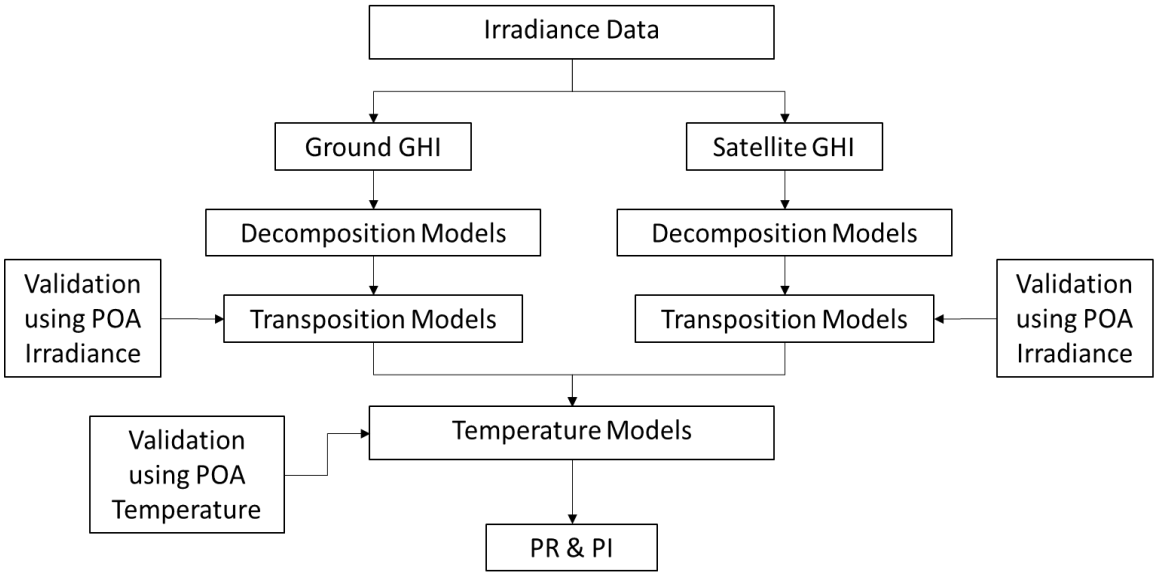

Fig. 3. Overall Procedure Developed at ASU-PRL to Determine Optimized Irradiance and Temperature Models to Produce High Accuracy PR and PI.

3.1 Determination of Optimal Irradiance Model

In this study, satellite modeled GHI data was used from SolarAnywhere. Since all systems evaluated are located very near to one another, it is assumed that the GHI seen by one system at a given time, is the same that is seen by all nearby systems. Shrestha *et al.*, also demonstrated the uncertainty that can come from using satellite based data [6]. In

order to correct for this, satellite based data was used as the input for all decomposition and transposition models, in which the resulting calculated POA irradiance was used and compared to two full years of POA irradiance measurements from a commercially owned system near the ASU Tempe campus (where 37 of the 38 PV plants are located). Within this thesis, a total of 12 decomposition models and 10 transposition models for each decomposition model, were evaluated. This results in 120 possible combinations that were evaluated. Next step is to determine the irradiance and thermal models' combination that work the best for the hot-dry climate of Arizona. All evaluated models were evaluated based on the previously reported models found by Lave [1], Wong [2], and Yang [3]. All irradiance models used are listed in the table below.

Irradiance Models	
Decomposition Models	Transposition Models
Liu and Jordan	Isotropic
Orgil and Hollands	Korokanis
Erbs	Badescu
Spencer	Sandia
Reindl 1	Willmot
Reindl 2	Temps and Coulson
Lam and Li	Klutcher
Skartveit and Olseth	Hay & Davies
Maxwell	Reindl
Louche	Perez
Vignola and McDaniels	
Perez	

Table 1. List of All Decomposition and Transposition Models Analyzed

The best combination of models was determined by taking the root mean square error (RMSE) and normalized root mean square error (NRMSE) for all combinations. These statistical values are frequently used to measure the difference between the values

predicted by a model and the values that are actually observed. The combination that was able to give the lowest RMSE and NRMSE results for two years of measured data was considered to be the most optimized model for the evaluation of all ASU systems or for hot-dry desert climate systems . By determining the best combination of a decomposition model and transposition model over the two years of measured data, it helped to reduce any uncertainties that may occur from use of SolarAnywhere satellite irradiance data.

3.2 Determination of Optimal Module Temperature Model

The evaluation of multiple module temperature models was conducted in a similar fashion as that of the irradiance models. In this study, 9 temperature models were evaluated and compared to module temperature readings using a commercially owned power plant.

3.2.1 Average Operating Temperature of a PV Power Plant

As was shown by Umachandran *et al.*, the temperature of all the cells within a PV module is not necessarily the same during operating conditions [9]. This effect is even more prominent in a PV power plant. ASU-PRL has recently began to study this effect by installing temperature sensors into a fixed horizontal tilt system. The temperatures of five modules in the power plant, located in the northeast corner, southeast corner, southwest corner, northwest corner, and center of the plant, were measured by attaching T-type thermocouples to the backsheets of the modules Figure 4 shows the layout of the PV plant and the location of the modules with installed temperature sensors.

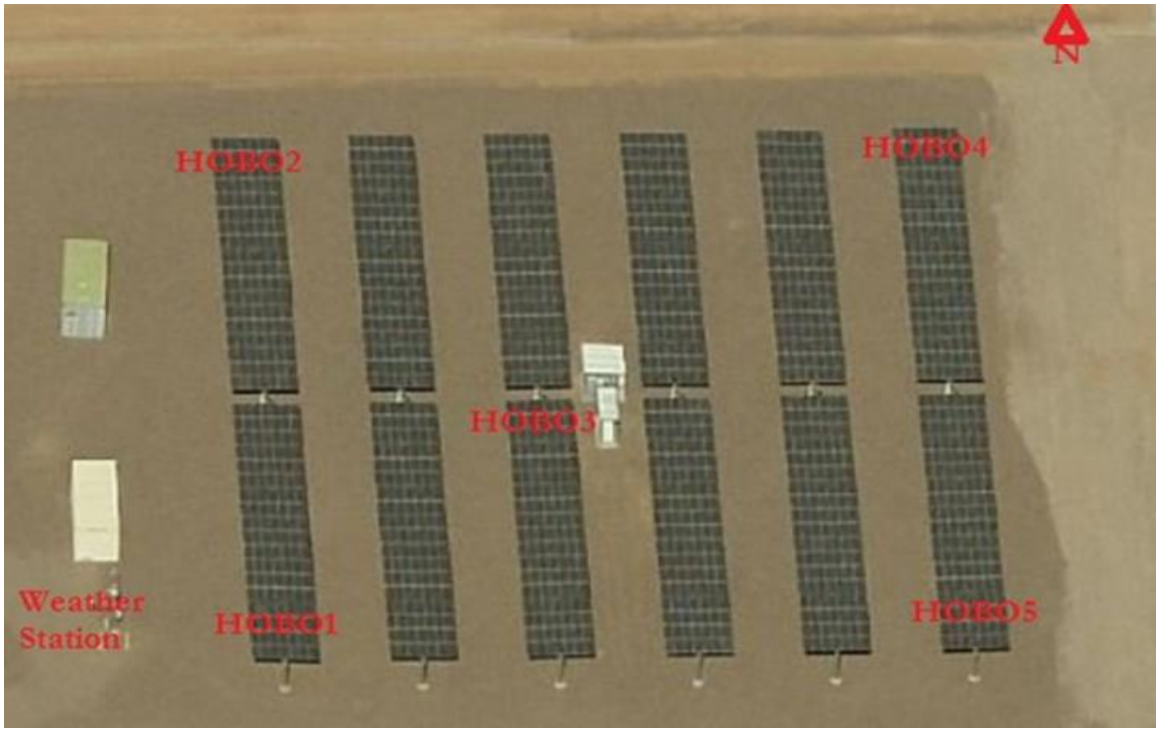

Fig. 4. Thermal Mapping Locations at a Fixed Horizontal Tilt PV system [Hobo is a Data Acquisition System Each Collecting Temperatures from Four Thermocouples Attached to Each of the Five Modules].

For each of the five PV modules, 4 temperature measurements are continuously taken using four thermocouples on backside of the PV modules. The 4 readings correspond to the center (T1), top corner (T2), bottom/short-frame (T3), and side/long-frame (T4). The diagram below shows an accurate depiction of where each thermocouple was placed. The average of these thermocouple readings from each module is considered as the temperature of that module.

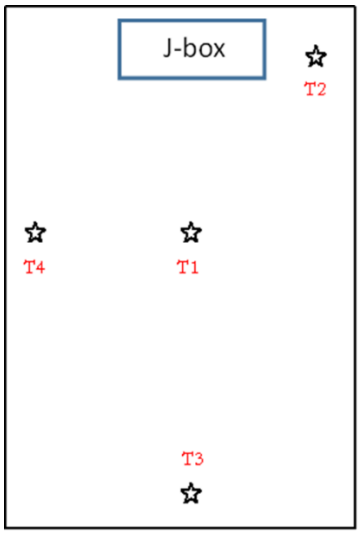

Fig. 5. Location of T-type Thermocouples on the Backsheet of a PV Module.

All thermocouples are connected to a four channel HOBO data logger. The data logger collects data every five minutes and stores in its internal memory. The device is said to be accurate to within ±0.6°C while having an operating range of -260°C to 400°C [9].

Fig. 6. Hobo 4 – Channel Temperature Data Logger

It is assumed, by all the thermal models used by the industry, all modules in a PV power plant operate at a single temperature. In order to obtain this single operating

temperature for the entire plant, all 20 module temperature measurements (5 modules each having 4 thermocouples) were averaged together. The plant readings were recorded for seven months, April to October.

3.2.2 Temperature Model Selection

The nine empirical temperature models which were evaluated in this work are listed in the table below. The model which most closely matched with the average measured module temperature of the PV power plant was selected for further analysis. This analysis was again conducted by using RMSE and NRMSE values as that of irradiance models described earlier. The input for these models were the GHI, wind speed, and ambient temperature data sets from SolarAnywhere. Satellite based data was used to verify the best thermal model since the evaluated PV systems will only have satellite generated data used for modeling the operating conditions.

PV Temperature Models
Simple Model
ASU Tang Model
Sandia King Model
NOCT Model
PVsyst Cell Model
PVsyst Module Model
Homer Model
Mattei 1 Model
Mattei 2 Model

Table 2. List of All PV Temperature Models Used to Calculate Operating Module Temperature.

3.3 Performance Analysis

Each of the 34 ASU PV power plants was evaluated for performance and degradation rate calculations through multiple methods. Hourly data was used in which it was then used to generate daily and monthly values for both PR and PI determinations. Degradation rate calculations were then based on the calculated PR and PI values. A degradation rate calculation based on each systems' kWh data was also determined. One previously measured system by ASU-PRL was used as the baseline system to determine the accuracy of all methods, while 4 other PV plants, which were measured by in-field IV measurements by ASU-PRL, were used to validate the statistical degradation rate calculation from metered raw kWh data.

3.3.1 Performance Ratio (PR) Analysis

As previously discussed, the performance ratio (PR) is the ratio of measured energy to expected energy (based on nameplate data and measured/translated insolation). For all ASU systems, daily PR values were calculated using measured kWh data and the calculated expected energy. The methodology of calculating performance ratio is similar to that previously reported by Shrestha *et al.* [6], but was slightly modified in order to fit the type of data that was available in this study. Do to the unavailability of site specific meteorological data and system operating conditions (POA irradiance and module temperatures) satellite generated data was used. Figure 7 shows a modified flowchart of the steps taken to calculate the degradation rate per year using daily PR values. The data was filtered out when the irradiance was less than 40 W/m^2. Any obvious outliers that were seen to not fit the overall trend of the year-to-year data sets were removed. For monthly

PR values, the average/median of the days with data availability corresponding for that particular month were used. The slope of a line for a particular month vs. number of years was then determined to be the degradation rate per year for that particular month leading to 12 slopes for 12 months of a year.

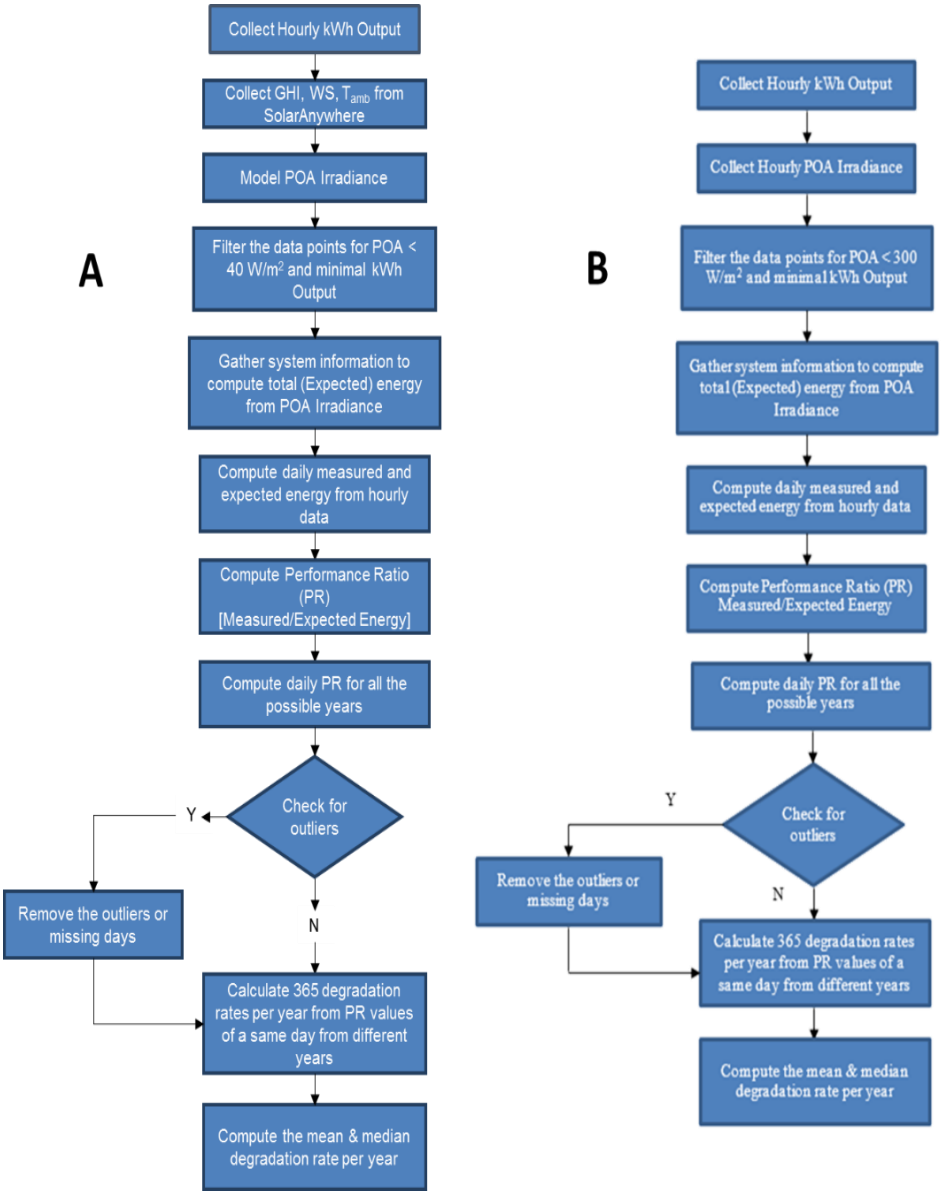

Fig. 7. A) New Method for Calculating Performance Ratio (PR) Using Optimized Irradiance Models from GHI Satellite Data. B) Previously Reported Method from Shrestha *et al.*

3.3.2 Performance Index (PI) Analysis

Performance index (PI), as previously mentioned, is more accurate than PR due to the fact that it corrects for other losses in a PV system, such as temperature, soiling,

balance of systems (BOS), wiring, etc. The ratio of the measured kWh data to the expected energy, having been corrected for irradiance, temperature, module mismatch, and inverter efficiency encompasses the PI values reported in this study. Again, for the 34 ASU systems being evaluated, the weather data and irradiance data were retrieved from the SolarAnywhere web database (using the 10X10 km resolution). Four previously measured systems by ASU-PRL are reported also reported in this study for both validation and degradation rate analysis. The POA irradiance and module temperature for the 34 newly evaluated ASU systems and one control system for validation, were calculated based on the optimized models, as discussed in the results and discussion chapter. The inverter efficiency was taken based on the listed California Energy Commission (CEC) efficiency or on the manufacture's data sheet. The module mismatch in a string was assumed to be a constant value for all plants (3.3%) and was developed from analysis of previously measured systems by ASU-PRL. Wiring losses were also assumed to be constant, regardless of system, by using a relative nominal value of 1.0% for ohmic losses of smaller plants. This is based on the general 1.5% that is used in PVSYST [10].

A comparison of the new developed flowchart as compared to that of one previously shown by Shrestha *et al.* [4] is shown in Figure 8. This procedure was carried out for all 34 ASU systems within the scope of this study.

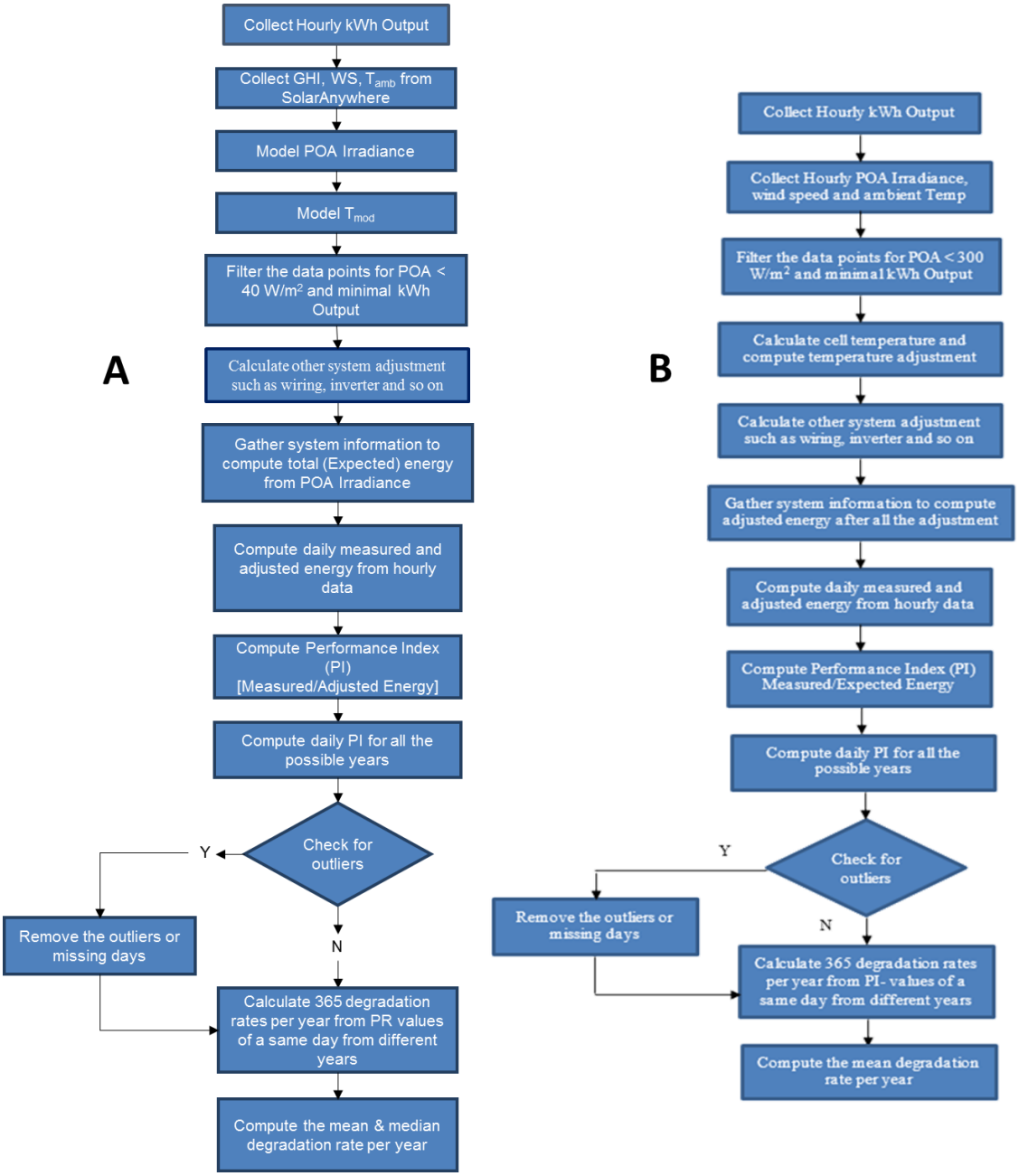

Fig. 8. A) New Method for Calculating Performance Index (PI) Using Optimized Irradiance and Temperature Models from Satellite GHI and Meteorological Data. B) Previously Reported PI Method from Shrestha *et al*.

3.3.2 kilowatt-hour Degradation Analysis

The kilowatt-hour degradation analysis that was originally presented by Shrestha *et al.* showed the possibility of using raw kWh data for calculating degradation rates. The kWh method that was originally developed by Shrestha *et al.*, used a similar approach as that of the PR and PI methods in which the degradation rate was calculated using year-over-year month approach leading to 12 degradation rates [6]. In this study, a statistical approach is used to calculate only one degradation rate instead of 12 degradation rates, which matches with the field measured I-V data.

In order to calculate the degradation rate the total daily output is summed for each day with each corresponding day having multiple values relating to the number of years the day has been "seen." Ideally, one would expect 365 slopes if we plot the year-over-year daily degradation versus number field exposed years. All data points are filtered for values that are less than 10 kWh since this means the system was not operating. The slope for all days is taken and divided by the first value of a particular day. This makes the assumption that the first day's production is always 100%. The standard deviation for all days is also calculated. The average of all daily kWh summations is taken. A filter of 15% times the average daily kWh generation is then applied to the standard deviation values of all days. Any day that had a standard deviation greater than the calculated value of 15% of the average daily kWh generation was removed. The remaining days were then filtered by their respective degradation rates. If a plant is less than 6 years old, any day having an annual degradation rate less -3.1% (gain in power) or greater than 3.0% (loss in power) was removed as outliers for c-Si modules. If a plant is greater than 6 years old, any day having an annual degradation rate less than -3.1% or greater than 1.0% was

removed. The median of the remaining days' degradation rates was then considered to be the rate at which the plant was degrading. As can be shown in Figure 9, the distribution of the data points is very widespread and contains many outliers, but after filtering, Figure 10, the distribution is narrower and the median value matches that of in field degradation measurements. The method for determining the degradation rate by use of metered kWh data is shown in Figure 11.

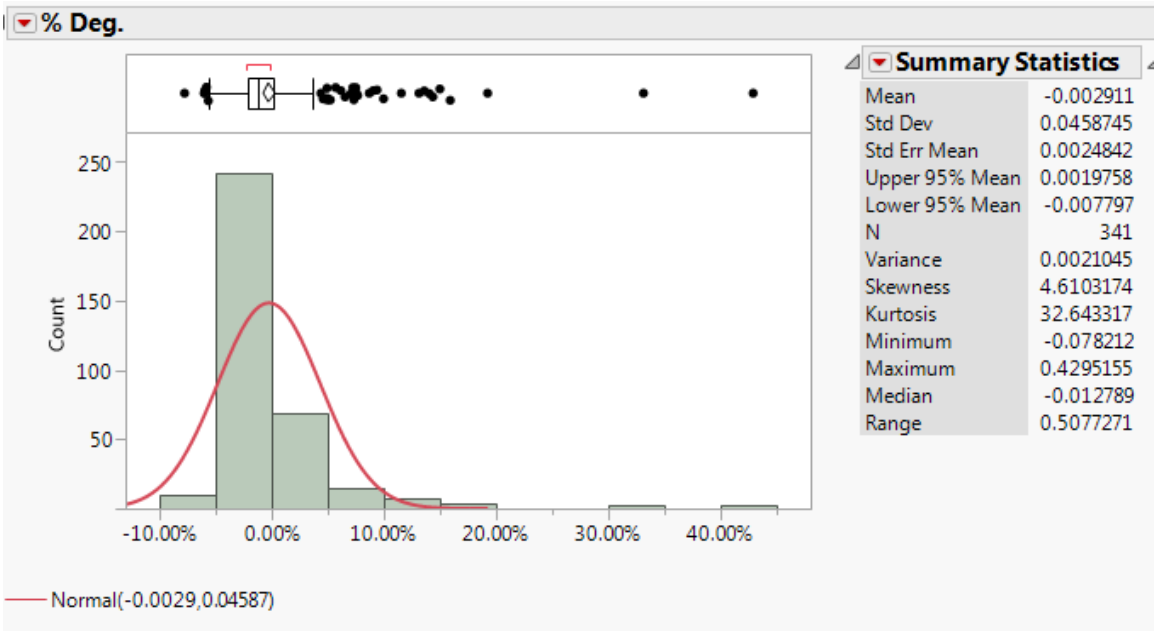

Fig. 9. Unfiltered Degradation Rates for All System Operating Days.

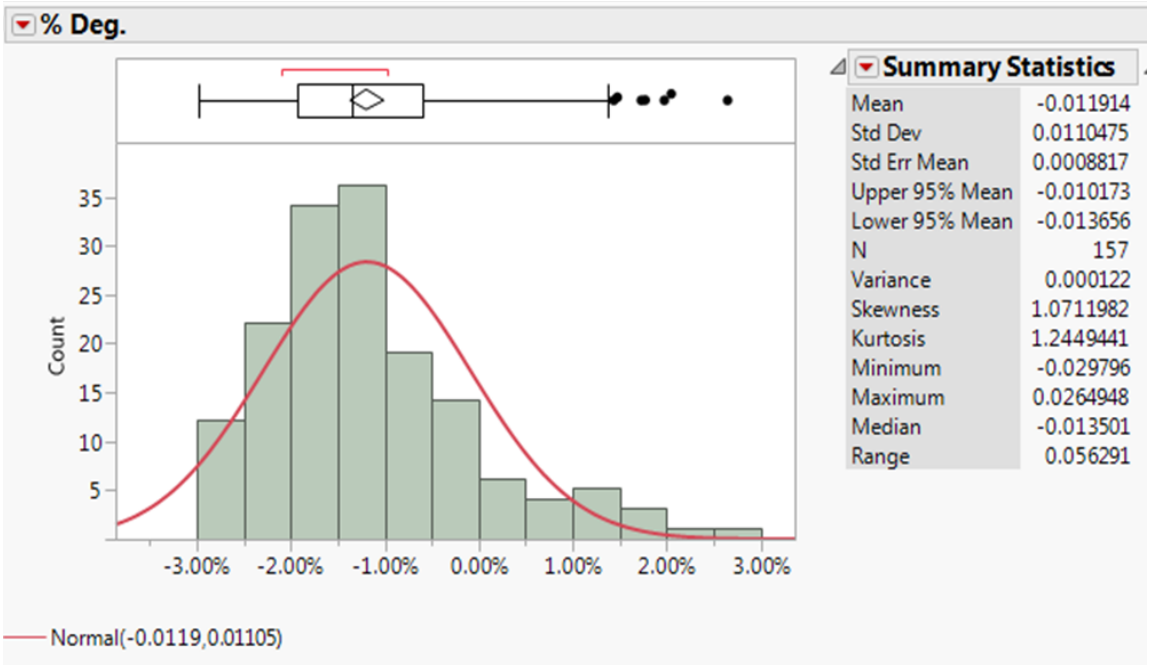

Fig. 10. Filtered Degradation Rates for All System Operating Days, Where the Median Matches Reported I-V Degradation Percent per Year.

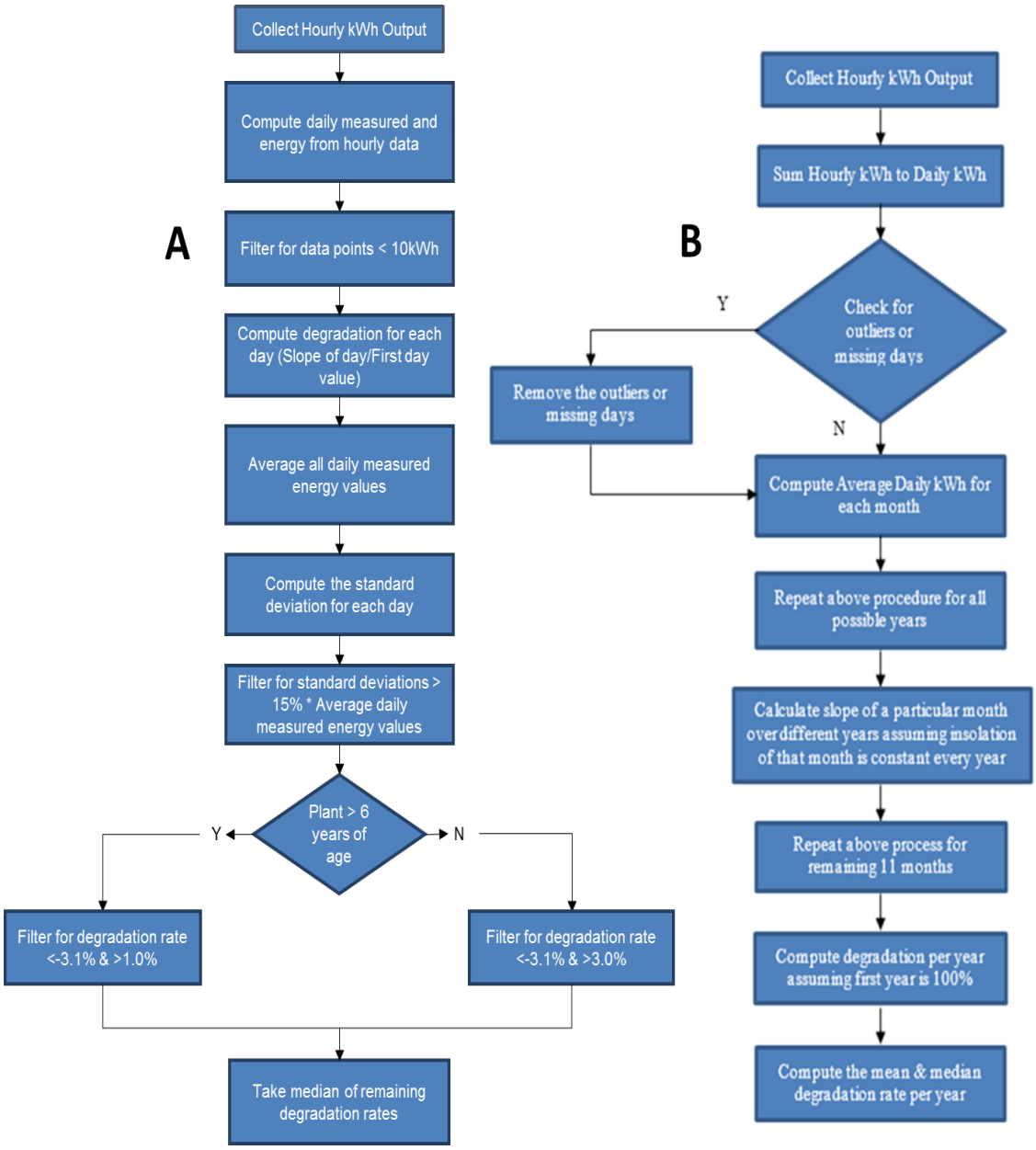

Fig. 11. A) Flowchart for Newer kWh Degradation Method Based on Statistical Analysis. B) Previously Reported kWh Method from Shrestha *et al.*

4.0 RESULTS AND DISCUSSION

The determination of optimal irradiance and temperature models is first analyzed in this section. The resulting irradiance and temperature models verified to best compare to measured data were then used as the models to evaluate the performance and degradation trend analysis of 38 commercial PV systems.

4.1 Irradiance Model Validations

As was previously mentioned in an earlier chapter, 12 decomposition models and 10 transposition models were analyzed to determine the best model for the hot-dry climate of Arizona. The GHI data \ irradiance data used in these models came from two different sources, satellite GHI and in-field measured GHI, to validate the differences, if any, between the calculated POA irradiance values and the real in-field measured POA irradiance values.

4.1.1 Irradiance Model Validations Based on In-field GHI

The GHI and POA irradiance data measured by a meteorological station at Arizona State University's Photovoltaic Lab was used to validate the multiple irradiance models used. The POA irradiance results from the all of the combinations of decomposition and transposition models, as well as the output POA irradiance from PVsyst, were analyzed and compared to two years of data, 2013 and 2014, collected from a Kipp and Zonen pyrometer at latitude tilt (33°) at ASU-PRL in Mesa, Arizona. The models were looked at two different perspectives: 1) how accurately the hourly data matched that collected from ASU-PRL and 2) how accurately models matched the total

yearly insolation measured at ASU-PRL. The weather station in which the data was collected from is shown below.

Fig. 12. Weather Station and Irradiance Sensors Used to Measure GHI and POA Irradiance (33° South Facing Tilt) for 2013 and 214 in Mesa, Arizona.

In order to fist look at how accurate all model combinations and PVsyst outputs were able to predict the measured POA irradiance, the calculated POA irradiances were analyzed by use of Root Mean Square Error (RMSE) and Normalized Root Mean Square Error (NRMSE). The results for the two years of data are shown below in Tables 3-6.

Root Mean Square Error (RMSE) for PRL GHI to POA in 2013										
	Transpostion Models									
Decomposition Models	Isotropic	Korokanis	Badescu	Sandia	Willmot	Temps.	Klutcher	Hay & Davies	Reindl	Perez
Liu and Jordan	43.27	88.56	42.92	43.63	51.88	47.11	46.15	94.07	56.22	58.46
Orgil and Hollands	29.95	29.92	39.84	29.75	44.82	34.51	32.06	46.33	47.60	32.27
Erbs	30.96	31.00	31.93	30.84	45.62	35.78	33.56	46.05	47.35	34.28
Spencer	76.12	72.34	87.86	75.22	77.73	43.20	60.78	72.17	65.71	94.92
Reindl 1	30.27	30.34	31.21	30.16	45.70	35.32	33.06	46.55	47.84	33.60
Reindl 2	43.61	42.71	46.80	43.35	49.45	40.05	39.57	49.74	50.59	45.42
Lam and Li	33.27	32.78	35.88	32.77	46.39	34.80	32.55	46.69	48.28	32.60
Skartveit and Olseth	26.71	26.25	29.52	26.08	32.15	30.12	26.96	33.60	35.76	26.25
Maxwell	56.10	53.61	63.73	54.98	42.00	35.79	39.67	38.82	37.37	40.55
Louche	57.03	54.69	64.54	55.98	44.86	38.14	40.34	41.79	39.15	40.78
Vignola and McDaniels	54.77	52.48	61.89	53.69	42.24	36.24	40.83	40.58	35.93	37.57
Perez	39.90	39.70	41.23	39.40	39.88	40.69	43.13	42.05	41.16	37.34
Pvsyst								14.63		18.82

Table 3. Root Mean Square Error for All Decomposition and Transposition Models When Converting Measured GHI Data, from PRL in 2013, to POA Irradiance (33° South Facing Tilt).

Normalized Root Mean Square Error (NRMSE) for PRL GHI to POA in 2013										
	Transpostion Models									
Decomposition Models	Isotropic	Korokanis	Badescu	Sandia	Willmot	Temps.	Klutcher	Hay & Davies	Reindl	Perez
Liu and Jordan	3.942%	8.068%	3.910%	3.975%	4.726%	4.292%	4.205%	8.570%	5.122%	5.325%
Orgil and Hollands	2.729%	2.725%	3.629%	2.710%	4.084%	3.144%	2.920%	4.221%	4.336%	2.939%
Erbs	2.820%	2.824%	2.909%	2.809%	4.156%	3.260%	3.057%	4.195%	4.313%	3.123%
Spencer	6.935%	6.591%	8.004%	6.852%	7.081%	3.936%	5.537%	6.575%	5.986%	8.647%
Reindl 1	2.758%	2.764%	2.843%	2.748%	4.163%	3.218%	3.012%	4.241%	4.359%	3.061%
Reindl 2	3.972%	3.891%	4.263%	3.949%	4.505%	3.649%	3.605%	4.531%	4.608%	4.138%
Lam and Li	3.031%	2.986%	3.269%	2.985%	4.226%	3.170%	2.965%	4.253%	4.398%	2.970%
Skartveit and Olseth	2.433%	2.391%	2.689%	2.376%	2.929%	2.744%	2.456%	3.061%	3.258%	2.391%
Maxwell	5.110%	4.884%	5.806%	5.009%	3.827%	3.261%	3.614%	3.536%	3.405%	3.694%
Louche	5.196%	4.982%	5.880%	5.100%	4.087%	3.474%	3.675%	3.807%	3.567%	3.715%
Vignola and McDaniels	4.990%	4.781%	5.638%	4.891%	3.848%	3.301%	3.719%	3.696%	3.273%	3.423%
Perez	3.635%	3.617%	3.756%	3.589%	3.633%	3.707%	3.929%	3.831%	3.750%	3.402%
Pvsyst								1.333%		1.714%

Table 4. Normalized Root Mean Square Error for All Decomposition and Transposition Models When Converting Measured GHI Data, from PRL in 2013, to POA Irradiance (33° South Facing Tilt).

Root Mean Square Error (NRMSE) for PRL GHI to POA in 2014										
	Transpostion Models									
Decomposition Models	Isotropic	Korokanis	Badescu	Sandia	Willmot	Temps.	Klutcher	Hay & Davies	Reindl	Perez
Liu and Jordan	46.50	90.43	46.29	46.73	50.41	49.65	48.59	52.52	52.31	61.09
Orgil and Hollands	35.16	35.01	36.68	34.89	43.86	37.74	35.43	44.85	45.47	35.68
Erbs	35.77	35.69	36.87	35.55	43.71	38.89	36.74	44.09	45.26	37.42
Spencer	71.30	68.24	80.66	70.54	71.09	46.98	58.88	66.26	61.55	90.99
Reindl 1	34.21	34.13	35.42	33.98	44.27	37.40	35.12	44.90	45.60	35.68
Reindl 2	44.00	43.38	46.45	43.81	47.34	42.12	40.84	47.64	47.98	45.58
Lam and Li	38.02	37.58	40.35	37.55	44.26	38.65	36.52	44.56	46.34	36.79
Skartveit and Olseth	32.16	31.67	34.78	31.56	35.52	33.67	30.80	37.16	38.82	30.55
Maxwell	56.28	53.88	63.64	55.19	42.86	35.87	39.79	39.53	36.69	40.13
Louche	60.84	57.05	65.78	59.87	43.77	42.34	40.85	41.65	36.92	44.58
Vignola and McDaniels	56.54	54.25	63.64	55.49	42.88	36.70	40.79	39.71	37.03	39.77
Perez	40.88	38.55	42.20	40.30	40.30	38.55	41.24	43.99	42.10	37.40
Pvsyst								15.23		20.43

Table 5. Root Mean Square Error for All Decomposition and Transposition Models When Converting Measured GHI Data, from PRL in 2014, to POA Irradiance (33° South Facing Tilt).

Normalized Root Mean Square Error (NRMSE) for PRL GHI to POA in 2014										
	Transpostion Models									
Decomposition Models	Isotropic	Korokanis	Badescu	Sandia	Willmot	Temps.	Klutcher	Hay & Davies	Reindl	Perez
Liu and Jordan	4.203%	8.174%	4.184%	4.224%	4.556%	4.487%	4.392%	4.747%	4.728%	5.522%
Orgil and Hollands	3.178%	3.164%	3.315%	3.153%	3.965%	3.411%	3.202%	4.054%	4.109%	3.224%
Erbs	3.233%	3.226%	3.333%	3.213%	3.950%	3.515%	3.321%	3.985%	4.091%	3.382%
Spencer	6.444%	6.168%	7.291%	6.376%	6.425%	4.246%	5.321%	5.989%	5.563%	8.224%
Reindl 1	3.092%	3.085%	3.201%	3.071%	4.002%	3.380%	3.175%	4.058%	4.122%	3.225%
Reindl 2	3.977%	3.920%	4.198%	3.960%	4.279%	3.807%	3.692%	4.306%	4.337%	4.120%
Lam and Li	3.436%	3.397%	3.647%	3.394%	4.000%	3.494%	3.301%	4.027%	4.188%	3.325%
Skartveit and Olseth	2.907%	2.863%	3.144%	2.853%	3.211%	3.043%	2.784%	3.359%	3.509%	2.762%
Maxwell	5.086%	4.870%	5.752%	4.988%	3.873%	3.242%	3.597%	3.573%	3.316%	3.627%
Louche	5.499%	5.156%	5.945%	5.412%	3.956%	3.826%	3.692%	3.765%	3.337%	4.029%
Vignola and McDaniels	5.111%	4.903%	5.752%	5.015%	3.876%	3.317%	3.686%	3.589%	3.347%	3.594%
Perez	3.695%	3.484%	3.814%	3.642%	3.642%	3.484%	3.727%	3.976%	3.805%	3.380%
Pvsyst								1.376%		1.847%

Table 6. Normalized Root Mean Square Error for All Decomposition and Transposition Models When Converting Measured GHI Data, from PRL in 2013, to POA Irradiance (33° South Facing Tilt).

When looking at the RMSE and NRMSE data from the above tables, it is clear that when converting from measured data, where the uncertainty is maintained at minimum, PVsyst is the most accurate source of irradiance translation. The interesting thing to note though, is that the Hay & Davies model, said to be the more robust model, is

actually more accurate than the Perez model, by ~.4%. This result is similar to the results that were reported in Lave *et al.* that the Hay & Davies model may want to be used when the diffused irradiance component is not directly measured [1]. While the translations shown here show that the PVsyst software does the most accurate job in predicting the hourly values of the POA irradiance, another important aspect that needs to be investigated is whether or not these values are slight under predictions or over predictions on the total insolation seen throughout the year.

In order to validate the amount of total energy that was predicted from the models and PVsyst, the hourly POA irradiance was summed for both years. In Tables 7 and 8, the percent difference of the predicted annual POA insolation versus that of the measured POA insolation is given for the years 2013 and 2014, respectively.

% Diff. of Modled Insolation vs. Measured Insolation for PRL GHI to POA in 2013										
	Transpostion Models									
Decomposition Models	Isotropic	Korokanis	Badescu	Sandia	Willmot	Temps.	Klutcher	Hay & Davies	Reindl	Perez
Liu and Jordan	3.501%	17.179%	2.663%	3.880%	4.623%	5.810%	5.167%	5.765%	4.796%	6.836%
Orgil and Hollands	-0.332%	0.332%	-1.359%	0.036%	1.983%	4.307%	3.336%	2.750%	4.201%	2.806%
Erbs	0.052%	0.683%	-1.530%	0.434%	2.253%	4.399%	3.487%	2.940%	4.250%	3.195%
Spencer	-6.373%	-5.203%	-9.277%	-6.000%	-5.128%	2.937%	-1.958%	-3.436%	-0.676%	-8.301%
Reindl 1	0.087%	0.728%	-1.493%	0.468%	2.325%	4.444%	3.579%	3.015%	4.349%	3.183%
Reindl 2	-0.363%	0.215%	-1.815%	0.010%	1.728%	4.055%	2.958%	2.417%	3.592%	1.704%
Lam and Li	-1.292%	-0.523%	-3.224%	-0.913%	1.553%	4.164%	3.282%	2.326%	4.120%	1.984%
Skartveit and Olseth	-1.791%	-1.034%	-3.625%	-1.407%	0.841%	3.347%	2.264%	1.254%	2.983%	1.145%
Maxwell	-7.388%	-6.176%	-10.418%	-7.001%	-5.600%	1.593%	-1.737%	-4.106%	-1.733%	-4.843%
Louche	-6.778%	-5.668%	-9.532%	-6.390%	-4.853%	1.852%	-1.345%	-3.486%	-1.048%	-3.826%
Vignola and McDaniels	-6.974%	-5.792%	-9.946%	-6.587%	-5.132%	1.878%	-1.371%	-3.608%	-1.089%	-4.286%
Perez	-1.843%	-1.281%	-3.256%	-1.457%	-0.661%	1.638%	1.051%	-0.143%	0.530%	0.380%
Pvsyst								0.977%		2.691%

Table 7. Percent Difference of Predicted Total Insolation for All Decomposition and Transposition Models vs. Measured POA Irradiance Data from PRL in 2013.

% Diff. of Modled Insolation vs. Measured Insolation for PRL GHI to POA in 2014										
	Transpostion Models									
Decomposition Models	Isotropic	Korokanis	Badescu	Sandia	Willmot	Temps.	Klutcher	Hay & Davies	Reindl	Perez
Liu and Jordan	3.334%	17.096%	2.489%	3.711%	4.396%	5.754%	4.979%	4.808%	4.370%	6.866%
Orgil and Hollands	-0.647%	0.012%	-2.358%	-0.293%	1.419%	4.167%	3.089%	2.179%	3.622%	2.676%
Erbs	-0.254%	0.385%	-1.832%	0.126%	1.667%	4.263%	3.249%	2.359%	3.686%	3.065%
Spencer	-4.722%	-3.596%	-7.549%	-4.345%	-3.735%	3.613%	-0.498%	-2.130%	0.514%	-6.812%
Reindl 1	-0.258%	0.379%	-1.892%	0.107%	1.734%	4.314%	3.354%	2.435%	3.777%	3.048%
Reindl 2	0.070%	0.606%	-1.266%	0.449%	1.669%	4.079%	3.019%	2.327%	3.405%	2.235%
Lam and Li	-1.293%	-0.531%	-3.235%	-0.928%	1.156%	4.203%	3.278%	1.924%	3.690%	2.078%
Skartveit and Olseth	-2.001%	-1.266%	-3.843%	-1.632%	0.568%	3.283%	2.081%	0.942%	2.686%	1.142%
Maxwell	-7.303%	-6.097%	-10.321%	-6.918%	-5.690%	1.673%	-1.692%	-4.212%	-1.842%	-4.610%
Louche	-6.640%	-5.588%	-9.515%	-6.253%	-5.131%	2.017%	-1.351%	-3.735%	-1.364%	-3.590%
Vignola and McDaniels	-7.076%	-5.889%	-10.060%	-6.691%	-5.524%	1.918%	-1.539%	-4.029%	-1.449%	-4.336%
Perez	-2.015%	-1.504%	-3.431%	-1.631%	-0.814%	1.583%	0.911%	-0.243%	0.492%	0.486%
Pvsyst								0.521%		2.369%

Table 8. Percent Difference of Predicted Total Insolation for All Decomposition and Transposition Models vs. Measured POA Irradiance Data from PRL in 2014.

When evaluating the models for predicted total insolation, it becomes apparent that there are some models that can more accurately predict the annual amount of solar radiation hitting a tilted surface on the Earth than those given by PVsyst. Some models seem to also have more variation year to year than others. One such example is than of Orgil and Hollands decomposition model with the Korokanis transposition model. In 2013, this model overpredicted the total insolation by 0.332%, whereas in the following year it was nearly identical with the measured value with only having 0.012% difference. This year to year variation is also evident in the outputs from PVsyst that show a difference of 0.456% and 0.322% for the Hay & Davies and Perez models, respectively.

From the data and models analyzed in this section, two conclusion can be drawn and implemented for the hot-dry climate of Arizona. The first conclusion that can be made is that when on site measured GHI data is available, PVsyst gives an accurate representation of the hour by hour value for the POA irradiance seen on a south facing tilted surface. If PVsyst is unavailable to be used, combination of the Skartveit and Olseth

decomposition model and Perez transposition model, also gives a good prediction as to the hour by hour amount of POA irradiance. In both the two years of observed data, this combination gave an NRMSE value of 2.39% and 2.76%. The second conclusion that can be made from this data set is that PVsyst generally over predicts the total yearly amount of insolation seen in the hot-dry climate of Arizona and that the more robust Hay & Davies transposition model should be used. The over prediction of total insolation can vary as much as little as 0.52% to as much as 2.37% depending on which model is used in the PVsyst software. In both years of analyzed data, the Hay & Davies was more accurate than the Perez model in predicting the hourly POA irradiance as well as yearly total POA insolation. While this model was the most accurate from PVsyst, it was shown to be outdone by multiple other decomposition and transposition model combinations as seen by the average percent difference for the two years of data in the table below.

Avg % Diff. of Modled Insolation vs. Measured Insolation for PRL GHI to POA										
	Transpostion Models									
Decomposition Models	Isotropic	Korokanis	Badescu	Sandia	Willmot	Temps.	Klutcher	Hay & Davies	Reindl	Perez
Liu and Jordan	3.417%	17.137%	2.576%	3.796%	4.509%	5.782%	5.073%	5.286%	4.583%	6.851%
Orgil and Hollands	-0.489%	0.172%	-1.858%	-0.128%	1.701%	4.237%	3.212%	2.464%	3.912%	2.741%
Erbs	-0.101%	0.534%	-1.681%	0.280%	1.960%	4.331%	3.368%	2.650%	3.968%	3.130%
Spencer	-5.548%	-4.399%	-8.413%	-5.172%	-4.432%	3.275%	-1.228%	-2.783%	-0.081%	-7.556%
Reindl 1	-0.085%	0.553%	-1.693%	0.288%	2.029%	4.379%	3.466%	2.725%	4.063%	3.116%
Reindl 2	-0.146%	0.410%	-1.541%	0.230%	1.699%	4.067%	2.988%	2.372%	3.499%	1.970%
Lam and Li	-1.293%	-0.527%	-3.229%	-0.921%	1.355%	4.184%	3.280%	2.125%	3.905%	2.031%
Skartveit and Olseth	-1.896%	-1.150%	-3.734%	-1.520%	0.705%	3.315%	2.172%	1.098%	2.835%	1.143%
Maxwell	-7.345%	-6.136%	-10.369%	-6.959%	-5.645%	1.633%	-1.714%	-4.159%	-1.788%	-4.726%
Louche	-6.709%	-5.628%	-9.524%	-6.322%	-4.992%	1.934%	-1.348%	-3.611%	-1.206%	-3.708%
Vignola and McDaniels	-7.025%	-5.840%	-10.003%	-6.639%	-5.328%	1.898%	-1.455%	-3.818%	-1.269%	-4.311%
Perez	-1.929%	-1.392%	-3.343%	-1.544%	-0.738%	1.611%	0.981%	-0.193%	0.511%	0.433%
Pvsyst								0.749%		2.530%

Table 9. Average Percent Difference of Predicted Total Insolation for All Decomposition and Transposition Models vs. Measured POA Insolation Data from PRL for 2013 and 2014.

One such combination is that of the Spencer decomposition model and Reindl transposition model, that gave an average percent difference of -0.081%. This is a drastic improvement over the average percent difference of 0.75% for the Hay & Davies model and 2.53% for the Perez model from PVsyst.

4.1.2 Irradiance Model Validations Based on Satellite GHI

Due to the cost of expensive irradiance sensors, system owners and installers do not wish to put many sensors in the field to measure the GHI of a particular location unless needed. Because of this reason, satellite base GHI data can also be used in which land areas are generally divided into tiles. These tiles can be smaller in size, giving higher accuracy results, or large in area, with lower resolution, but costing less to purchase. Due to the lack of available on site GHI data, SolarAnywhere data was used to generate the GHI seen by all systems within the Phoenix-Metro region of Arizona. This was more specifically done for the Tempe area, as shown by the map below. Since satellite data itself contains some uncertainties, it became necessary to verify all decomposition models and transposition models, as well as PVsyst, in order to validate which models are again most accurately predicting the measured POA irradiance. The same procedure was done for satellite data as was previously shown for measured in-field GHI data. The calculated POA irradiance was once again compared to the measured POA irradiance of a commercial PV power plant located in the same region as that of the selected tile. The results of the RMSE and NRMSE for the two years of measured data are shown in Tables 8-11.

Fig. 13. Tile selection from SolarAnywhere based on site locations.

Root Mean Square Error (RMSE) for Satellite GHI to POA in 2009										
	Transpostion Models									
Decomposition Models	Isotropic	Korokanis	Badescu	Sandia	Willmot	Temps.	Klutcher	Hay & Davies	Reindl	Perez
Liu and Jordan	23.23	23.28	23.10	23.30	24.75	27.68	39.40	24.82	24.59	25.05
Orgil and Hollands	20.56	20.65	20.33	20.60	22.42	28.90	23.21	22.51	22.70	19.18
Erbs	17.31	17.38	17.10	17.36	23.13	26.06	23.39	26.14	26.00	18.82
Spencer	27.85	27.64	28.52	27.83	33.15	30.19	25.29	32.20	28.75	31.39
Reindl 1	20.87	20.95	20.63	20.91	22.73	28.87	23.50	22.82	23.00	19.71
Reindl 2	21.31	21.32	21.29	21.37	24.78	26.36	24.02	24.80	23.82	23.61
Lam and Li	17.05	17.09	16.95	17.08	22.58	26.49	24.25	22.68	22.93	18.34
Skartveit and Olseth	10.57	10.66	10.38	10.62	19.23	23.28	19.89	19.26	19.56	12.45
Maxwell	23.27	23.11	23.80	23.23	20.17	31.87	24.54	20.33	11.96	14.02
Louche	27.80	27.74	28.01	27.76	31.49	35.15	31.77	29.64	24.59	27.61
Vignola and McDaniels	18.24	18.12	18.66	18.18	14.39	29.48	20.73	14.66	13.92	12.87
Perez	34.02	34.14	33.70	34.06	34.44	38.91	28.46	36.61	26.00	31.06
Pvsyst								11.35		12.76

Table 10. Root Mean Square Error for All Decomposition and Transposition Models When Converting Satellite GHI Data, from SolarAnywhere in 2009, to POA Irradiance (10° South Facing Tilt).

Normalized Root Mean Square Error (NRMSE) for Satellite GHI to POA in 2009										
	Transpostion Models									
Decomposition Models	Isotropic	Korokanis	Badescu	Sandia	Willmot	Temps.	Klutcher	Hay & Davies	Reindl	Perez
Liu and Jordan	2.193%	2.198%	2.181%	2.200%	2.337%	2.613%	3.720%	2.343%	2.321%	2.365%
Orgil and Hollands	1.941%	1.950%	1.919%	1.945%	2.116%	2.729%	2.192%	2.126%	2.143%	1.811%
Erbs	1.634%	1.641%	1.615%	1.639%	2.184%	2.461%	2.209%	2.468%	2.455%	1.777%
Spencer	2.630%	2.610%	2.692%	2.628%	3.130%	2.850%	2.388%	3.041%	2.715%	2.964%
Reindl 1	1.970%	1.979%	1.948%	1.974%	2.146%	2.726%	2.219%	2.154%	2.171%	1.861%
Reindl 2	2.012%	2.013%	2.010%	2.018%	2.340%	2.488%	2.268%	2.342%	2.249%	2.229%
Lam and Li	1.610%	1.614%	1.601%	1.612%	2.132%	2.501%	2.289%	2.142%	2.165%	1.731%
Skartveit and Olseth	0.998%	1.006%	0.980%	1.003%	1.815%	2.198%	1.878%	1.819%	1.847%	1.176%
Maxwell	2.197%	2.182%	2.247%	2.193%	1.905%	3.009%	2.317%	1.919%	1.130%	1.324%
Louche	2.625%	2.619%	2.645%	2.621%	2.973%	3.319%	2.999%	2.799%	2.322%	2.607%
Vignola and McDaniels	1.722%	1.711%	1.762%	1.717%	1.359%	2.784%	1.957%	1.384%	1.314%	1.216%
Perez	3.212%	3.223%	3.182%	3.216%	3.252%	3.674%	2.687%	3.457%	2.455%	2.933%
Pvsyst								1.071%		1.205%

Table 11. Normalized Root Mean Square Error for All Decomposition and Transposition Models When Converting Satellite GHI Data, from SolarAnywhere in 2009, to POA Irradiance (10° South Facing Tilt).

Root Mean Square Error (RMSE) for Satellite GHI to POA in 2010										
	Transpostion Models									
Decomposition Models	Isotropic	Korokanis	Badescu	Sandia	Willmot	Temps.	Klutcher	Hay & Davies	Reindl	Perez
Liu and Jordan	24.31	24.35	24.20	24.37	26.99	28.64	36.63	27.27	26.87	26.00
Orgil and Hollands	18.55	18.61	18.38	18.59	22.14	27.42	24.53	22.22	22.39	21.24
Erbs	19.54	19.60	19.37	19.58	22.37	27.55	24.84	22.45	22.40	20.82
Spencer	30.20	30.01	30.81	30.19	31.18	32.73	27.74	30.29	26.47	33.92
Reindl 1	19.25	19.31	19.08	19.29	22.13	27.67	25.06	22.25	22.42	22.00
Reindl 2	23.28	23.29	23.27	23.33	25.24	27.95	25.56	27.58	25.44	27.64
Lam and Li	19.81	19.85	19.73	19.84	22.15	28.36	26.13	22.28	22.52	20.91
Skartveit and Olseth	11.15	11.23	10.97	11.20	21.48	23.49	19.98	21.46	21.72	13.00
Maxwell	19.94	19.82	20.35	19.90	18.75	29.94	24.43	18.62	16.65	17.92
Louche	37.78	37.69	38.05	37.76	23.69	43.13	33.33	20.70	20.13	25.44
Vignola and McDaniels	18.61	18.50	19.00	18.56	13.42	29.83	23.03	13.48	13.26	13.72
Perez	40.87	40.99	40.51	40.89	40.87	45.16	31.40	43.10	26.25	29.14
Pvsyst								11.25		12.72

Table 12. Root Mean Square Error for All Decomposition and Transposition Models When Converting Satellite GHI Data, from SolarAnywhere in 2010, to POA Irradiance (10° South Facing Tilt).

Normalized Root Mean Square Error (NRMSE) for Satellite GHI to POA in 2010										
	Transpostion Models									
Decomposition Models	Isotropic	Korokanis	Badescu	Sandia	Willmot	Temps.	Klutcher	Hay & Davies	Reindl	Perez
Liu and Jordan	2.289%	2.293%	2.279%	2.295%	2.541%	2.697%	3.449%	2.567%	2.530%	2.448%
Orgil and Hollands	1.746%	1.753%	1.731%	1.750%	2.085%	2.582%	2.310%	2.092%	2.109%	1.999%
Erbs	1.839%	1.845%	1.823%	1.844%	2.106%	2.594%	2.339%	2.114%	2.109%	1.960%
Spencer	2.844%	2.826%	2.901%	2.842%	2.936%	3.081%	2.612%	2.852%	2.492%	3.194%
Reindl 1	1.812%	1.818%	1.796%	1.816%	2.084%	2.605%	2.360%	2.095%	2.111%	2.071%
Reindl 2	2.192%	2.193%	2.191%	2.197%	2.377%	2.632%	2.407%	2.597%	2.395%	2.602%
Lam and Li	1.865%	1.869%	1.857%	1.868%	2.085%	2.670%	2.460%	2.098%	2.120%	1.968%
Skartveit and Olseth	1.050%	1.057%	1.033%	1.055%	2.022%	2.212%	1.881%	2.021%	2.045%	1.224%
Maxwell	1.878%	1.866%	1.916%	1.873%	1.766%	2.819%	2.300%	1.753%	1.567%	1.687%
Louche	3.557%	3.549%	3.583%	3.555%	2.230%	4.061%	3.138%	1.949%	1.895%	2.395%
Vignola and McDaniels	1.753%	1.742%	1.789%	1.748%	1.263%	2.808%	2.169%	1.269%	1.248%	1.291%
Perez	3.848%	3.860%	3.814%	3.850%	3.848%	4.252%	2.956%	4.058%	2.472%	2.743%
Pvsyst								1.059%		1.198%

Table 13. Normalized Root Mean Square Error for All Decomposition and Transposition Models When Converting Satellite GHI Data, from SolarAnywhere in 2010, to POA Irradiance (10° South Facing Tilt).

Again, when looking at the RMSE and NRMSE data from the above tables, it is easy to see that when converting from satellite generated GHI data, where the uncertainty can be as much as 5% [11], PVsyst is shown to not be the most accurate source of irradiance translation. When using the satellite GHI data for translating to POA irradiance, the most accurate model was found to be the combination of the Skartveit and Olseth decomposition model and Badescu transposition model. This model showed to slightly outperform the NRMSE of the Hay & Davies model found in PVsyst by 0.09% and 0.03% in 2009 and 2010, respectively. As shown in the two figures below, the accuracy of the Skartveit and Olseth – Badescu model is on par with that of the results generated from PVsyst. There are only a few outliers each year and only occurred when the measured POA was less than 100 W/m^2 where the system would be producing little to no energy.

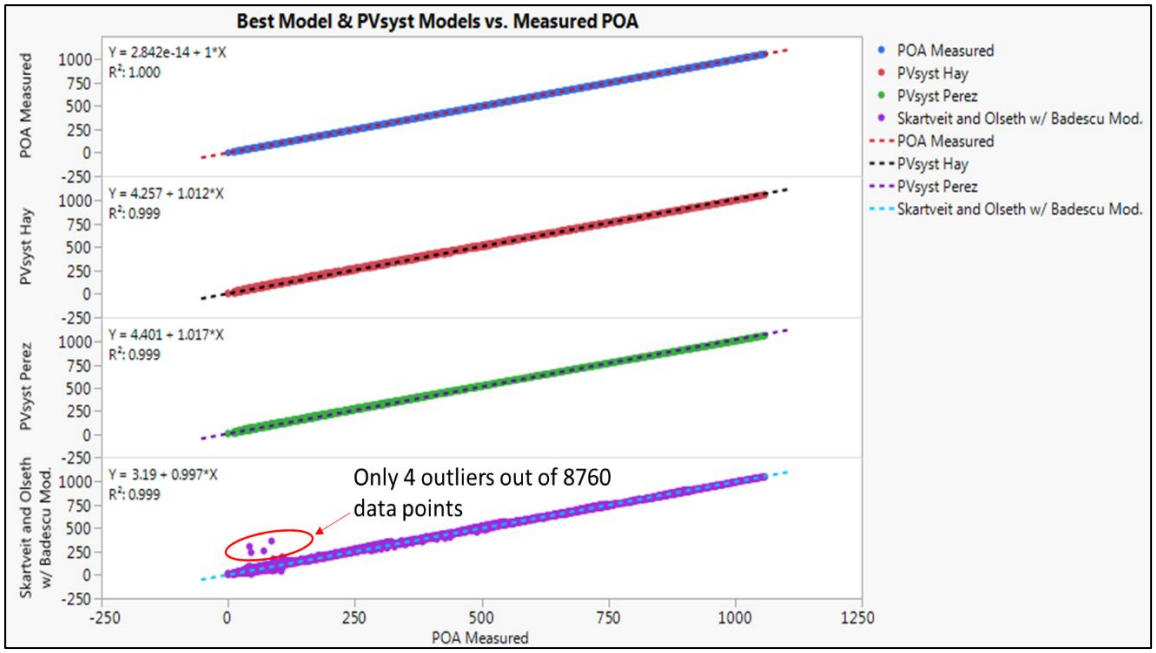

Fig. 14. Correlation comparison of PVsyst Models and Best Decomposition Model and Transposition Model vs. Measured Hourly POA Irradiance for 2009.

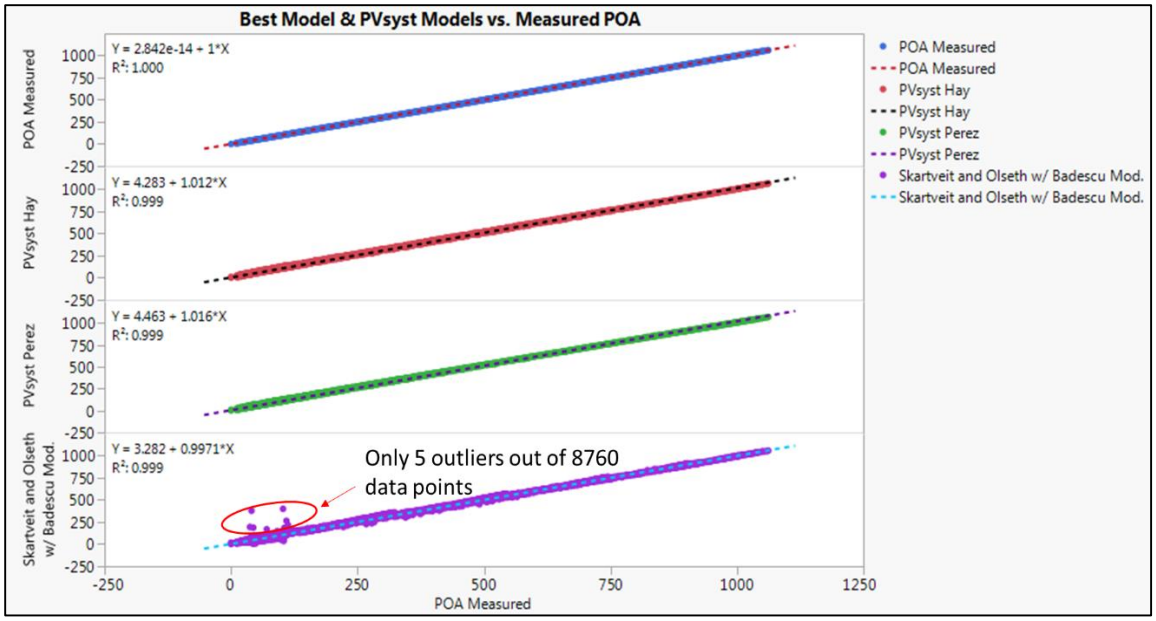

Fig. 15. Correlation Comparison of PVsyst Models and Best Decomposition Model and Transposition Model vs. Measured Hourly POA Irradiance for 2010.

It was also found again that the more robust Hay & Davies model was able to outperform the Perez model in PVsyst. This means that for the hot-dry climate of Arizona, when using PVsyst, the Hay & Davies transposition model should be used no matter if the input data is in-field measured GHI or satellite generated GHI. To determine if the best model was that of Hay & Davies from PVsyst or the Skartveit & Olseth – Badescu model, the deciding factor would be which model more closely represented the total annual energy since both translation methods gave nearly identical NRMSE values. The two figures below show the over prediction of the models for each year as compared to the measured total insolation.

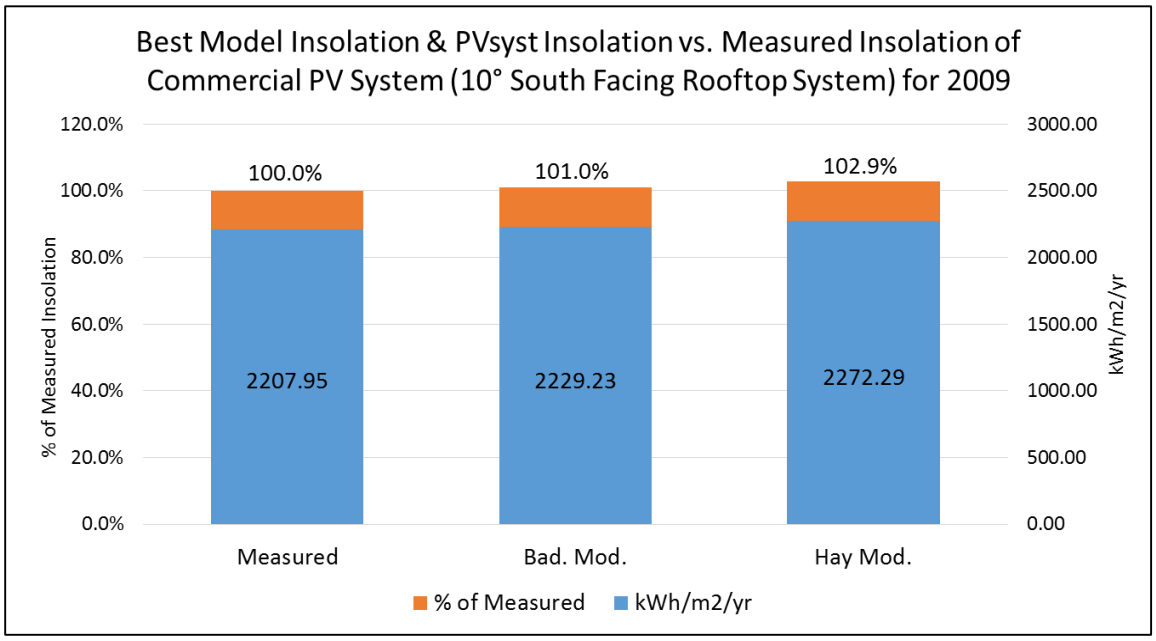

Fig. 16. Skartveit & Olseth – Badescu Model Insolation and PVsyst Hay & Davies Model Insolation Compared to the Measured Insolation of a Commercial PV System (10° South Facing Rooftop) for 2009.

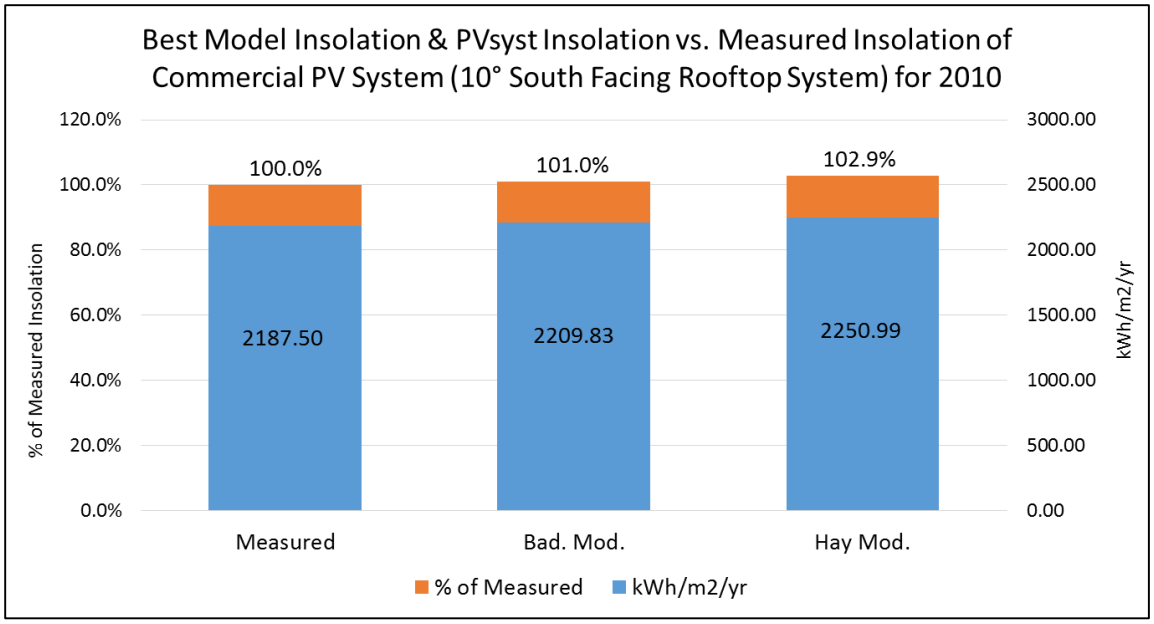

Fig. 17. Skartveit & Olseth – Badescu Model Insolation and PVsyst Hay & Davies Model Insolation Compared to the Measured Insolation of a Commercial PV System (10° South Facing Rooftop) for 2010.

When looking at the total insolation for both years, it is evident that the more effective model is that of the Skartveit & Olseth – Badescu model since it only over predicts the total insolation by 1.0% as compared to that of the PVsyst Hay & Davies model that over predicts by 2.9%. To verify this, the average monthly percent variation of the model POA irradiance compared to that of the measured POA irradiance was averaged for both years of data. The results of this are shown in Figure 18.

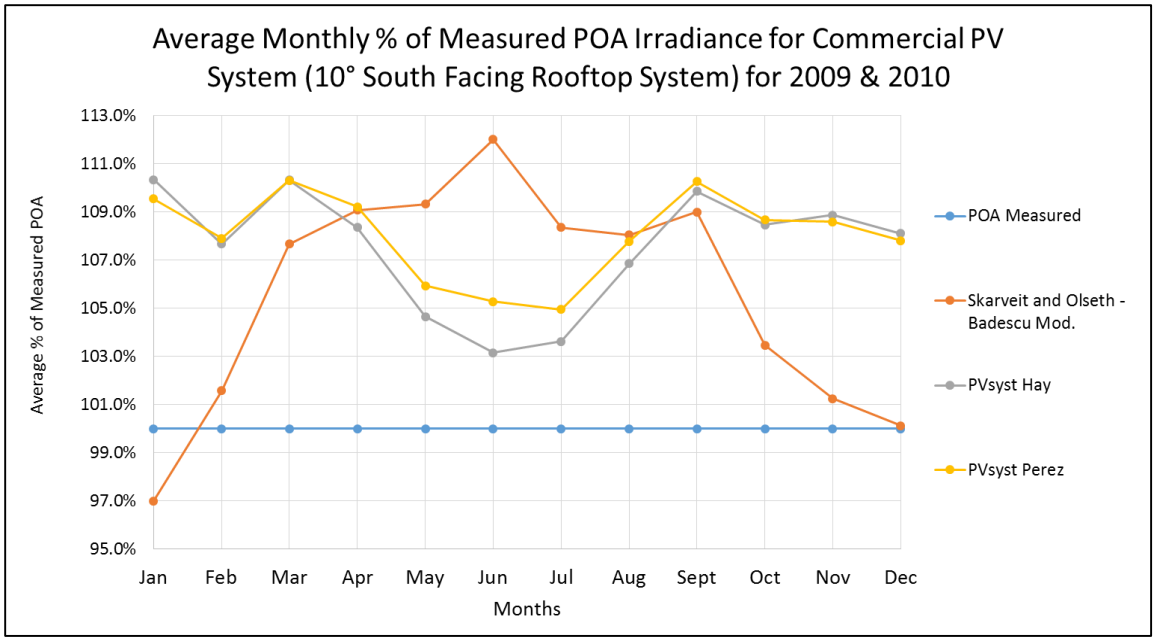

Fig. 18. Average Percent Monthly Variation of POA Irradiance from PVsyst Models and Skartveit & Olseth – Badescu as Compared to Measured POA Irradiance for a Commercial PV System from 2009 to 2010.

As can be seen from the graph above, both the Hay & Davies and Perez PVsyst models are shown to over predict the POA irradiance by a minimum of 3.0% for a single month and can be as much as 10.4%. The Skartveit & Olseth – Badescu model was shown to have more variance in it since it under predicts by 3.0% in a single month and can then over predict by 12.0% in a summer month. This graph indicates that for the summer months (May-August) PVsyst's Hay & Davies model showed the least amount of variation, but during the other months, the Skartveit & Olseth – Badescu showed to have the least amount of monthly variations. Because of this it was decided that a hybrid model of PVsyst's Hay & Davies model and the Skartveit & Olseth – Badescu model would be the best way to minimize the RMSE and NRMSE. When this was done, the

RMSE values were reduced to 9.29 W/m^2 and 9.50 W/m^2 for 2009 and 2010, respectively. This results in the NRSME values falling to 0.878% for 2009 and 0.895% for 2010, the lowest observed values. Since these values were seen to give the lowest errors for predicting hourly POA irradiance data, the hybrid model was determined to be the most optimal model. While the model showed improvement on the hour by hour basis, it was shown to still have an over prediction of 1.3%. This value is still far better than those produced from PVsyst and only adds an additional .3% over prediction to that of the Skartveit & Olseth – Badescu model.

When looking at the translation of satellite generated GHI data into POA irradiance data, some important conclusions can be made. First, it has been shown that there are multiple combinations and models that give highly accurate results. One such model is that of the Skartveit & Olseth decomposition and Badescu transposition model. This model showed to be better than both the Hay & Davies PVsyst models on both the hour to hour POA irradiance results and annual POA insulation. While this model alone was shown to be more accurate than the PVsyst models, it still had some months with high variations as compared to measured POA irradiance. In order to compensate for this, the hybrid model of Skartveit & Olseth – Badescu and PVsyst's Hay & Davies model was developed to give the lowest found RMSE and NRMSE values for two years of measured data. This hybrid model also showed to have a drastic improvement on the total annual insulation prediction as compared to the PVsyst models by decreasing the over prediction percentage from 2.9% to 1.3%. The second conclusion that can thus be drawn is that when looking to reduce the overall variations seen in models throughout the year, a

developed hybrid model that uses the months of lowest variability of multiple models can result in a highly accurate irradiance model on both the hour to hour POA irradiance basis as well as annual POA insolation predictions.

4.2 Temperature Model Validations

The second most important feature when performing performance analysis on PV module(s)/arrays/systems is to have an accurate measurement of operating temperature of the PV module(s) that are being analyzed. As was done with the irradiance models in the previous section, measured data was compared to calculated data from different temperature models. As was previously discussed in an earlier chapter, the measured data was collected from a commercial PV system in which all temperatures were averaged together to give one overall operational temperature of the system. Due to a lack of in field measured data, the meteorological and GHI data was only validated using data obtained by use of SolarAnywhere. The results given are thus based on the temperature model that most accurately reproduced the measured onsite measured module temperatures.

The model that was shown to have the smallest RMSE and NRMSE values was again assumed to be the best model for use of predicting operating PV module temperatures using satellite based data. This is shown in Figures 19 and 20 below.

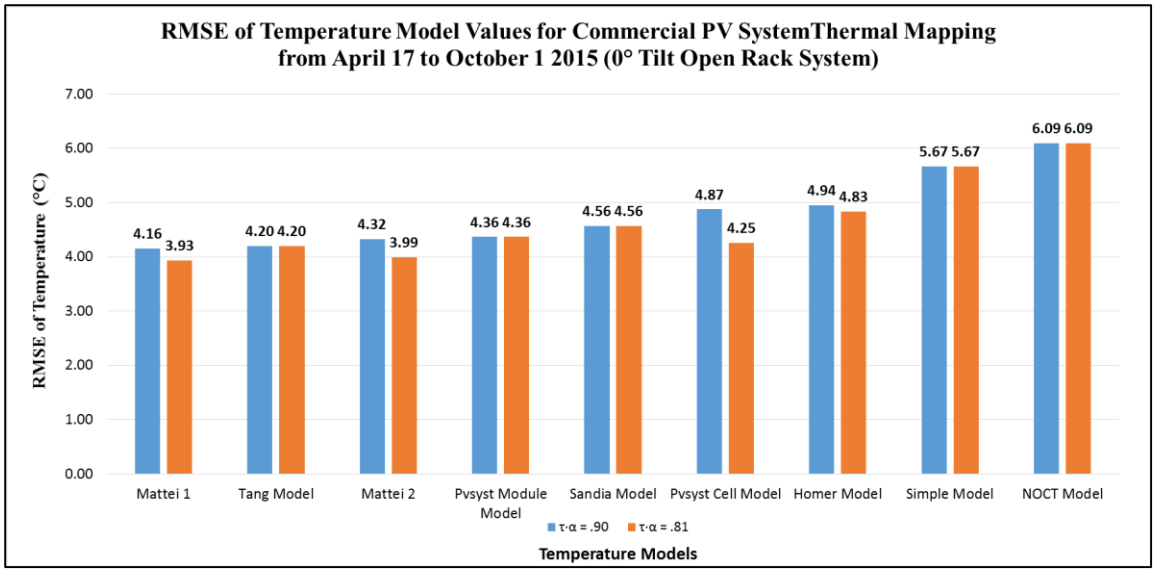

Fig. 19. RMSE Values of Thermal Models with Coefficient values of the Transmittance of the System Times the Absorption Coefficient of the PV Module ($\tau \cdot \alpha$) Set to Either 0.90 (Blue Bars) or 0.81 (Orange Bars).

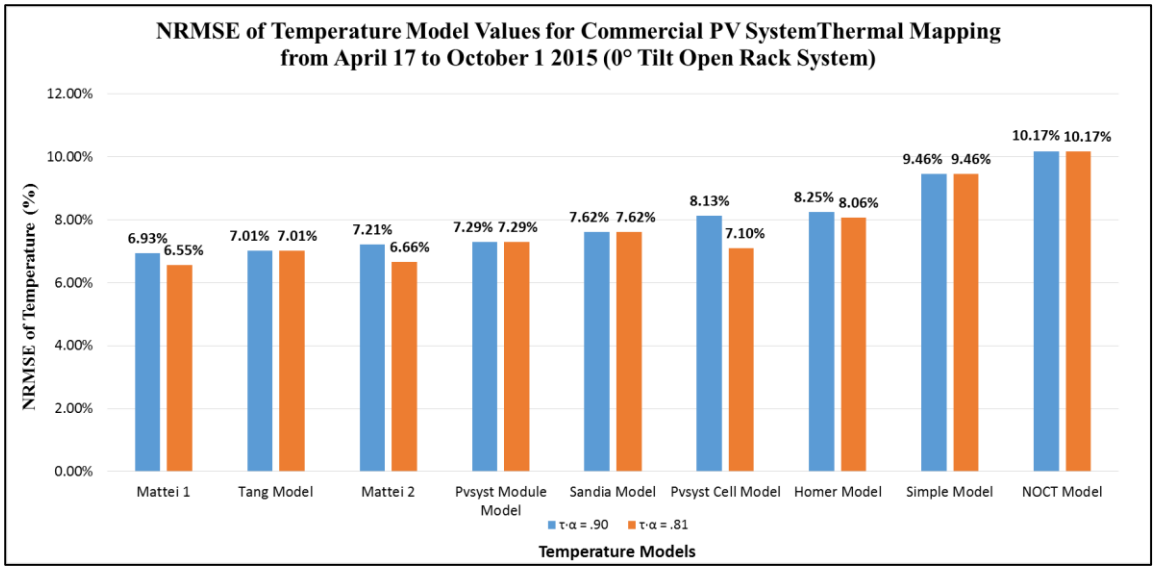

Fig. 20. NRMSE Values of Thermal Models with Coefficient Values of the Transmittance of the System Times the Absorption Coefficient of the PV Module ($\tau \cdot \alpha$) Set to Either 0.90 (Blue Bars) or 0.81 (Orange Bars).

As it can be seen on the above graphs, some models (Mattei 1. Mattei 2, PVsyst Cell Model, and Homer Model) use two coefficients identified as the transmittance of system (τ) and the absorption coefficient of the PV module (α). These two coefficients are multiplied to generate a constant multiplier. This constant multiplier is generally set to 0.9 [4], but was shown to be optimized to 0.81 by Mattei [12]. Because of this, all models were evaluated using both values to see the results. It is to be noted that the PVsyst models used the values given by the software for the constant heat transfer coefficient (U_0) and convective heat transfer coefficient (U_1) of 25.0 W/m^2K and 1.2 W/m^2sK, respectively, regardless of which constant multiplier value (0.90 or 0.81) was used.

The resulting conclusion from the graphs above indicate that the temperature model designated as Mattei 1, produces the most accurate prediction of operating module temperatures. This model was consistently the best model regardless of whether or not the constant multiplier was set to 0.90 or 0.81. The interesting thing to note is that the majority of the temperature models were shown to all be close to one another. Another note that can be made is some models tended to over predict the operating temperature of a PV module. Since the performance of a PV module is inversely proportional to the operating temperature, this results in performance models that may slightly under predict the actual amount of energy that is being produced depending on the thermal model that was used.

When looking at which model most accurately predicts the in-field measurement conditions, model that perfectly predicts the measured values would produce an R^2-value

equal to 1.00 when predicted values are plotted against measured values. The results of this plot are shown in Figure 21.

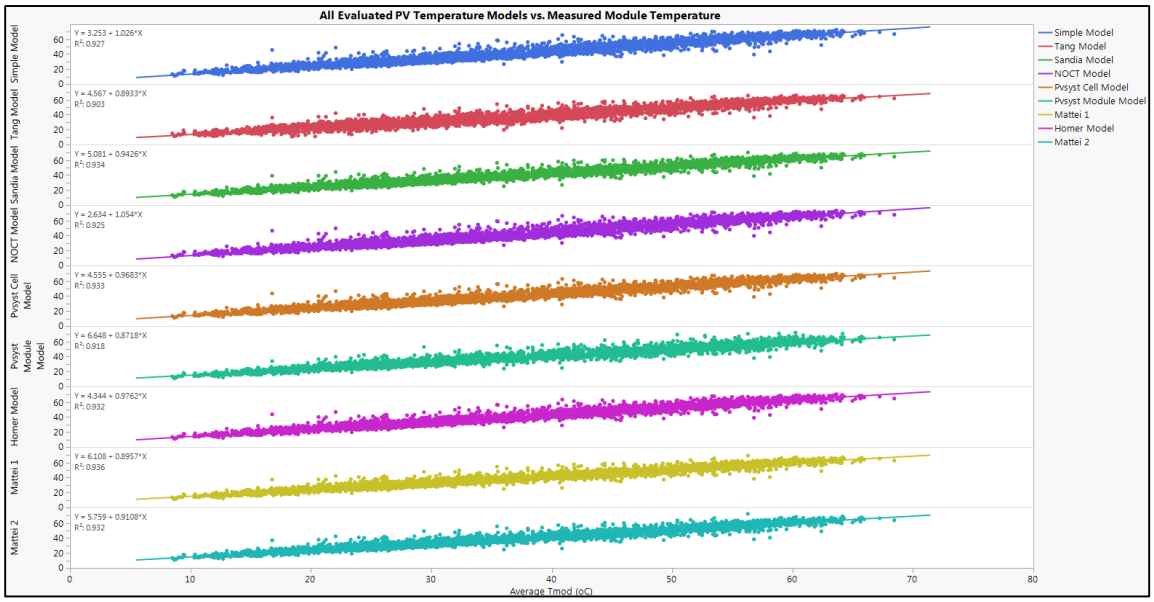

Fig. 21. Correlation of Predicted Module Temperature for All Thermal Models Compared to Actual Measured Module Temperature.

The above graph shows that again, while Mattei 1 was the model that most correlated with the measured temperature values, all other models still had a very high correlation of greater than 90%. This means that for quick operating temperature calculations, the Simple Model method, which only needs ambient temperature and POA irradiance, can be used. For high accuracy predictions though, for things such degradation rate calculation and large scale energy generation predictions, more complicated models such as Mattei 1, PVsyst, and Sandia models need to be used. As can be concluded from the analysis performed in this section, the thermal model that gave most accurate prediction of operating module temperature for the hot-dry climate of Arizona was that of the Mattei 1 model, based on the 7 months of available data.

4.3 Performance Validation

The degradation rate, and thus the resulting trend of degradation, is calculated for 38 commercial PV plants in the Phoenix-Metro area of Arizona. Because of this, it is critical to know whether the calculated degradation rates are accurate to what the modules are actually experiencing. In order to validate the process, the degradation rate found through in-field IV measurements as reported by [6] was used as the validation parameter. This degradation rate should be identical to all methods of performance analysis (PR, PI, and kWh) that are performed in this thesis. The system used to validate all performance models was chosen due to the fact the system was only unavailable for 59 days of the total 3,431 days the system was evaluated for. The graph below shows the availability of the system with any down times resulting in a break in the bar chart (white spaces).

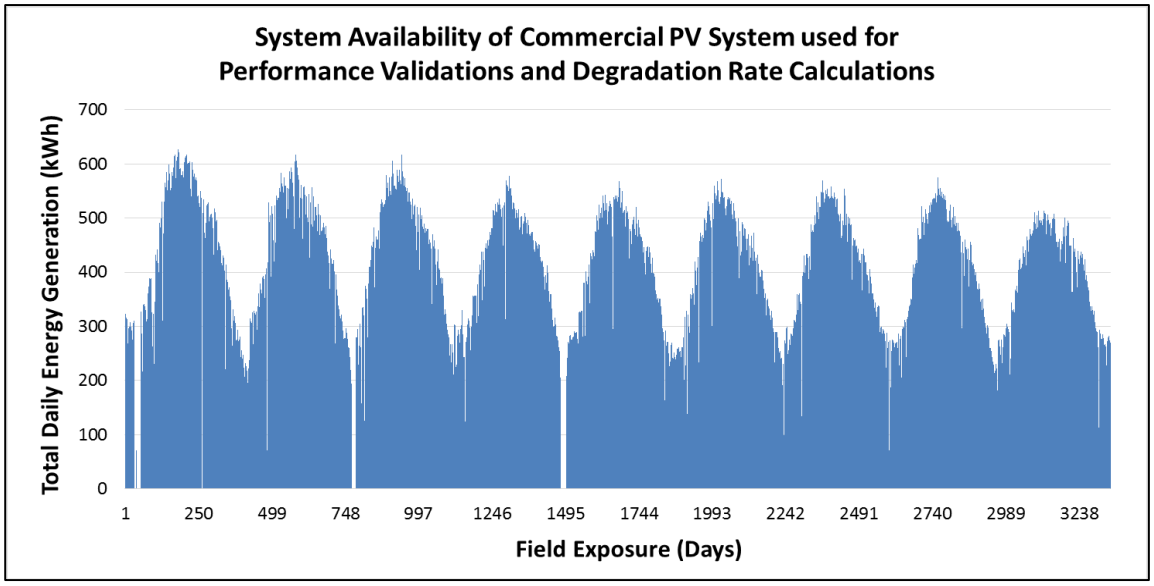

Fig. 22. System Availability Check of Commercial PV System Used for Performance Validations and Degradation Rate Calculations.

4.3.1 Performance Ratio (PR) Validation

As stated earlier, the determination of the performance ratio (PR) was done per the IEC 61724 standard. This means that the expected energy production of the system is only corrected for POA irradiance and not for any other system losses. In order to accurately calculate the degradation rate of the PV system based on PR, the steps as discussed in the methodology section were followed. This first involved calculating the expected amount of energy to be produced from the system based on the POA irradiance. The performance ratio was then calculated for 365 days every year and then filtered for any outliers. The resulting days were then evaluated based on a month to month basis. To determine the typical daily performance ratio of a particular month, the median data point of the filtered data set was taken. This was done for every year where a particular month had measured data. A plot of these values is shown below in Figure 23.

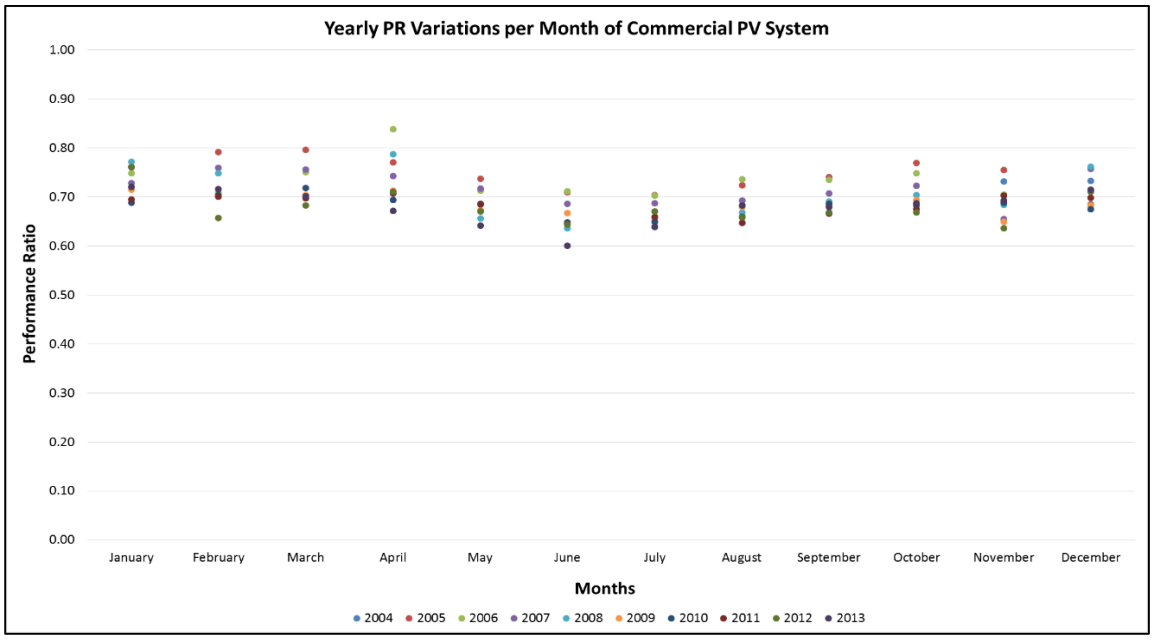

Fig. 23. Typical Monthly PR Values for 10 Year Old Commercial PV System.

From the plot, it is noticeable that the PR of the summer months (May – August) typically have a lower value than those of the remaining months. This can be attributed to the fact that operating temperatures are not accounted for and in the hot-dry climate of Arizona, module operating temperatures can as high as 50°C on open rack systems. These high operating conditions are thus causing a severe loss in performance, this will be analyzed in more detail later on in the section. As can be seen the above plot each month has a total of 9 PR values (except for November and December that each have 10) that were calculated for each year of field exposure. The slope of these data points, for each month, were taken in order to calculate the degradation rate of the plant. This results in a final 12 degradation rates being calculated for the plant. The resulting degradation rates are shown in Table 12.

Monthly PR Degradation											
Month	**2004**	**2005**	**2006**	**2007**	**2008**	**2009**	**2010**	**2011**	**2012**	**2013**	**Degradation (%/yr)**
January		0.7737	0.7589	0.7358	0.7902	0.7173	0.6755	0.6959	0.7777	0.7233	-0.57%
February		0.8002	0.7076	0.7723	0.7458	0.6954	0.7031	0.7082	0.6376	0.7162	-1.19%
March		0.7947	0.7566	0.7506	0.6896	0.6999	0.7160	0.6968	0.6687	0.6968	-1.23%
April		0.7636	0.8441	0.7418	0.7920	0.7039	0.6913	0.6967	0.6989	0.6687	-1.68%
May		0.7435	0.7110	0.7097	0.6581	0.6633	0.6801	0.6732	0.6709	0.6298	-1.04%
June		0.7213	0.7197	0.6836	0.6356	0.6679	0.6510	0.6558	0.6511	0.6026	-1.20%
July		0.7036	0.7047	0.6835	0.6356	0.6537	0.6456	0.6547	0.6682	0.6338	-0.73%
August		0.7296	0.7436	0.6926	0.6679	0.6811	0.6590	0.6448	0.6482	0.6779	-1.00%
September		0.7466	0.7407	0.7207	0.6919	0.6763	0.6819	0.6730	0.6638	0.6690	-1.08%
October		0.7837	0.7590	0.7143	0.7007	0.6824	0.6845	0.6705	0.6621	0.6851	-1.32%
November	0.7313	0.7598	0.7023	0.6496	0.6807	0.6465	0.6885	0.7004	0.6251	0.7014	-0.69%
December	0.7460	0.6799	0.6860	0.7600	0.7863	0.6755	0.6656	0.6965	0.7203	0.7198	-0.18%

Table 14. Table of Calculated PR for Each Month of System Operation and the Resulting Calculated Degradation Rate.

As was reported by Shrestha *et al.* the consistency of the irradiance that hits the Earth's surface for the Phoenix-Metro area has high and low variance months [6]. Due to this fact the 7 months with the least variation (April – October) were used in order to

calculate the actual degradation rate of the plant. The average of these seven months' degradation rates was then stated as being the systems true degradation rate. This results in the degradation rate of 1.15%/yr being calculated by use of PR values. The measured in-field IV degradation rate of this plant was stated to be 1.37%/yr. The under predicted PR degradation rate is similar to the trend reported by Shrestha *et al.* that showed the use of PR giving lower degradation rates than those measured by in-field IV curve measurements [6].

The results of this plant show that the PR method, PR values, and degradation rate calculation were all validated and can then be used for further plant evaluations. The results here show the typical trend of PR giving an under predication of module degradation by about 0.2%. The PR values were also shown to have a wide variance since the values only account for irradiance correction and no other performance criteria, such as temperature, module mismatch, and etc.

4.3.2 Performance Index (PI) Validation

The performance index of a system is the most accurate representation of the systems current performance and overall working health due to the fact that it accounts for all known losses. The performance index (PI) was used to correct for irradiance and other system losses (temperature, inverter efficiency, module mismatch, and wiring losses). Again as stated in an earlier chapter, the wiring losses was assumed to be a nominal 1.0% based on previous works [10]. The mismatch that can occur between modules was assumed to be a constant value of 3.3%. This value was calculated based on in-field IV measurements of multiple commercial PV power plants measured by ASU-

PRL. The string power and summed individual module powers were analyzed to see the mismatches that could occur. In order to make sure the value was as accurate as possible only the best performing strings and median performing strings were analyzed. The mismatch values were found to vary from as little as 0.84% to as much as 5.5%. The average of all calculated mismatch values was taken to be the typical mismatch values seen in the hot-dry climate of Arizona.

The steps used to calculate the degradation rate based on PI was carried out as described in the methodology. The operating temperature of the PV system was calculated by use of POA irradiance and meteorological data generated from SolarAnywhere. These values were used as the input to the Mattei 1 model, found to be the most accurate temperature model in an earlier section, to generate the operating temperature of the PV system. The efficiency of the inverter (found from manufacturer's datasheet), module mismatch, and wiring losses were also used to generate the predicted adjusted energy that should be produced by the system. As was done with the PR values, a table was generated for the typical PI value seen by the plant per month for each year of field exposure. The distribution of these values for each month can be seen in Figure 24 below.

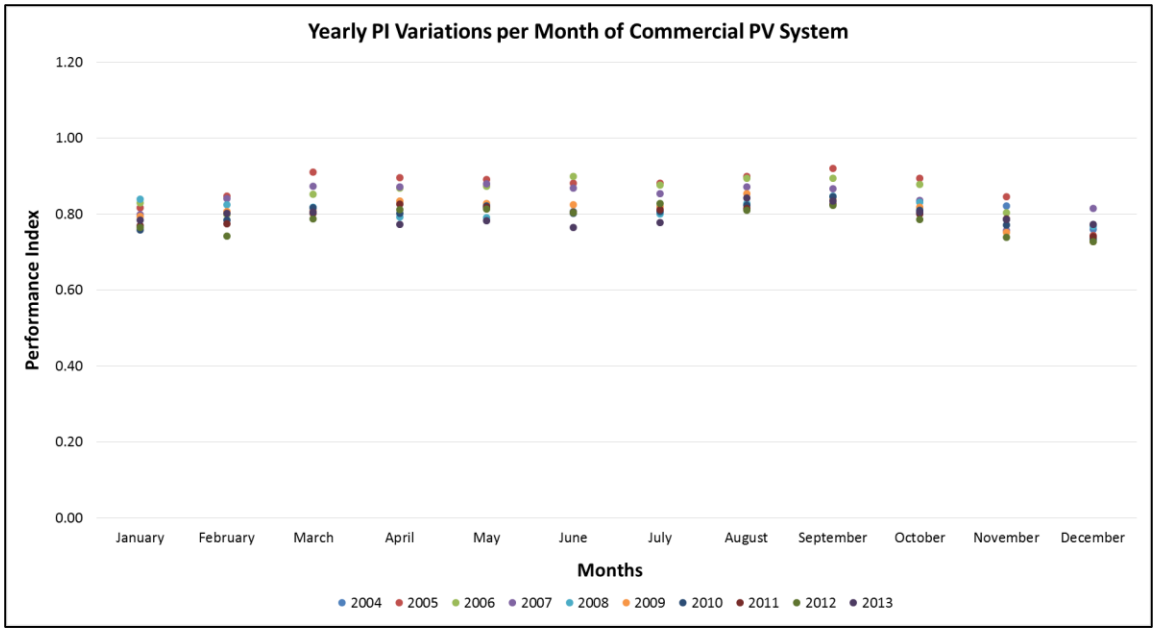

Fig. 24. Typical Monthly PI Values for 10 Year Old Commercial PV System.

When looking at the plot above, it is to first notice the difference in the trend of the PI values calculated for the summer months (May – August) as compared to those previously shown for PR. Since PI accounts for all known system losses, the high operating temperature of the PV systems is corrected for and thus results in a more uniform PI value from month to month instead the large variation that is seen in PR. The above plot shows that each month has a total of 9 PI values (except for November and December that each have 10) that were again calculated for each year of field exposure. The slope was once again take for these data points, for each month, and were again used to calculate the degradation rate of the plant. This results in a final 12 degradation rates being calculated for the plant, now based on PI values. The resulting degradation rates are shown in Table 15.

Monthly PI Degradation											
Month	2004	2005	2006	2007	2008	2009	2010	2011	2012	2013	Degradation (%/yr)
January		0.828605	0.83311	0.79923	0.8597	0.797777	0.7471	0.765698	0.757136	0.780963	-1.00%
February		0.856074	0.79916	0.856101	0.832131	0.810133	0.786821	0.783089	0.726636	0.797259	-1.07%
March		0.927003	0.868458	0.871282	0.810118	0.801344	0.807692	0.798585	0.778127	0.807002	-1.50%
April		0.896946	0.867588	0.870853	0.792075	0.831282	0.798425	0.815906	0.791167	0.771245	-1.39%
May		0.891603	0.869959	0.878712	0.781336	0.824748	0.817185	0.81388	0.810917	0.76881	-1.27%
June		0.886403	0.909258	0.865197	0.811285	0.826142	0.802574	0.807014	0.808834	0.765333	-1.52%
July		0.886772	0.884735	0.859829	0.79468	0.825672	0.798714	0.816546	0.823379	0.769625	-1.23%
August		0.90908	0.918926	0.874139	0.829284	0.853667	0.829696	0.817352	0.805208	0.835394	-1.25%
September		0.934142	0.899499	0.870947	0.847068	0.830249	0.844474	0.831786	0.818266	0.829571	-1.24%
October		0.909346	0.883253	0.833486	0.830805	0.811641	0.802992	0.800237	0.782851	0.798894	-1.40%
November	0.825406	0.851101	0.804735	0.741769	0.781439	0.747931	0.770626	0.787819	0.73512	0.790623	-0.70%
December	0.75912	0.746006	0.748784	0.822565	0.791249	0.712192	0.731649	0.763629	0.716782	0.780355	-0.18%

Table 15. Table of Calculated PI Values for Each Month of System Operation and the Resulting Calculated Degradation Rate.

The same seven months, when the irradiance variations are the lowest, were again averaged to find the degradation rate of the PV system. This value was found to be 1.33%/yr. The calculated value is nearly identical to that of the measured IV curve degradation rate of 1.37%/yr. This value shows that the losses accounted for in the PI calculation are good representations of the general losses seen by PV power plants in the hot-dry climate of Arizona.

The results of this plant show that the PI method, PI values, and degradation rate calculation were all validated and can then be used for further plant evaluations. The results here show the how accurate the degradation rate calculated from PI is compared to the measured in-field IV degradation rate. The PI degradation rate was found to be only 0.02%/yr less than the measured value, well within the percent error that could occur from instruments used in field. The PI values were also shown to have a lesser variance than those of PR since the calculated PI values account for all losses experienced by the PV power plant.

4.3.3 kilowatt-hour (kWh) Degradation Validation

The newly developed statistical method for calculating the degradation rate is analyzed in this section. The values obtained here were calculated after following the Because of the newer method, the calculated kWh based degradation rates for 4 commercial PV power plants are compared to the measured degradation rates obtained by ASU-PRL [6,13]. In the figure below, the calculate kWh degradation rates are shown against the measured values.

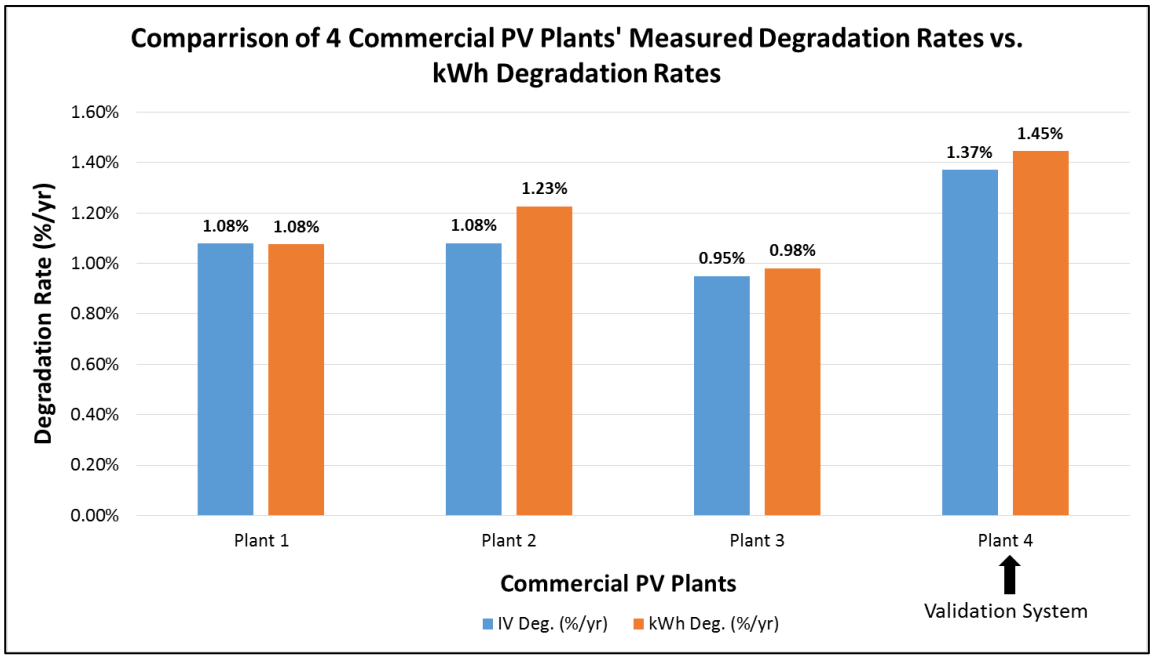

Fig. 25. Comparison of Measured IV Degradation Rates and Calculated kWh Degradation Rates for 4 Commercial PV Power Plants in the Phoenix-Metro Area of Arizona.

The above graph shows that the overall accuracy of the newly developed model is on par, if not better than, the degradation rate that can be calculated by using PR values. Unlike PR that generally under predicts the real degradation rate observed by a PV power

plant, the newly developed kWh degradation method seems to slightly over predict the actual degradation rate. The benefit of this new method though is that it is statistically based, with not manual data filtration necessary, and it also does not involve any type of modeled data or measured data, except inverter kWh values and date/time.

When performing the kWh degradation analysis, it was found that the needed filters used for removing outlier data points varied by the age of the plant. For new plants, less than 5 years of age, the degradation rates were filtered for a wider array of values, between -3.0%/yr and 3.0%/yr. For the older plants, it was found that a filter of -3.0%/yr and 1.0%/yr were applied.

From the results shown in this section, the use of raw kWh data for degradation rate calculation is highly accurate when based on the calculated statistical values. The values used in the statistical analysis have no set statistical reason for being applied, other than it was discovered to give similar, if not identical, degradation rates to those of measured in-field IV curved degradation rates measured by ASU-PRL. While the degradation rates calculated from this new kWh method are accurate, without having any other system performance data, it is not as useful as PR or PI when wanting/needing to analyze other system performance factors such as the amount of energy loss to temperature effects, the rate of soiling, and etc.

The filtering of the kWh data can also be represented when looking at the energy generation of the resulting Julian Days that were used to calculate the degradation rate. This new statistical method shows an ability to remove a large amount of outliers in order

to develop an accurate degradation rate. A comparison of the unfiltered data and resulting filtered data can be seen in Figures 26 – 29.

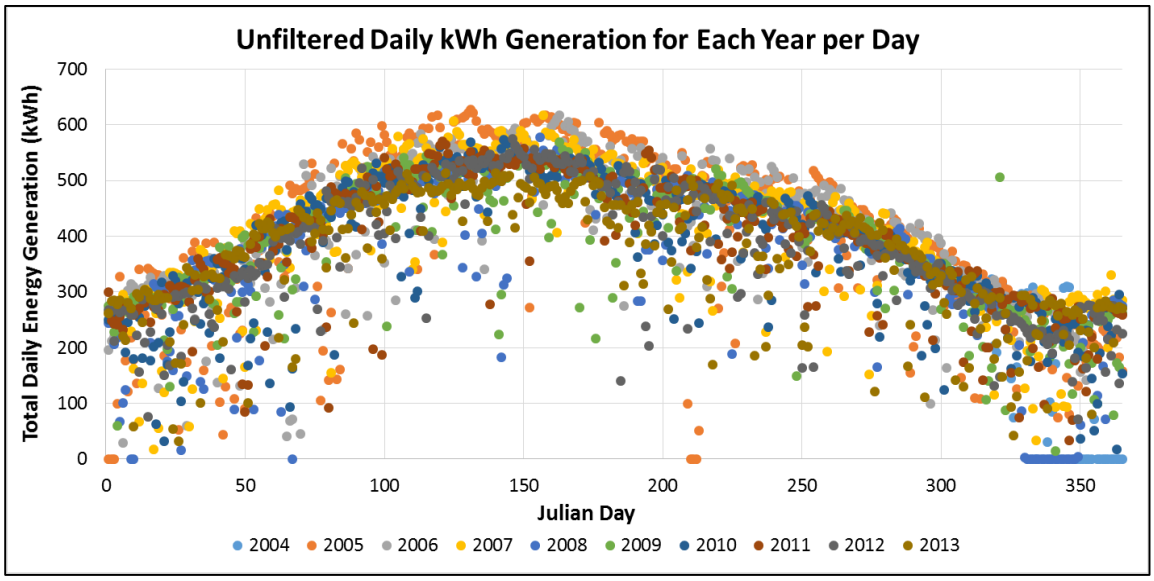

Fig. 26. Unfiltered Daily kWh Generation for Each Year per Julian Day.

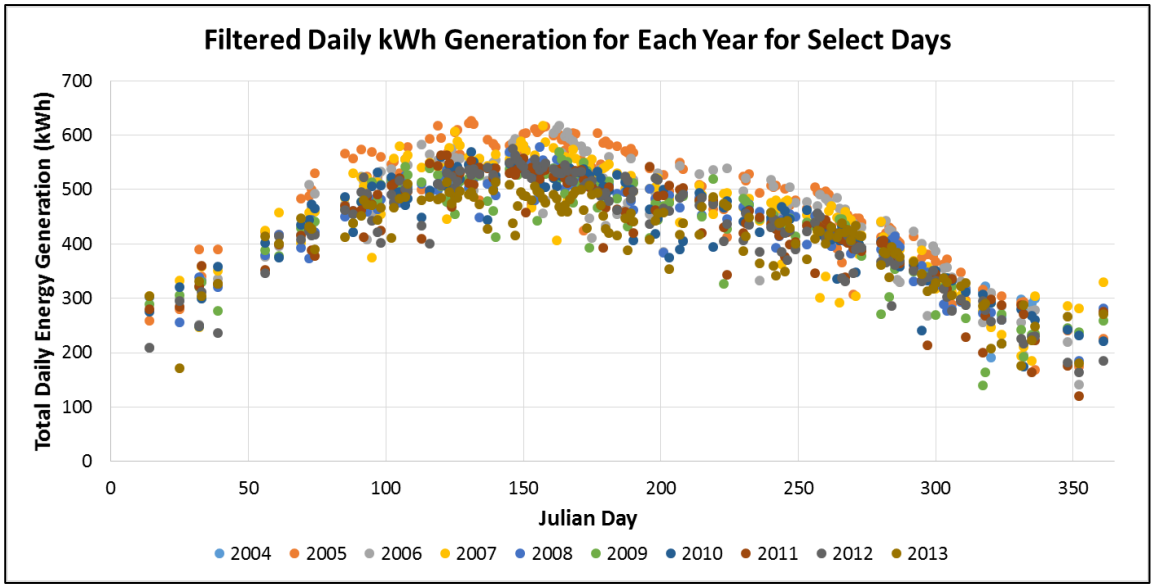

Fig. 27. Filtered Daily kWh Generation for Each Year per Selected Julian Day Used for Degradation Rate Calculation.

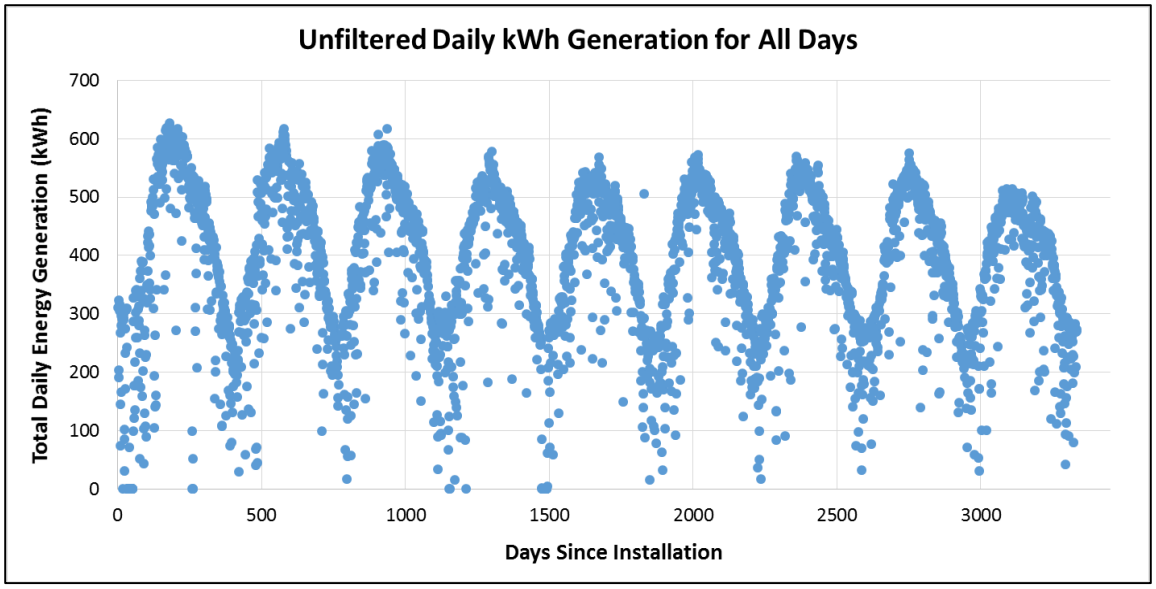

Fig. 28. Unfiltered Daily kWh Generation for All Days from First Measured Day to Last Measured Day.

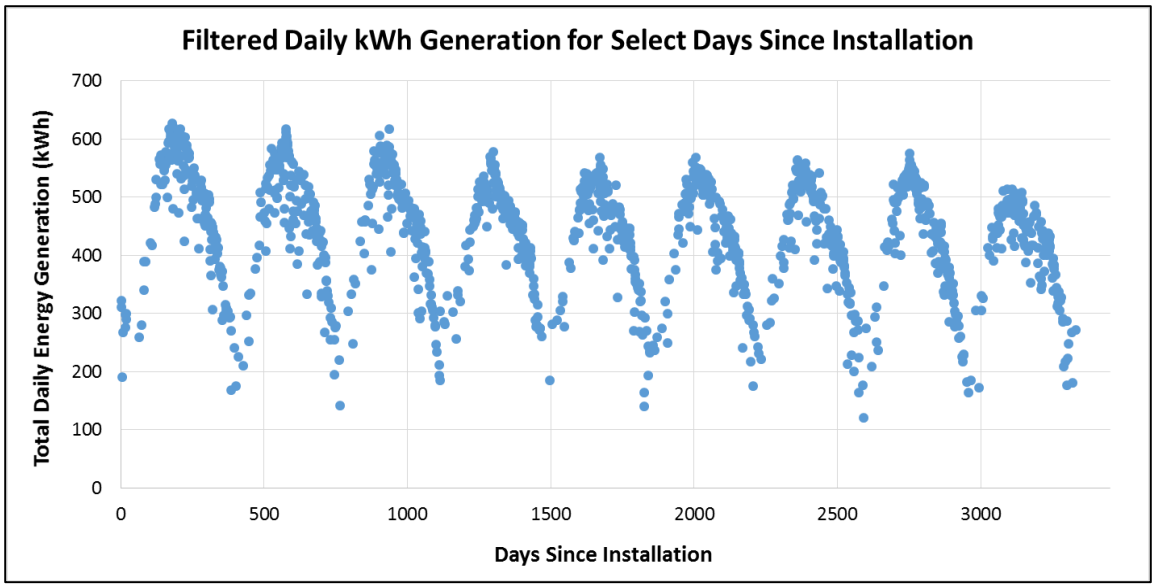

Fig. 29. Filtered Daily kWh Generation from First Measured Day to Last Measured Day Based on Selected Days Used for Degradation Rate Calculation.

4.3.4 Analysis of System Operating Conditions

When calculating the performance of a system using PI, it becomes possible to also look at the affects that other conditions, such as system and temperature losses, having on the performance and the amount of energy that is being lost due to these factors. As stated earlier, system losses are typically assumed to be a constant nominal value since the only component that really degrades is the PV modules that comprise the PV power plant. Looking at the amount of energy loss due to temperature can give system owners a better understanding of the amount and variation of lost energy production that can occur from month to month and year to year. This can be seen in Figure 30 below.

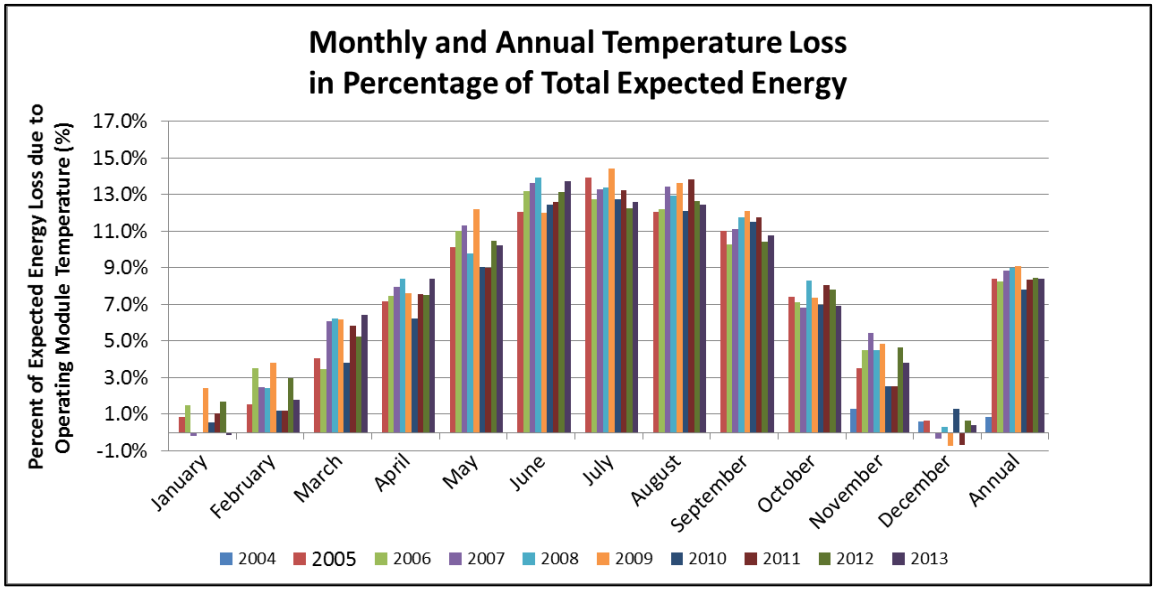

Fig. 30. Percent of Expected Energy Production Lost to Thermal Losses Based on Monthly and Yearly Basis for a 10 Year Old Commercial Rooftop PV System.

The above graph gives a very distinct picture of the amount of energy that this system loses on a yearly basis and the amount of very that can occur between the losses seen in the summer months and those seen in the winter months. On an annual basis (excluding the first year where the system was only installed for two months) this system averages a loss of 8.5% of the expected energy production due solely to performance losses from temperature. This value is shown to be rather consistent since there is little variation from the smallest annul value, 7.80%, and the highest annual loss of 9.08%. A simple reason for this variation could be that the average annual ambient temperatures were respectively lower and higher, resulting in the operating temperatures of the PV modules also being lower or higher than the average. One can also look at break down of loss factors and actual performance of the system by looking at the percent contribution of each individual loss and generation component as seen in Figure 31.

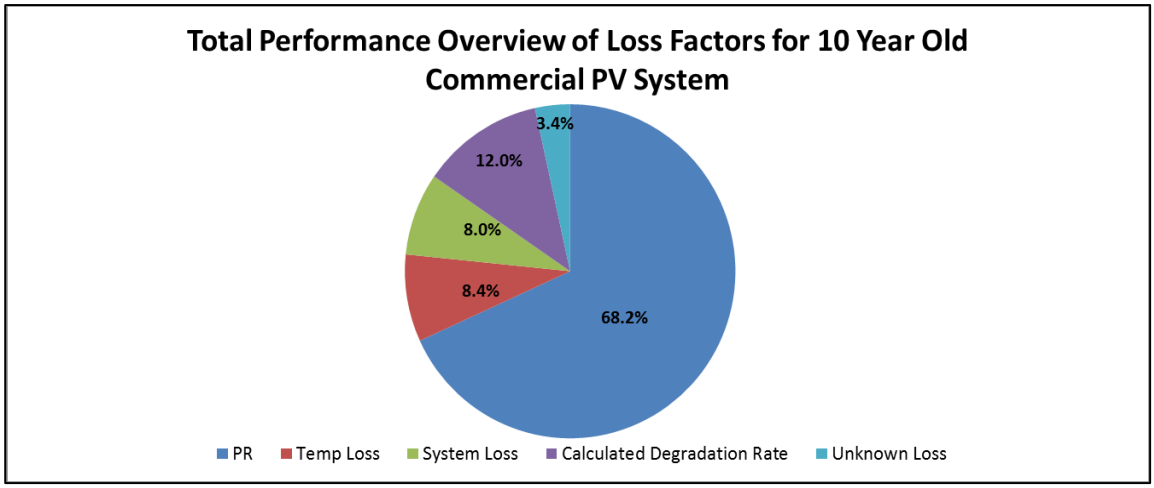

Fig. 31. Performance Overview of Loss Factors for a 10 Year Old Commercial Rooftop PV System in the Phoenix-Metro Area and Hot-Dry Climate of Arizona.

From the above pie chart, it becomes easily visible that the overall assumptions of system losses and calculated thermal losses accurately predict the actual conditions found for the power plant. When using the calculated degradation rate, which was already verified to be nearly identical to the measured IV curve degradation rate, it can be seen that the degradation rate of the modules accounts for 12.0% of the overall losses experienced by the system since installation. The system losses, accumulating of inverter efficiency, module mismatch, and wiring losses, is found to be a total of 8.0% of the overall losses of the system. As stated earlier the amount of energy lost to just operating temperatures is 8.4% of the total expected energy (this is slightly lower than the average annual values since it also includes the first two months of installation in the first year). The unknown losses, accounting for 3.4% of the total expect energy, can be attributed to a single or combination of factors such as soiling, under assumption of wiring losses, under assumption of module mismatch, and/or an over assumption on the efficiency of the inverter.

The results presented in this section show the usage of calculated and/or assumed operating parameters of a PV system in order to develop an overall picture of the affects these parameters are having on the system output. It is important to note the large amount of fluctuation that can occur throughout the year for the amount of energy lost to operating temperatures of the PV modules within the system. This large fluctuation shows that when installing a system, it is important for PV system designers and owners to account for this variance and that on average, an open rack rooftop system will lose 8.5% of the expected energy production per year to thermal losses alone in the hot-dry

climate of Arizona. This section also shows the validation of the assumed wiring losses and module mismatch factors as being reasonable assumptions that can made for use in predicting the adjusted energy expected to be produced by a PV system in the Phoenix-Metro area of Arizona.

4.4 Degradation Rate and Linearity Analysis

The analysis and degradation rates of 38 PV systems are analyzed to determine the trend, whether linear or not, of degradation seen by crystalline silicon PV power plants in the hot-dry climate of Arizona. In order to develop these degradation rates, the same performance analysis based on (PR, PI, and kWh) were used to look at the variances that could occur. All systems had the same analysis done as that shown in the previous sections and can be found in Appendix A. The age of the power plants evaluated range from 2 to 16 years of age with the majority of the systems being less than 5 years of age. The degradation trend of all PV power plants based on PR, PI, and kWh, can be seen in Figures 32 – 34, respectively.

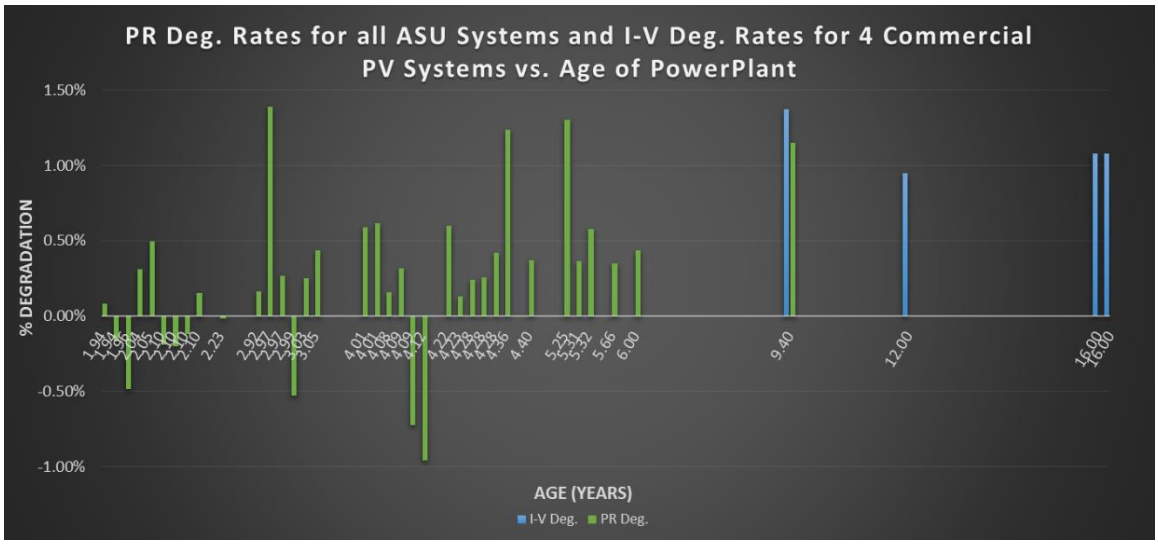

Fig. 32. Calculated Degradation Rates for All 38 Evaluated ASU and Commercial Systems Based on PR and In-Field IV Curve Measurements, Where Available.

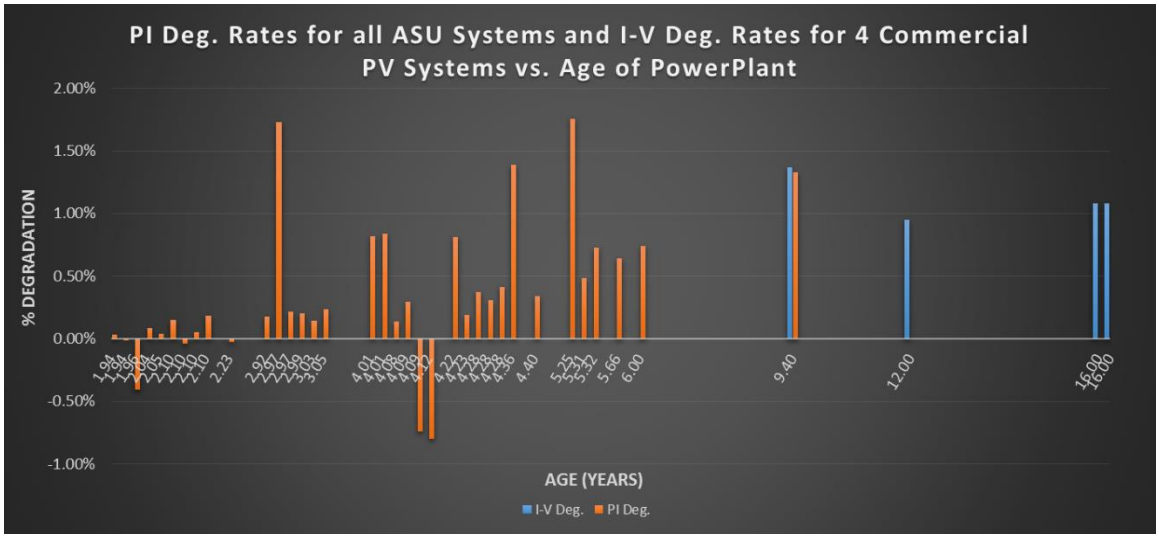

Fig. 33. Calculated Degradation Rates for All 38 Evaluated ASU and Commercial Systems Based on PI and In-Field IV Curve Measurements, Where Available.

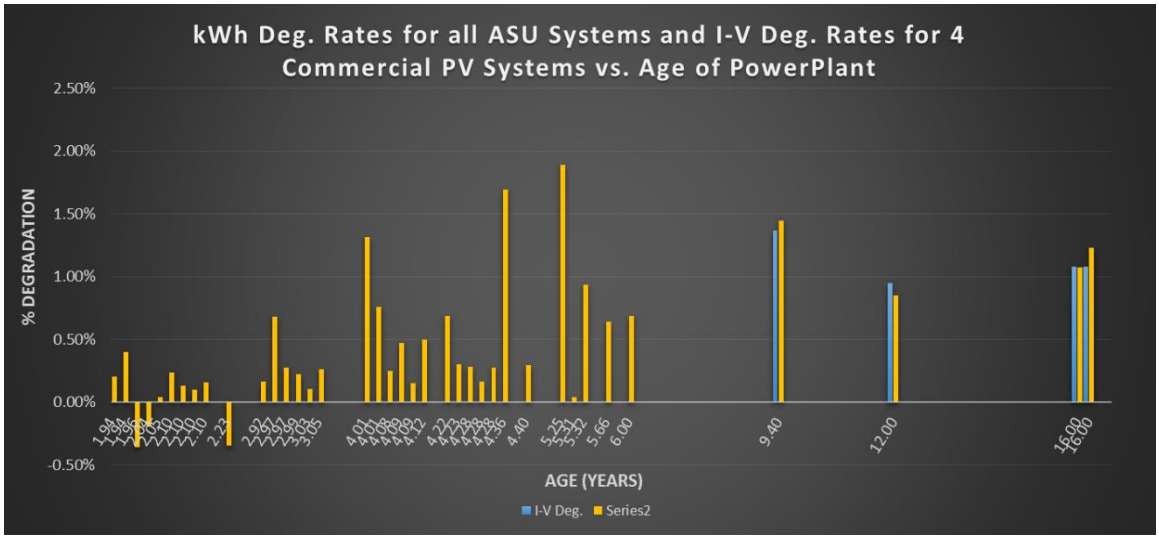

Fig. 34. Calculated Degradation Rates for All 38 Evaluated ASU and Commercial Systems Based on kWh and In-Field IV Curve Measurements, Where Available.

When looking at the above graphs, it is easy to see that there are some systems in which the degradation rates are shown to be excessively high or even negative (indicating increased performance). High degradation rates can be attributed to site specific issues that may occur such as shading losses, blown fuses, heavy soil deposition, and etc. When looking at the hourly kW generation, it is easy to see that there is a large amount of losses that are not typical of crystalline silicon based PV technologies, as shown in Figure 35. For systems that are less than 3 years old, they may show a negative degradation that indicates an increasing performance trend. This is not possible, but due to year to year variations, it is possible that the second year could produce slightly more energy than the first year and since there is smaller number of data points available, this trend can be exaggerated. When looking at the degradation rates report by the PI calculated method, a few of the older ASU systems, around 4 years of age, also show an increase in system performance. This again is easy to explain when looking at the hourly kW generation of

the system since there is a trend of high degradation rates and then a sudden increase in performance after a few years. This could be indicative of either a modules that were exceeding the manufactures degradation rate warranty and were replaced, inverters that were down for long periods of time before either being fixed or replaced, and any other system performance factor that was corrected at a later date. An example of one these systems is shown in Figure 36.

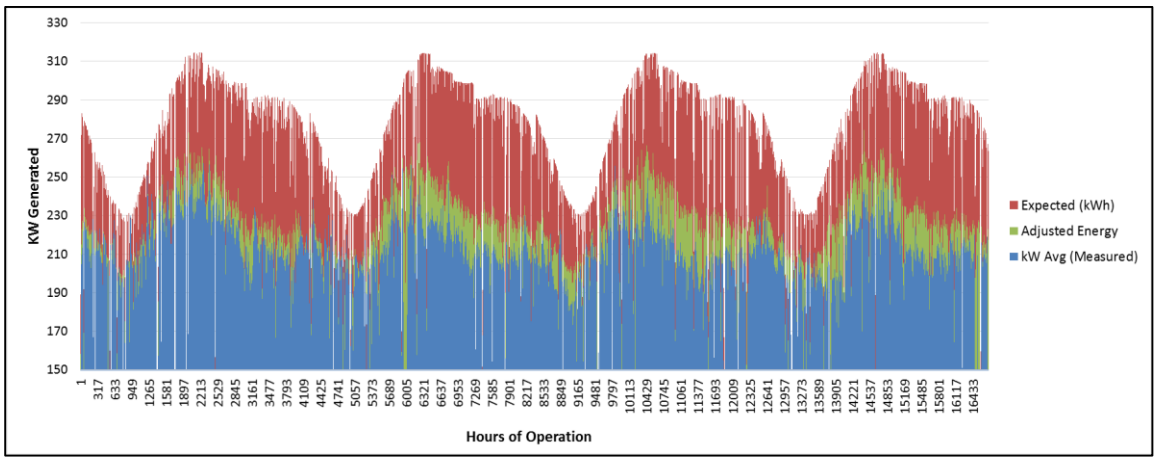

Fig. 35. Hourly kWh Generation for One ASU System That Shows a High Amount of Degradation.

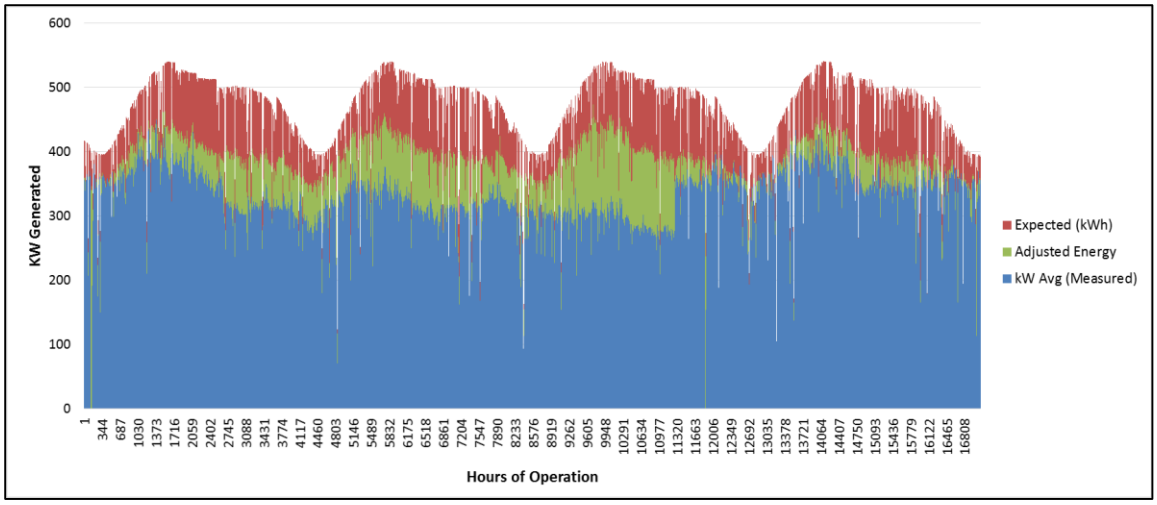

Fig. 36. Hourly kWh Generation for One ASU System That Shows a High Amount of Degradation and Then a Sudden Increase in Performance in the Later Years.

In the above figures, the ratio between either the measured values (blue) and expected energy (red) will yield the PR or measured values and adjusted expected energy (green) will yield the PI. Since the expected energy for either PR or PI will always remain constant, one show expect for the difference between the initial values to be very little and gradually increase over time, such as that of system used for performance validation in Figure 37.

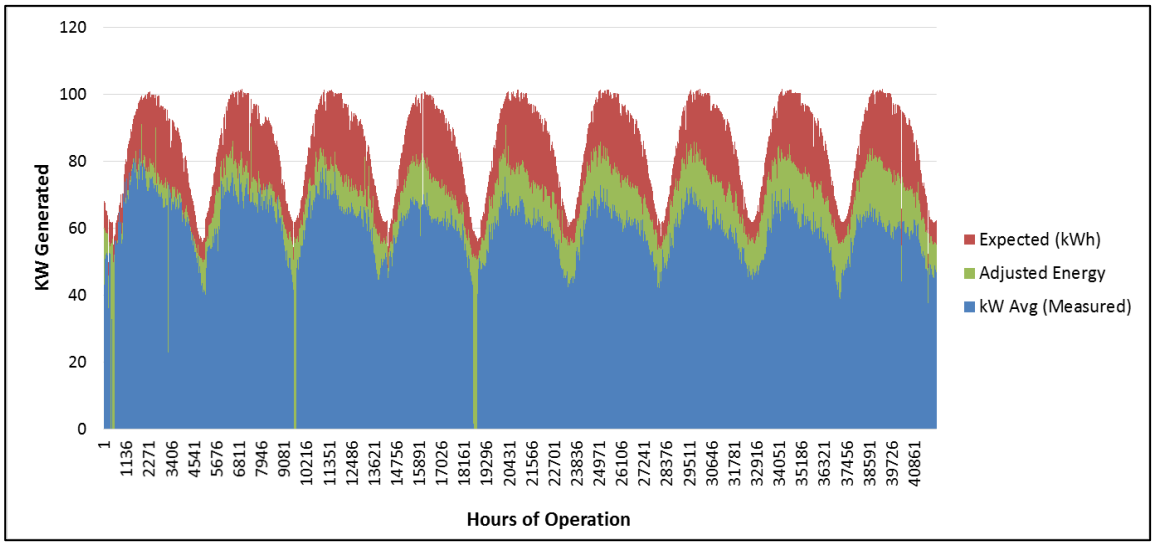

Fig. 37. Hourly kWh Generation for a Commercial PV System Used in Performance Validation That Shows a Gradual Increase in the Difference Between the Measured Values and Expected or Adjusted Energy Values.

Another issue that was also noticed is that some systems had a high DC to AC ratio resulting in inverter clipping. This poses a challenge for looking at the actual degradation rates seen by a system since the output of the plant will not show a decrease in performance until the PV modules have degraded to a level where the inverter size is no longer undersized as compared the amount of energy being produced. An example of inverter clipping is shown in Figure 38 below.

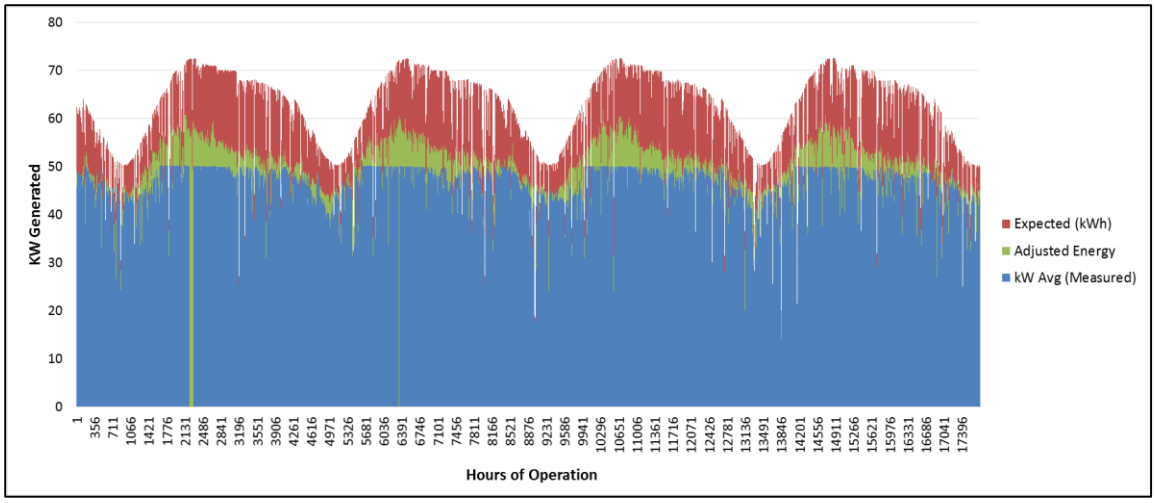

Fig. 38. Hourly kWh Generation for One ASU System That Shows Inverter Clipping and thus the Unavailability of Looking at a Degradation Trend.

The systems that show unrealistic degradation rates due to either inverter clipping or other unknown issues were chosen to be removed since they would skew the trend of the data set. The list of all the systems and whether or not they were used in this analysis is shown in Table 14. The degradation rates of PR, PI, and kWh were then graphed again in order to develop a clearer analysis of the trend of degradation seen by multiple PV power plants in Arizona, as shown in Figures 39 – 41.

System Name	Age (Years)	DC System Size (kW)	Tilt(°)	Inverter Clipping?	PI Deg. Rate (%/yr)	Used for Analysis?
ASU-U	1.94	230.4	12	No	0.03%	Yes
ASU-AC	1.94	252.54	10	No	-0.02%	No
ASU-AH	1.96	86.22	5	No	-0.41%	No
ASU-X	2.04	250.56	10	No	0.08%	Yes
ASU-AF	2.05	310.32	8	No	0.04%	No
ASU-AA	2.10	204.6	10	No	0.15%	Yes
ASU-AB	2.10	224.4	10	No	-0.04%	No
ASU-Z	2.10	89.1	10	No	0.05%	Yes
ASU-R	2.10	66	12	Yes	0.18%	No
ASU-T	2.23	254.1	12	Yes	-0.03%	No
ASU-S	2.92	69.3	12	Yes	0.17%	No
ASU-J	2.97	214.86	20	No	1.73%	No
ASU-Y	2.97	138.6	10	Yes	0.22%	No
ASU-AE	2.99	246.06	10	No	0.21%	Yes
ASU-Q	3.03	65.82	12	Yes	0.15%	No
ASU-AD	3.05	166.38	10	Yes	0.23%	No
ASU-AG	4.01	2132.48	8	No	0.82%	No
ASU-L	4.01	705.6	20	Yes	0.83%	No
ASU-G	4.08	144.48	20	No	0.13%	Yes
ASU-E	4.09	57.12	20	No	0.29%	Yes
ASU-I	4.09	188.16	20	No	-0.74%	No
ASU-N	4.12	497.28	20	No	-0.80%	No
ASU-K	4.22	168	20	Yes	0.81%	No
ASU-B	4.23	63.84	20	Yes	0.19%	No
ASU-D	4.28	94.08	20	No	0.38%	Yes
ASU-H	4.28	64.68	20	No	0.30%	Yes
ASU-P	4.28	67.2	15	Yes	0.41%	No
ASU-F	4.36	94.08	20	No	1.39%	No
ASU-C	4.40	63.84	20	No	0.34%	Yes
ASU-G	5.25	289.8	20	No	1.76%	No
ASU-V	5.31	248.64	11	No	0.48%	No
ASU-M	5.32	141.12	20	No	0.73%	Yes
ASU-A	5.66	150.15	20	No	0.64%	Yes
ASU-O	6.00	23.1	20	No	0.74%	Yes
CT	9.40	97.2	5	No	1.33%	Yes
G	12.00	249.9	1-axis	No		Only for kWh analysis

BRO1	16.00	113.4	0	No		Only for kWh analysis
BRO2	16.00	113.4	0	No		Only for kWh analysis

Table 16. Filtration of Systems Used in This Analysis Based on Inverter Clipping, Unrealistic Degradation Rates, and Quality of Data Sets (Systems ASU-AF and ASU-V).

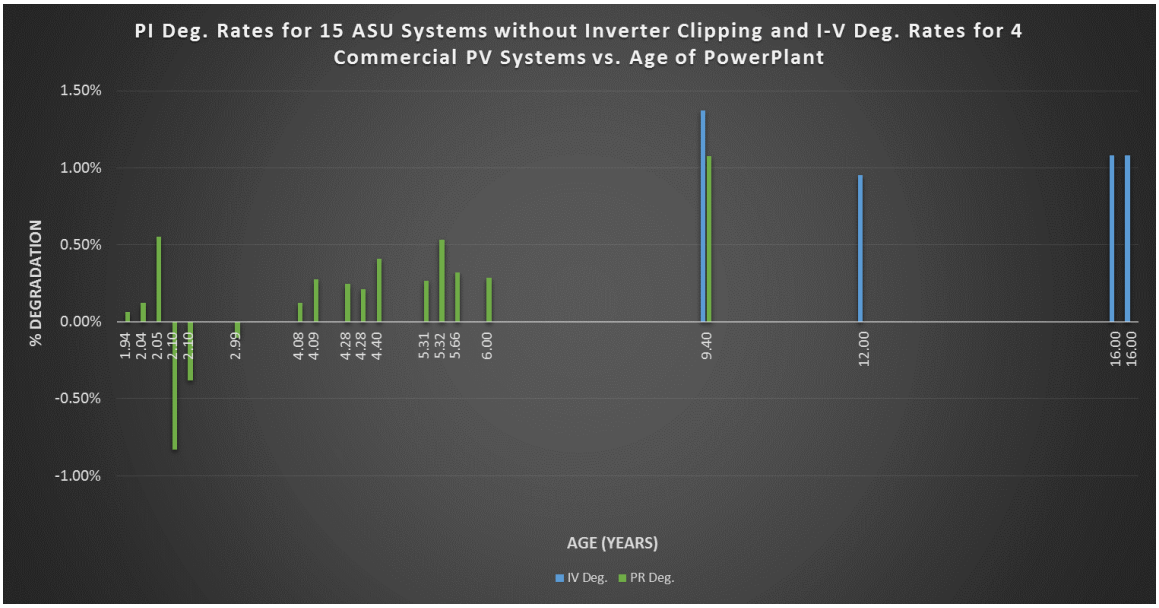

Fig. 39. Calculated Degradation Rates for All Filtered ASU and Commercial Systems Based on PR and In-Field IV Curve Measurements, Where Available.

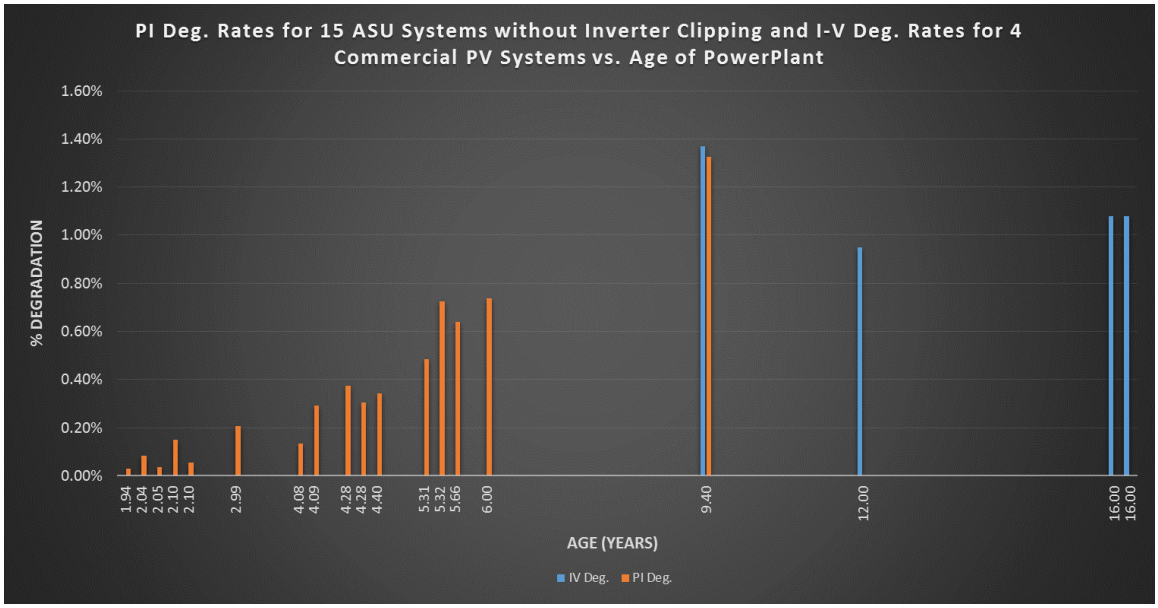

Fig. 40. Calculated Degradation Rates for All Filtered ASU and Commercial Systems Based on PI and In-Field IV Curve Measurements, Where Available.

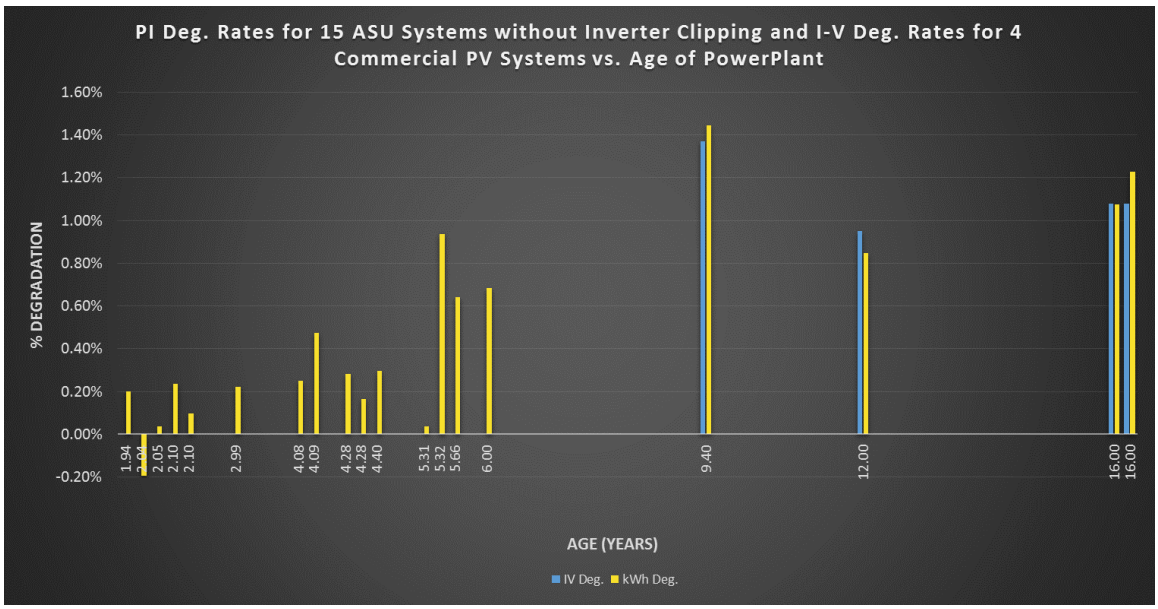

Fig. 41. Calculated Degradation Rates for All Filtered ASU and Commercial Systems Based on kWh and In-Field IV Curve Measurements, Where Available.

The resulting filtered degradation rates that are shown in the three graphs above show an overall trend of increasing degradation as systems age. As seen in the PR and kWh degradation graphs, there are still a few systems that show to have an increase in performance. This is likely due the small number of data points and robustness of the two methods in calculating system degradation rates. Without having the high accuracy of PI calculations, other various performance that can affect a PV system are exaggerated and thus affect the calculated degradation rates. This is why all degradation trend analysis is conducted on reported PI values since they have been validated to be the most accurate performance measurements without having in-field measured IV data.

Figure 40 is an interesting graph due to fact that if it is typically assumed that for all crystalline PV systems, the degradation is linear in nature. If this was the case, all lines would be around the same degradation rate, typically ~1.0%, no matter the age of the system. Since this is not the case, it could be construed that the degradation rates of crystalline silicon PV systems is not truly linear. To view this possibility in detail the, distribution of yearly PI for the evaluated PV power plants is analyzed. In order to view whether or not a system is linear, a minimum of 4 data points was determined to be needed since any systems less than 4 years of age would show a high linear correlation due to the lack of available data. This results in a total of 10 systems that can be evaluated for degradation trend analysis by use of PI. The figures below show the degradation trend for 4 of the 10 systems, both linear and non-linear, for all 12 months of PI values or for the 7 months of PI values used to calculate the reported degradation rates.

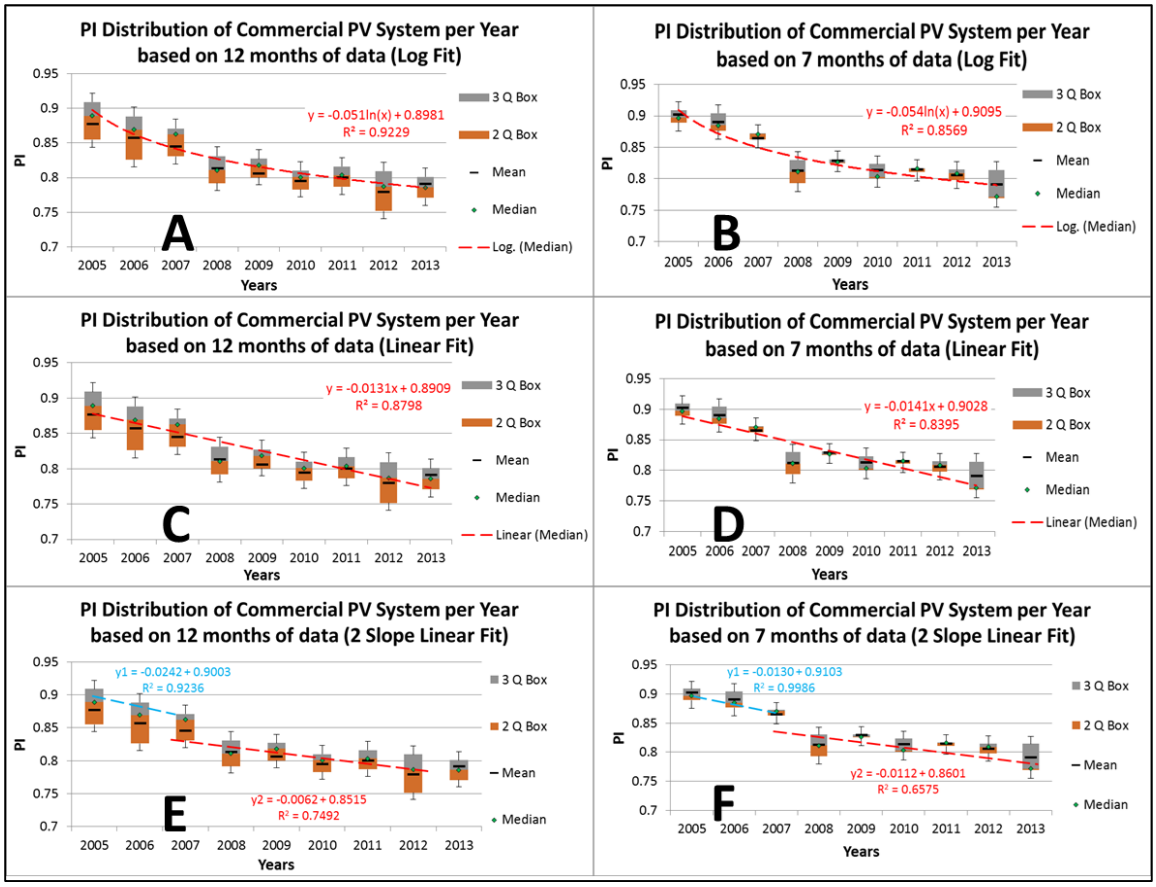

Fig. 42. Degradation Trend Analysis of Commercial PV system

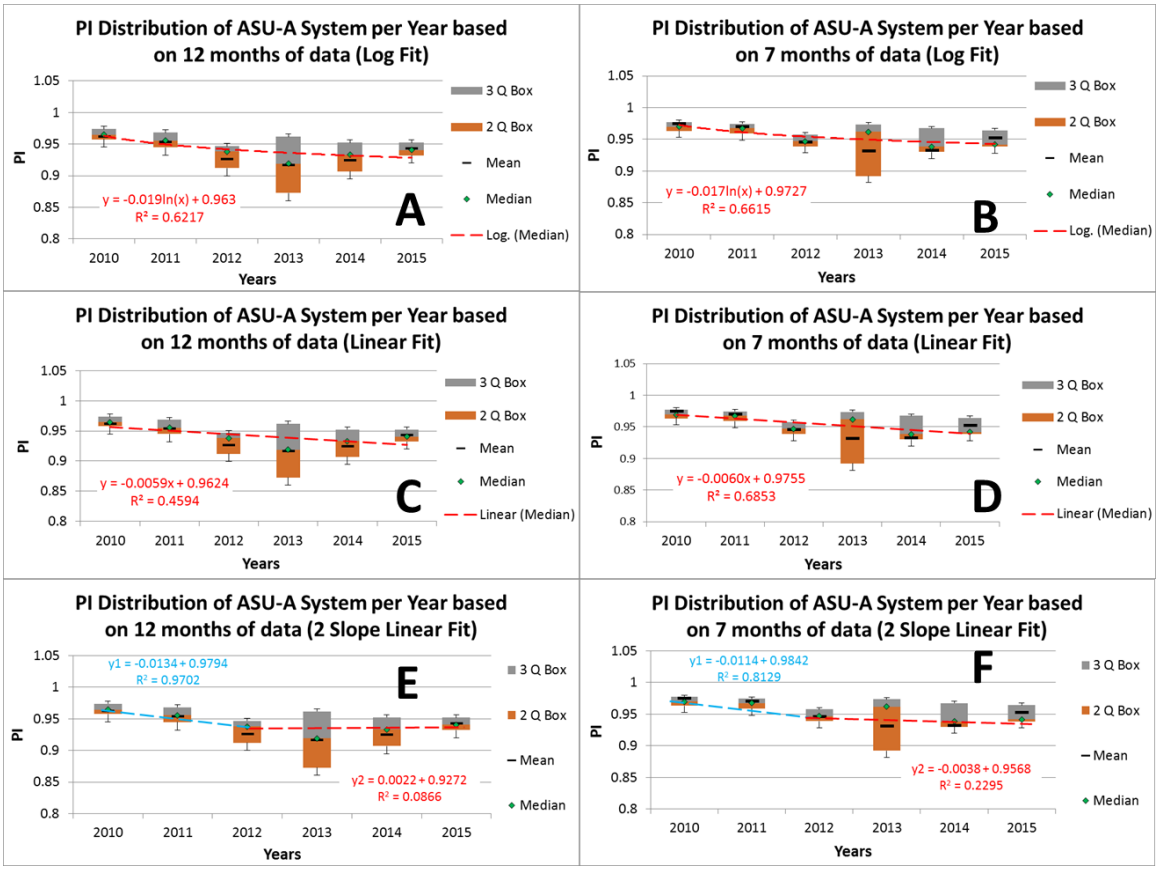

Fig. 43. Degradation Trend Analysis of ASU-A PV System

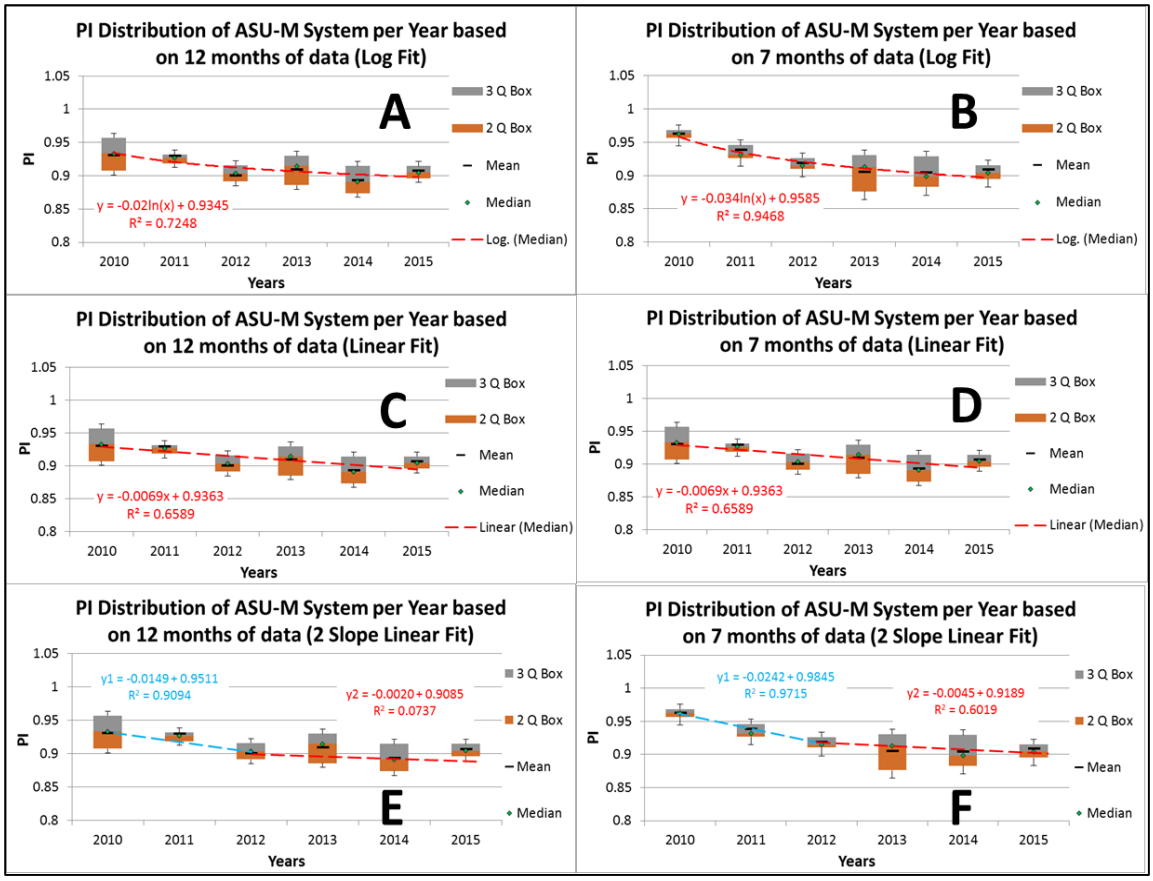

Fig. 44. Degradation Trend Analysis of ASU-M PV System

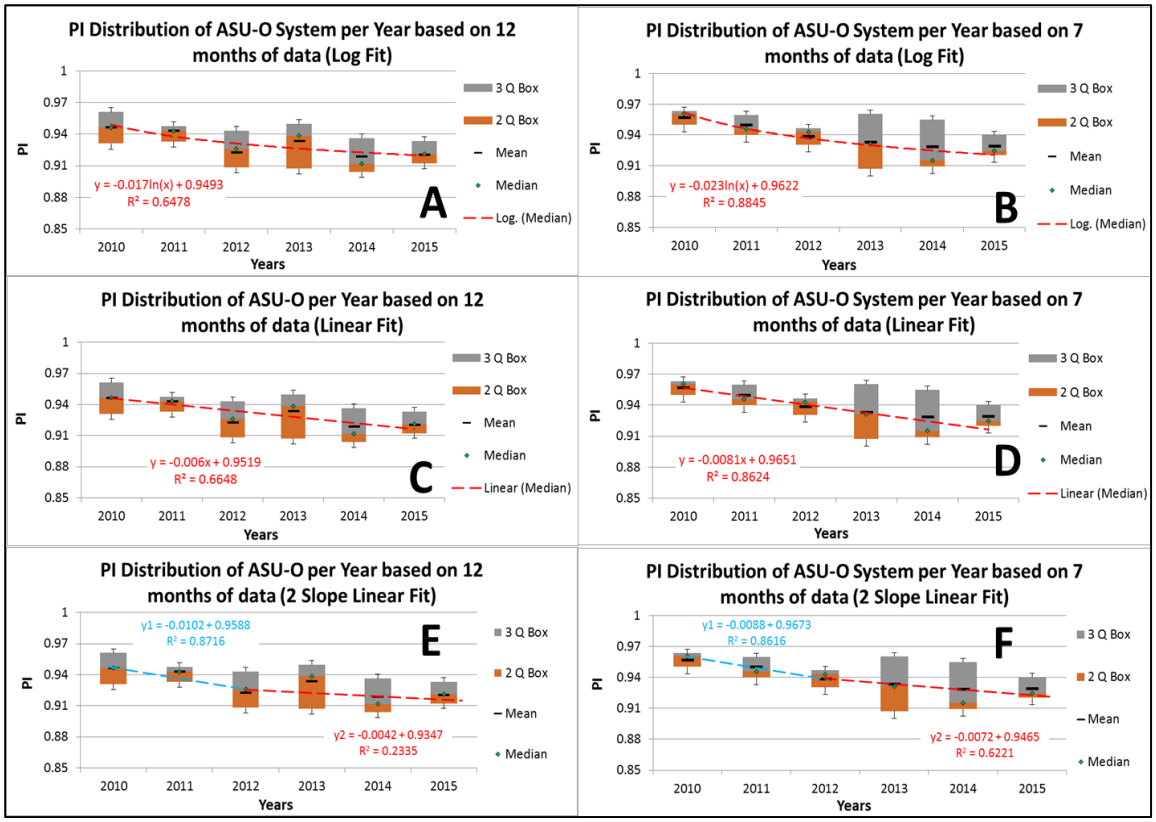

Fig. 45. Degradation Trend Analysis of ASU-O PV System

In the above graphs the degradation trend analysis is shown using the median with either: **A)** Distribution of PI values per year based on 12 months data using a log fit, **B)** Distribution of PI values per year based on 7 months data using a log fit, **C)** Distribution of PI values per year based on 12 months data using a linear fit, **D)** Distribution of PI values per year based on 7 months data using a linear fit, **E)** Distribution of PI values per year based on 12 months data using a 2 slope linear fit, and **F)** Distribution of PI values per year based on 7 months data using a 2 slope linear fit.

When looking at the results from these plots, it can be seen that the general trend is for the logarithmic degradation to have a higher correlation value than that of a linear trend line, but as the systems increase in age, the difference in correlation values

decreases. What this may tend to indicate is that in the initial years, the systems do not degrade linearly, but after a period of time, the degradation rates may seem to then level out into a consistent linear degradation. The graph below also shows the comparison of the calculated degradation rate of the "good" ASU systems for PR, PI, and kWh methods as compared to IV measurements previously found at older PV sites by ASU-PRL.

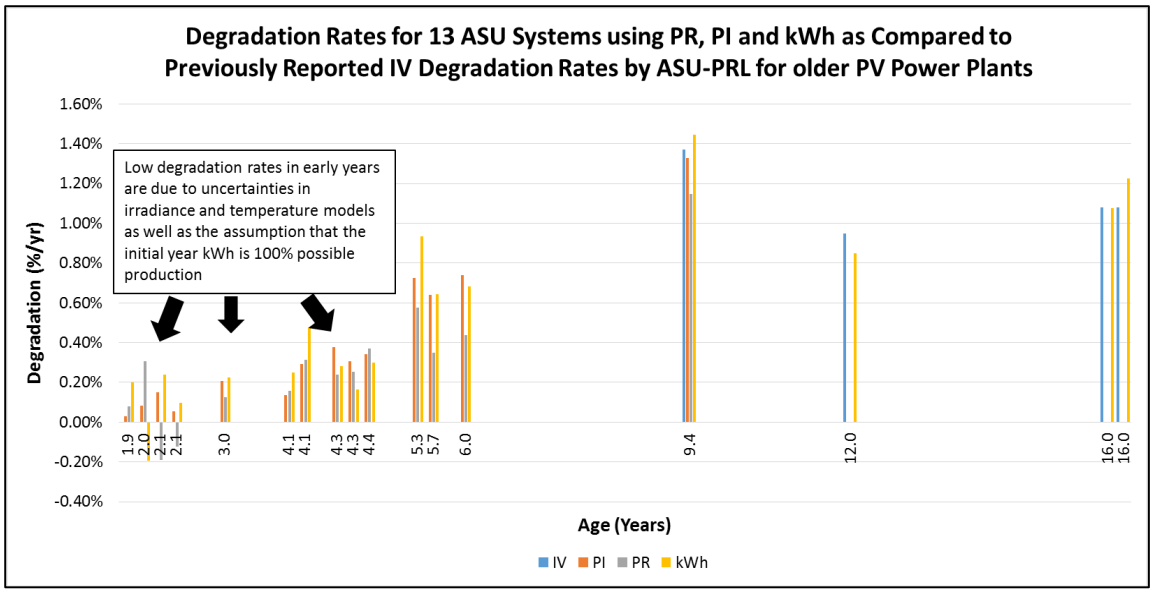

Fig. 46. Degradation Rates for 13 Evaluated ASU PV Systems Using PR, PI, and kWh Methods as Compared to Previously Reported IV Degradation Rates by ASU-PRL.

From the above graph, it is noticeable that the calculated degradation rates for systems that have less than 5 years of field exposure have severely lower degradation rates than what would typically expected to be found. There are two reasons for these low degradation rates. The first reason is due to the fact there are uncertainties that arise from the use of modeling irradiance and module temperature values, instead of having physically measured values. The irradiance values, as taken from SolarAnywhere, have a

built in uncertainty of 5% before even being converted to POA irradiance values. By using this data source, it is possible that the year over year (YOY) degradation rate may occasionally have an increase in performance from the first year to the second. The second reason for this occurrence may stem from the fact that the insolation from one year to another may have changed drastically in which one year had more rain than another, or more soil deposition occurred, or etc. These types of occurrences do occur as shown by Figure 47 below.

Fig. 47. Overview of Degradation Trend of Commercial PV System Where Some Year

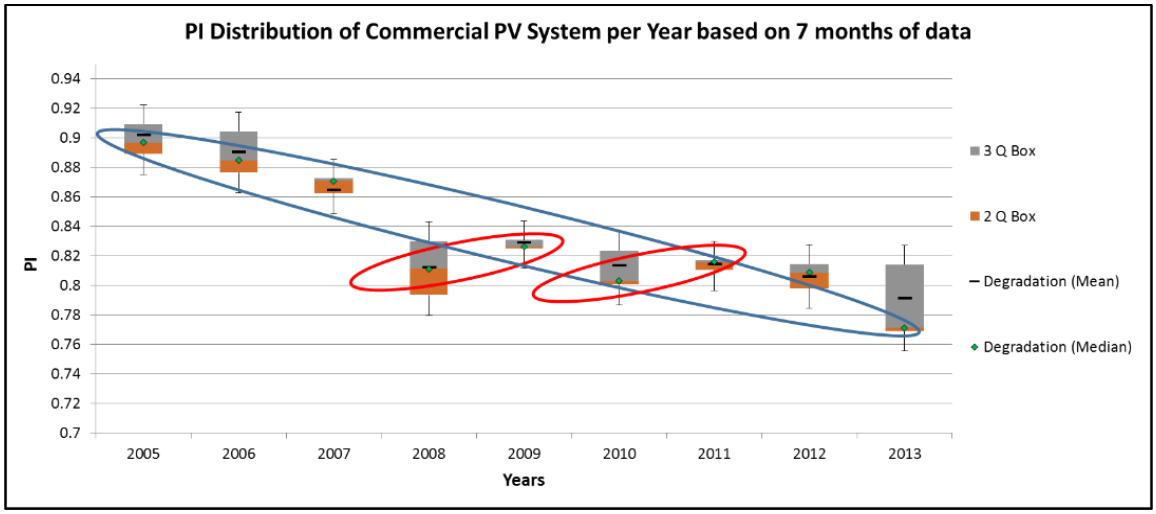

Over Year Degradation Rates Show a Positive Slope (Red Ovals) as Compared to the Overall Negative Trend (Blue Ovals).

Positive YOY degradation rates have been seen relatively frequently by the industry. As reported by Black & Veatch, the YOY degradation analysis can vary as much as ±20% [14]. The figure below, as shown in the Black & Veatch report, presents the overall distribution of YOY degradation rates for a total of 73,829 degradation rates

of non-SunPower systems (Red) and 45,636 degradation rates for SunPower systems (Blue).

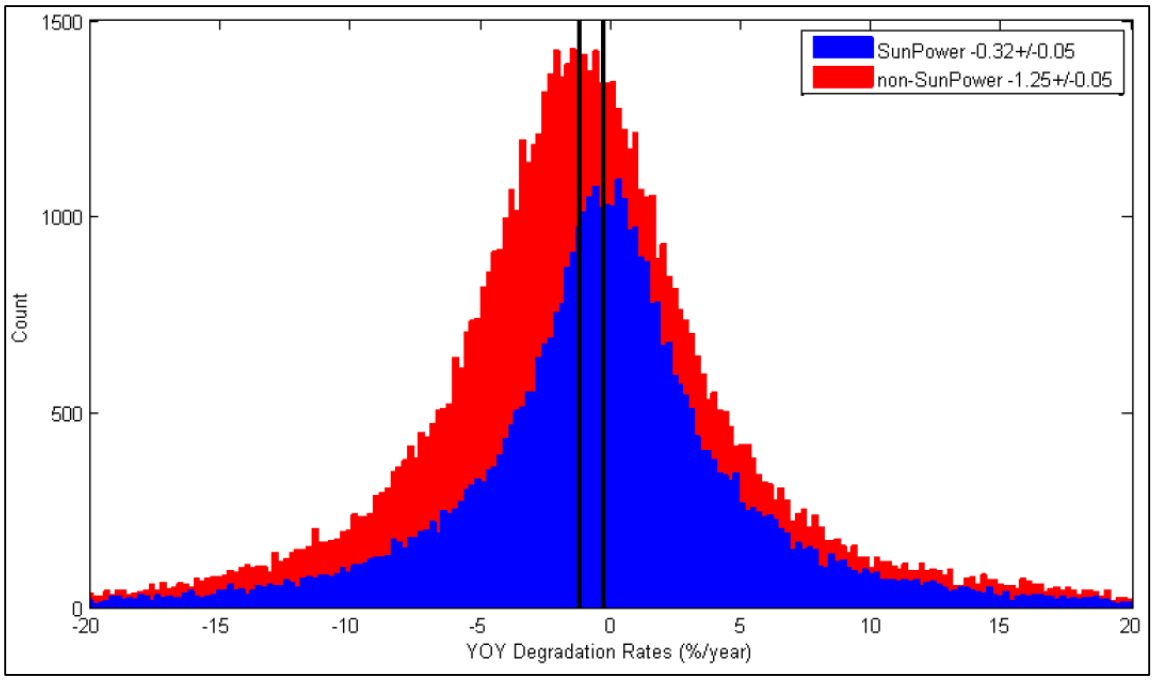

Fig. 48. Histograms of all Site Level YOY Degradation Rate Data for SunPower and Non-SunPower Systems.

The results presented in this section give indications to the non-linear degradation trend that seems to occur in crystalline silicon based PV modules and PV power plants. This non-linearity is seen to closely resemble that of a logarithmic degradation in the early years of PV power plants. For current long-term warranty and energy prediction models, linear assumptions still prove to be practically accurate, but may need to be adjusted for systems with less than five years of age, perhaps using a double-slope approach. Due to a lack of available systems, most systems evaluated range between 4 to 6 years in age. The continuation of this study as the systems increase in age or evaluating

other systems of an older age is encouraged to develop a definitive answer to the overall degradation trend experience by crystalline silicon PV modules in the hot-dry climate of Arizona.

5.0 CONCLUSION

From the results that were discussed in the previous chapter, important conclusions for the type of irradiance, temperature, performance models that best operate in the hot-dry climate of Arizona can be drawn. The best irradiance model found for correcting in-field measured GHI data to POA irradiance was that of PVsyst. The commercial software showed to have the best RMSE (14.63 W/m^2 and 15.23 W/m^2) and NRMSE (1.33% and 1.38%) values for the two years of measured data, 2013 and 2014. These values were found by using the Hay & Davies transposition model. The Hay & Davies model, said to be the more robust model, gives the best results compared to that of the other transposition model used in PVsyst, the Perez transposition model, since it is more accurate by ~.4%. When using satellite generated GHI, it was found that while PVsyst did give accurate irradiance results, it was not the most accurate. The most accurate overall model was that of the combination of the Skartveit and Olseth decomposition model and Badescu transposition model. The Skartveit and Olseth – Badescu model gave the best RMSE (10.38 W/m^2 and 10.97 W/m^2) and NRMSE (0.98% and 1.03%) values for the two years of measured data, 2009 and 2010. This model also performed better than the PVsyst model when predicating the overall insolation that could be expected for a particular location. This was shown by the Skartveit and Olseth – Badescu model reducing the overall over predication of PVsyst's best model, Hay &

Davies, from an average 2.9% to only 1.0%. To further generate the most accurate hourly irradiance model for converting satellite GHI into POA irradiance, a hybrid model of the PVsyst Hay & Davies model and that of the Skartveit and Olseth – Badescu model was developed. This model was able to reduce the RSME values from 10.38 W/m^2 and 10.97 W/m^2 to 9.29 W/m^2 and 9.50 W/m^2 for 2009 and 2010, respectively. This results in the NRSME values falling to 0.878% for 2009 and 0.895% for 2010, the lowest observed values. Since these values were seen to give the lowest errors for predicting hourly POA irradiance data, the hybrid model was determined to be the most optimal model for the hot-dry climate of Arizona.

The best model for predicting the operating temperature of crystalline silicon PV modules in the hot-dry climate of Arizona was determined to the be Mattei 1 thermal model since it gave the lowest RMSE and NRMSE values for the 7 months of measured in-field module temperature data. As was shown in an earlier chapter, for quick operating temperature calculations, the Simple Model method, which only needs ambient temperature and POA irradiance, can be used for a rough idea the operating conditions being seen by a PV module. For high accuracy predictions though, for things such degradation rate calculation and large scale energy generation predictions, more complicated models such as Mattei 1, PVsyst, and Sandia models need to be used, with the Mattei 1 method giving the most accurate results for the hot-dry climate of Arizona.

The performance models used, Performance Ratio, Performance Index, and kilowatt-hour methods, also showed differences in the calculated degradation rates. While it was shown that the best method, after the IV method, for calculating degradation

rates is by using PI values, the developed kWh degradation rate calculation gives similar results to that of PI, but without the need of using sophisticated modeling for temperature and irradiance. The developed kWh degradation model does produce better results than those of the PR calculation, but cannot be used to determine any specific system component losses since it is purely a statistical calculation without having any other operating conditions being taken into consideration.

The trend and rate of degradation for crystalline silicon PV systems was found to be slightly nonlinear with logarithmic degradation rates having more correlation than that of the single slope linear degradation rates. When reviewing this trend, it was only observed in systems that were 5 or more years old, since any systems younger then this had too few data points to make conclusions about the trend of the data sets. The graphs and data presented in an earlier chapter help support the idea of using a two slope regression model where the first three years seem to degrade at a higher rate than the proceeding years. The degradation rate of systems in Arizona was calculated with an average rate of 1.43%/yr in the first three years and an average rate of 0.67% for years greater than three, when using systems that have 5 or more years of field exposure. The overall average degradation rate (using the standard one slope method) of the 13 ASU PV power plants that were analyzed showed an average degradation rate of only 0.31%yr. This value is not close to the expected value of ~1.0%/yr and should not be used when looking at the overall degradation rate of the hot-dry climate of Arizona since the uncertainties in irradiance and temperature models and assumptions in the kWh method heavily dominate calculated degradation rates for systems less than 5 years of age.

Again when comparing the degradation rates found in this study, new systems (installed within ~5 years) show an average degradation of 0.70%/yr (when averaging the calculated degradation rates from PI single slope method with 7 months data for plants ~5 years old), while old systems (installed ~10 years or more) show an average degradation rate of 1.12%/yr (when averaging the in-field measured IV curves of systems ~10 years old or more). The two different degradation rates could be attributed to an improvement in the quality of modules that are being installed in newer systems, but without having intermediate data, this cannot be stated for certain.

This study shows that the rate and trend of degradation can only be assumed as true when: A) there is a large data set available in which a system has 5 or more years of field exposure, B) the on-site measured values (POA irradiance, module temperature, weather, etc.) are used for calculating performance and degradation rate analysis instead of modeled data, and C) in-field measured IVs are performed when the system(s) is initially installed and then are measured again at set incremental periods of time. The method discussed in C would give the most accurate degradation rate since it would directly measure the modules performance and be the least susceptible to error. In both methods A and B, the system also must not have inverter clipping, long system down times, or any sudden increases in performance (without knowing the reason why) in order to have accurate performance and degradation calculations.

Continuation and future work of this study is suggested since it as these systems continue age it will be critical to see if the proposed second slope will continue to be linear or if there is another non-linear degradation that may occur at later years after a

greater amount of time in the field. From the control commercial PV power plant, it was seen that there was no other non-linear degradation that occurred in later years, but a larger sample size should be used in order to conduct a statistically accurate conclusion on this phenomenon. Determining the effective ness of the kWh technique on larger utility sized systems (>1 MW) in the same climate and in different climates is also advised in order to determine whether or not the filtration ranges used are representative of all climatic conditions or only that of Arizona. The determination of optimal irradiance and temperature models for other climates should also be one of further study in order to better understand the variances that can occur between region to region so that the optimal type of PV system can be used and the behavior of the PV system can better be predicated and modeled.

REFERENCES

[1] Lave, Matthew, William Hayes, Andrew Pohl, and Clifford W. Hansen. "Evaluation of Global Horizontal Irradiance to Plane-of-Array Irradiance Models at Locations Across the United States." IEEE Journal of Photovoltaics 5 (2015): 597-606. Web. 6 July 2015.

[2] Wong, L.T., and W.K. Chow. "Solar Radiation Model." Applied Energy 69 (2001): 191-224. Elsevier. Web. 6 July 2015.

[3] Yang, Dazhi, Zibo Dong, Andre Nobre, Yong Sheng Khoo, Panida Jirutitijaroen, and Wilfred M. Walsh. "Evaluation of Transposition and Decomposition Models for Converting Global Solar Irradiance from Tilted Surface to Horizontal in Tropical Regions." Solar Energy 97 (2013): 369-87. Elsevier. Web. 5 July 2015.

[4] Schwinshackl, C., M. Petitta, J.E. Wagner, G. Belluardo, D. Moser, M. Castelli, M. Zebisch, and A. Tetzlaff. "Wind Effect on PV Module Temperature: Analysis of Different Techniques for an Accurate Estimation." Energy Procedia 40 (2013): 77-86. Elsevier, 2013. Web. Oct. 2015.

[5] Olukan, Tuza A., and Mahieddine Emziane. "A Comparative Analysis of PV Module Temperature Models." Energy Procedia 62 (2014): 694-703. Elsevier. Web. Oct. 2015.

[6] Shrestha, Sanjay. "Determination of Dominant Failure Modes Using Combined Experimental and Statistical Methods and Selection of Best Method to Calculate Degradation Rates." Thesis. Arizona State University, 2014. Dec. 2014. Web. June 2015.

[7] IEC 61724 First edition, “Photovoltaic system performance monitoring –Guidelines for measurement, data exchange and analysis”, 1998-04.

[8] T. Townsend, C. Whitaker, B. Farmer, and H. Wenger. “A new performance index for PV system analysis”, CH3365-4/94/0000-1036 IEEE First WCPEC, 1994.

[9] Umachandran, Neelesh. "Spatial Temperature Uniformity and Statistical Determination of Dominant Degradation Modes in PV Modules." Thesis. Arizona State University, 2015. July 2015. Web. 8 Aug. 2015.

[10] PVsyst. Computer software. Www.pvsyst.com. Vers. 6.3. N.p., n.d. Web. Aug. 2015.

[11] "SolarAnywhere." SolarAnywhere. N.p., n.d. Web. Sept. 2015.

[12] Mattei, M., G. Notton, C. Cristofari, M. Muselli, and P. Poggi. "Calculation of the Polycrystalline PV Module Temperature Using a Simple Method of Energy Balance." Renewable Energy 31 (2006): 553-67. Elsevier, 13 May 2005. Web. 15 Oct. 2015.

[13] Mallineni, Jaya. "Failure and Degradation Modes of PV Modules in a Hot Dry Climate: Results after 4 and 12 Years of Field Exposure." Thesis. Arizona State University, 2013. 2013. Web. Nov. 2015.

APPENDIX A

PERFORMANCE ANALYSIS

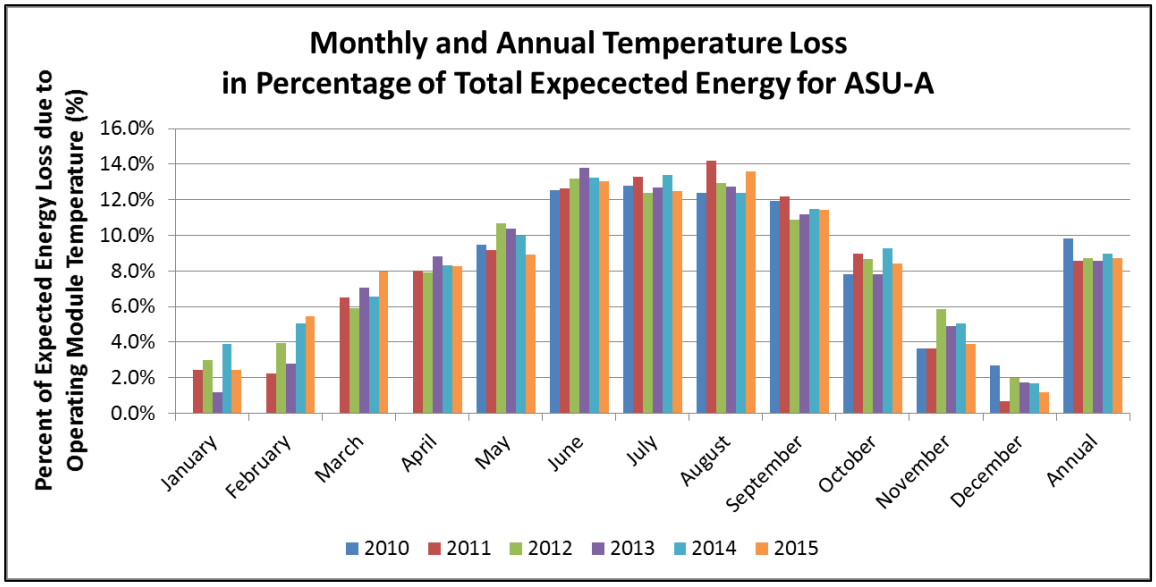

Fig. 49. Percent of Expected Energy Production Lost to Thermal Losses Based on Monthly and Yearly Basis for ASU-A System.

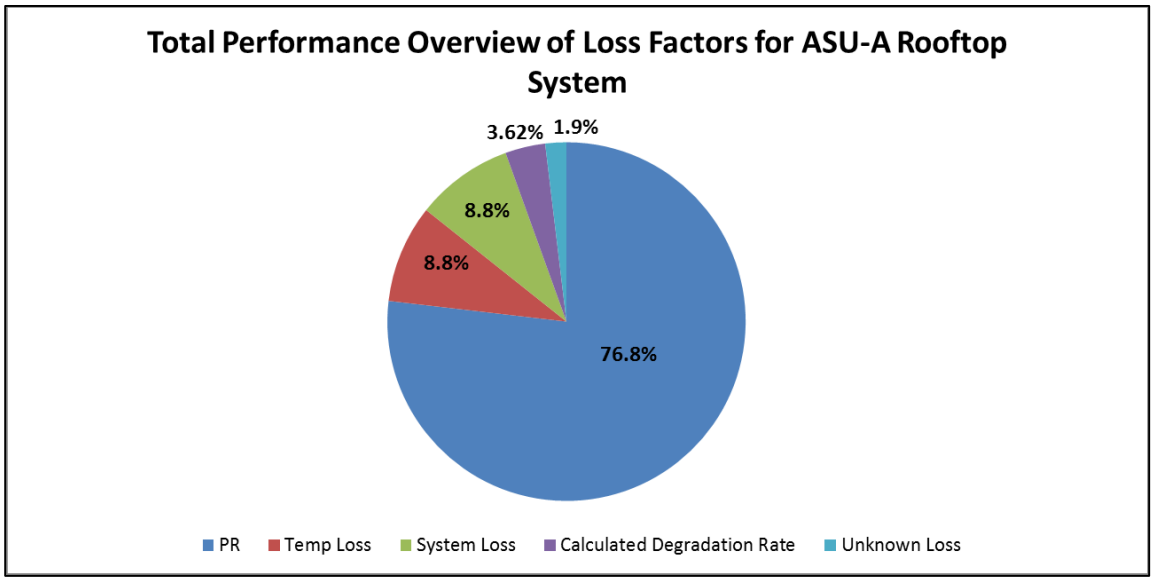

Fig. 50. Performance Overview of Loss Factors for ASU-C Rooftop PV System in the Phoenix-Metro Area of the Hot-Dry Climate of Arizona.

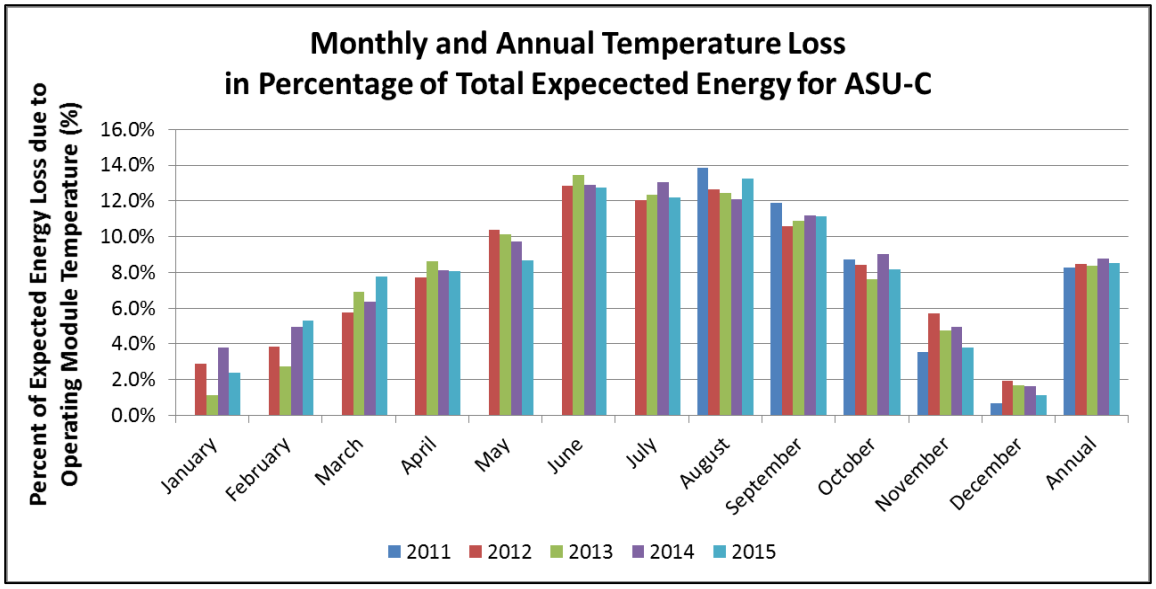

Fig. 51. Percent of Expected Energy Production Lost to Thermal Losses Based on Monthly and Yearly Basis for ASU-C System.

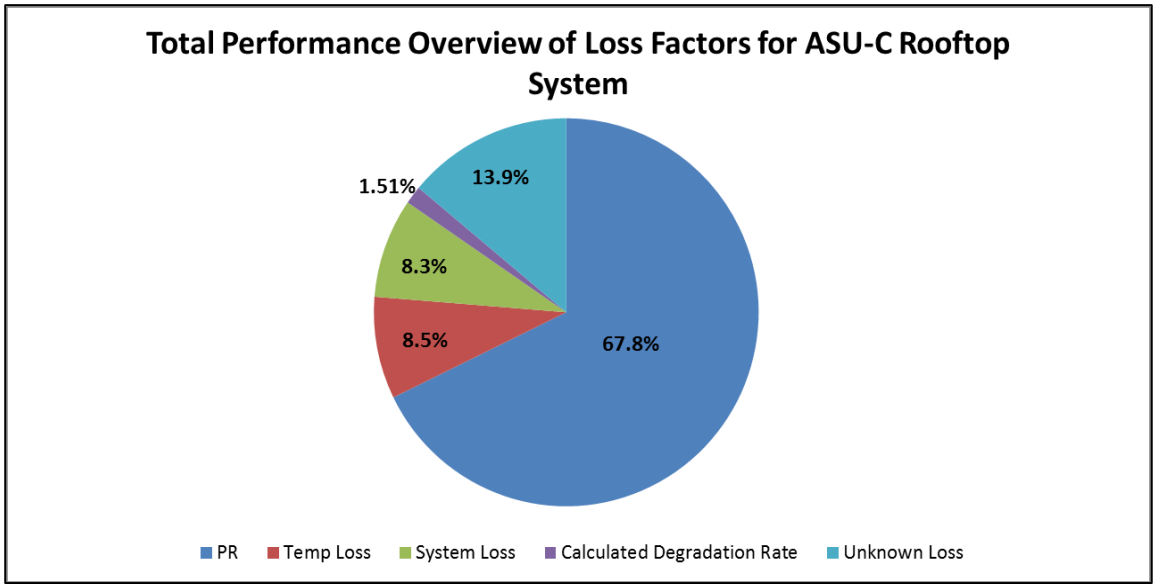

Fig. 52. Performance Overview of Loss Factors for ASU-C Rooftop PV System in the Phoenix-Metro Area of the Hot-Dry Climate of Arizona.

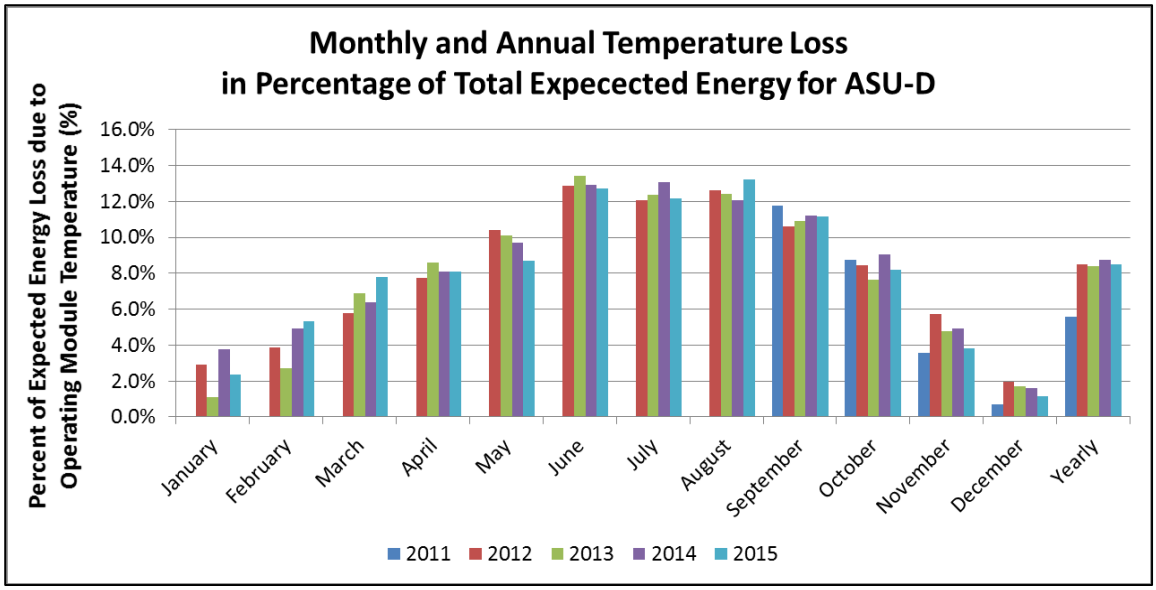

Fig. 53. Percent of Expected Energy Production Lost to Thermal Losses Based on Monthly and Yearly Basis for ASU-D System.

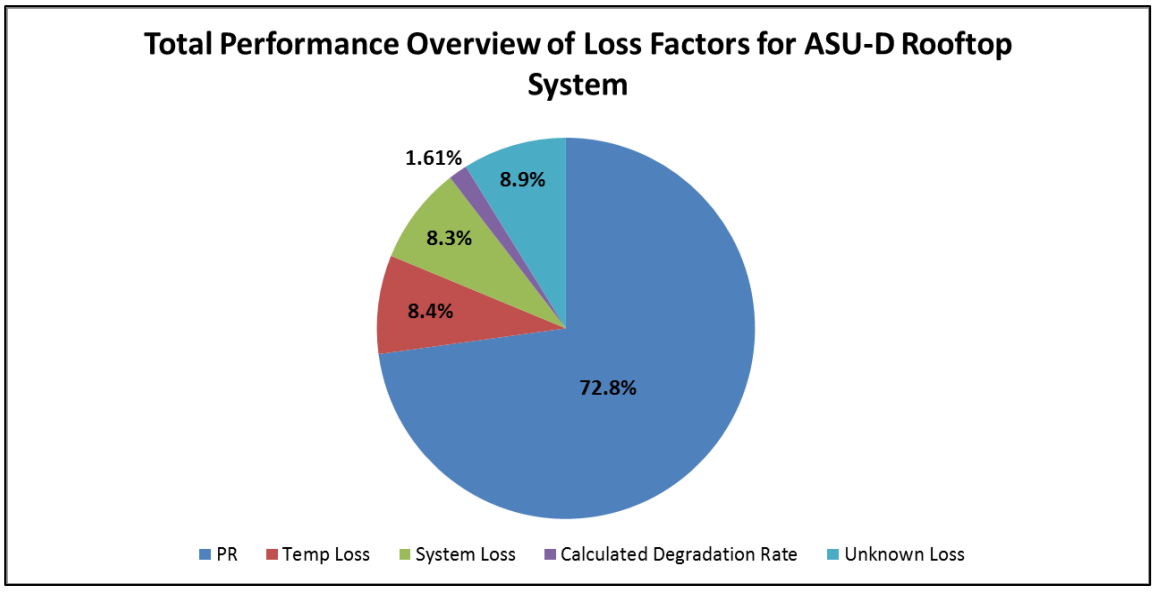

Fig. 54. Performance Overview of Loss Factors for ASU-D Rooftop PV System in the Phoenix-Metro Area of the Hot-Dry Climate of Arizona.

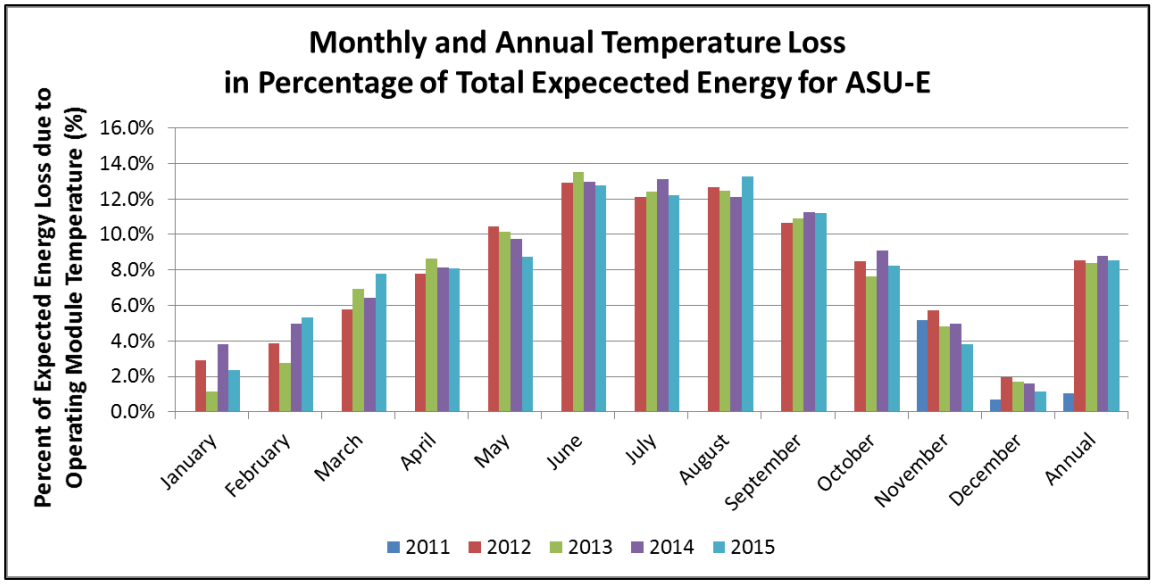

Fig. 55. Percent of Expected Energy Production Lost to Thermal Losses Based on Monthly and Yearly Basis for ASU-E System.

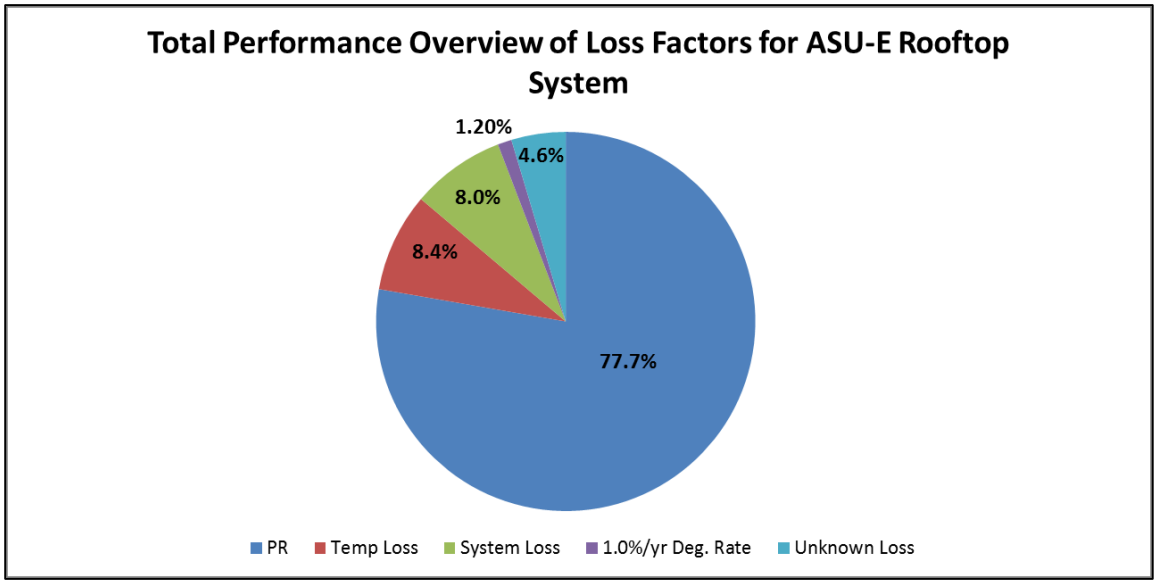

Fig. 56. Performance Overview of Loss Factors for ASU-E Rooftop PV System in the Phoenix-Metro Area of the Hot-Dry Climate of Arizona.

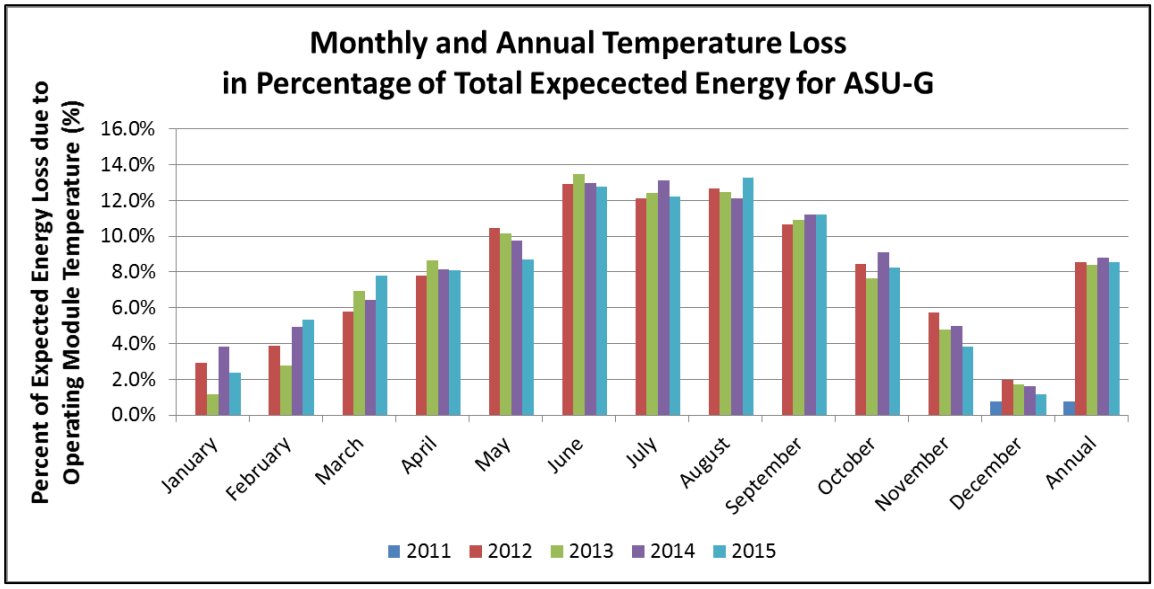

Fig. 57. Percent of Expected Energy Production Lost to Thermal Losses Based on Monthly and Yearly Basis for ASU-G System.

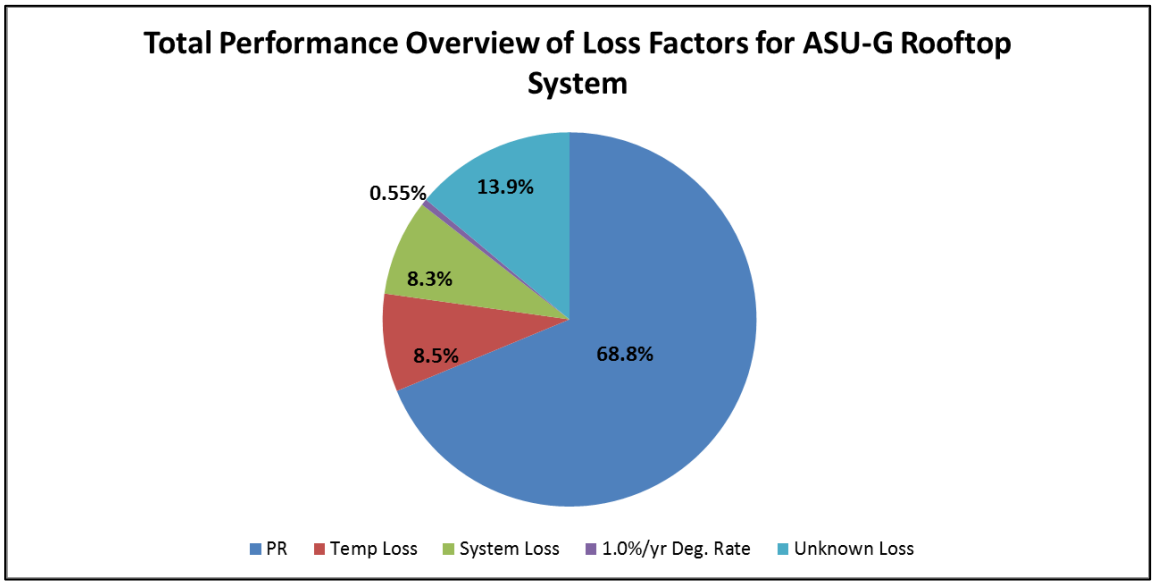

Fig. 58. Performance Overview of Loss Factors for ASU-G Rooftop PV System in the Phoenix-Metro Area of the Hot-Dry Climate of Arizona.

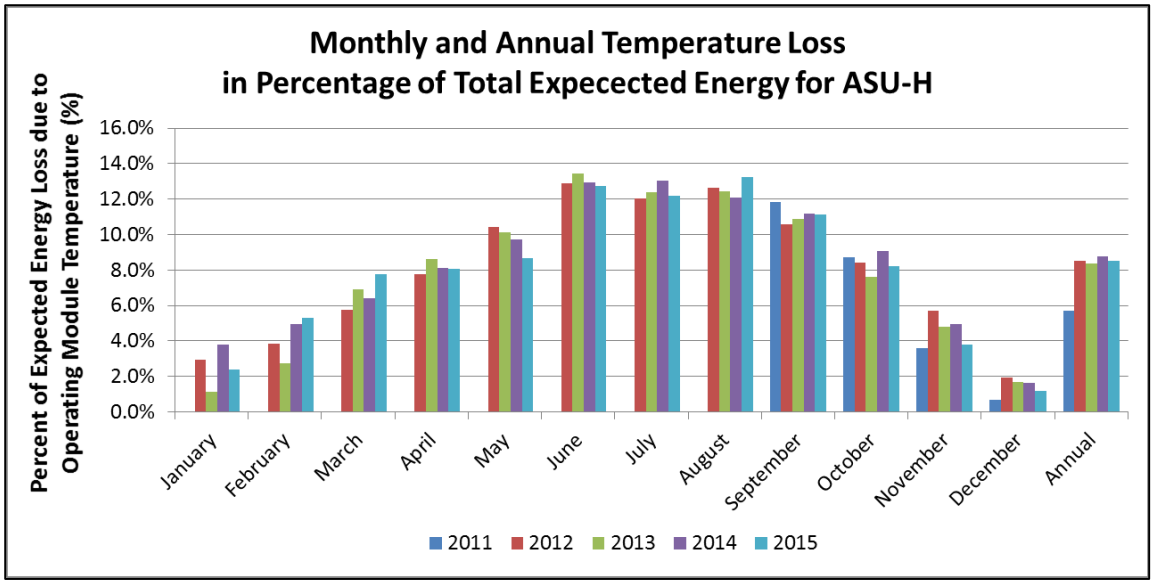

Fig. 59. Percent of Expected Energy Production Lost to Thermal Losses Based on Monthly and Yearly Basis for ASU-H System.

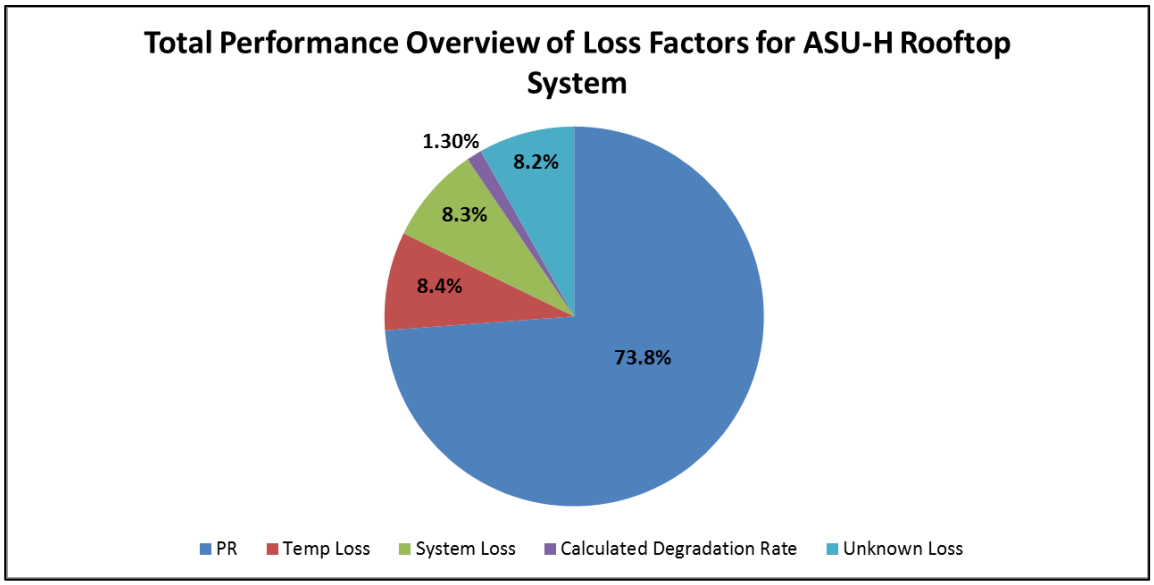

Fig. 60. Performance Overview of Loss Factors for ASU-H Rooftop PV System in the Phoenix-Metro Area of the Hot-Dry Climate of Arizona.

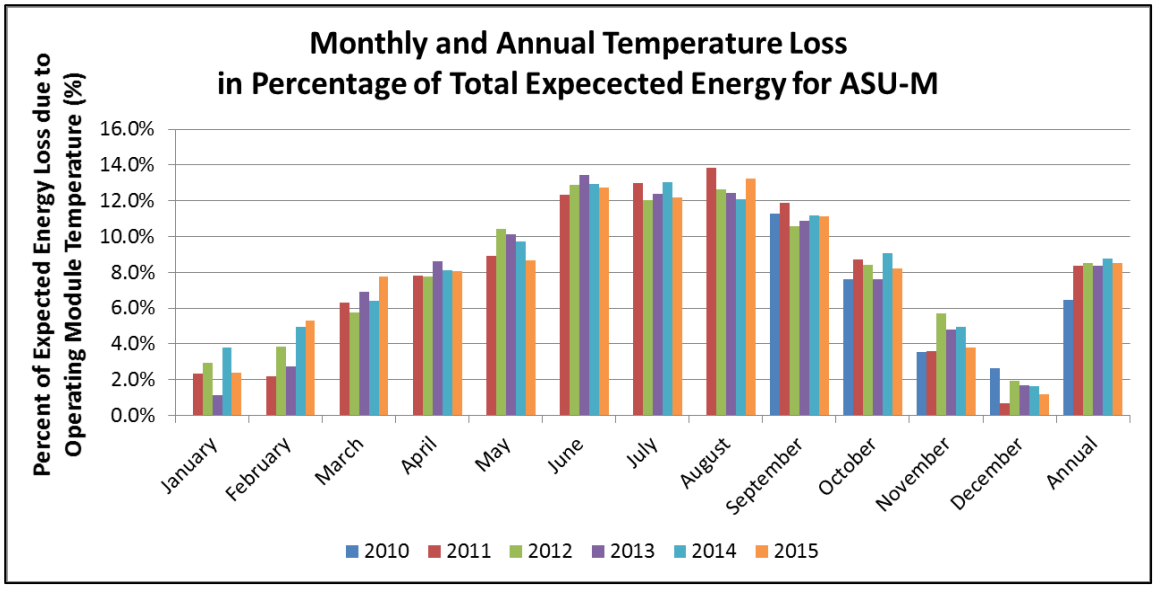

Fig. 61. Percent of Expected Energy Production Lost to Thermal Losses Based on Monthly and Yearly Basis for ASU-M System.

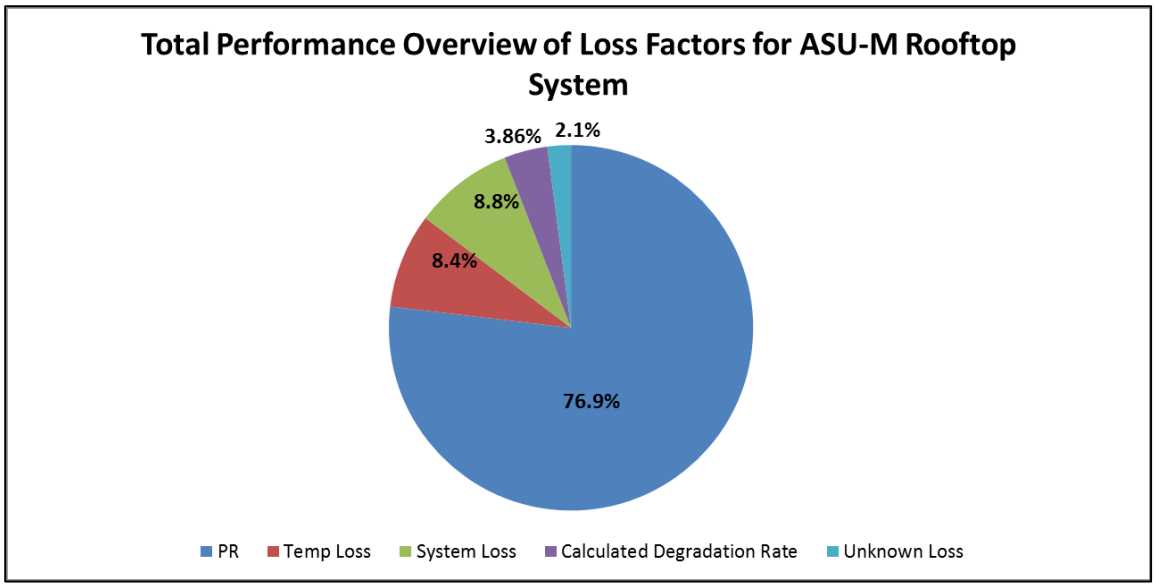

Fig. 62. Performance Overview of Loss Factors for ASU-H Rooftop PV System in the Phoenix-Metro Area of the Hot-Dry Climate of Arizona.

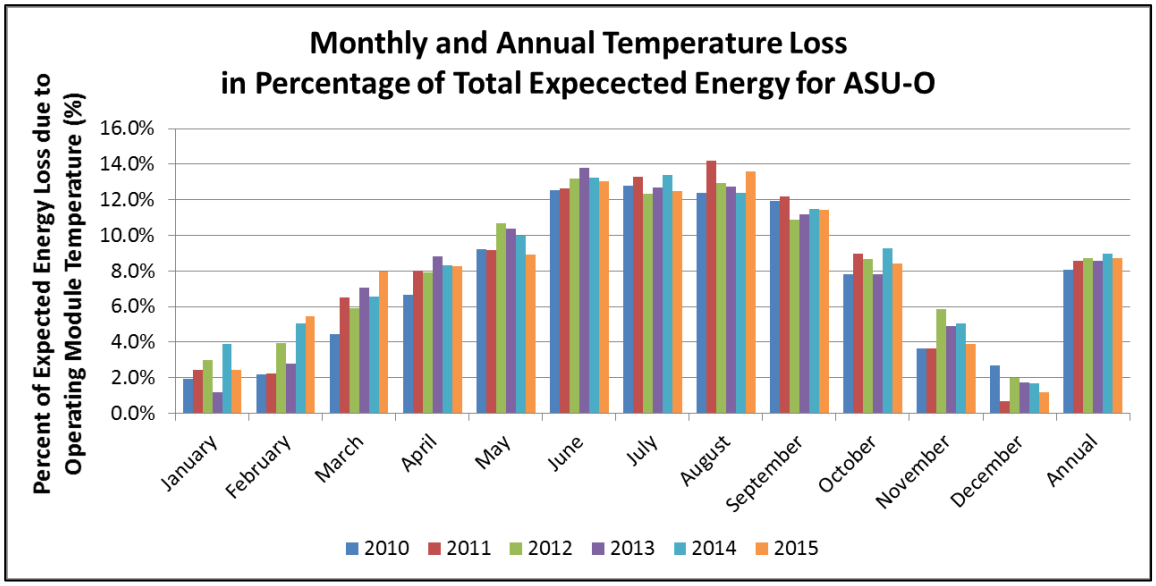

Fig. 63. Percent of Expected Energy Production Lost to Thermal Losses Based on Monthly and Yearly Basis for ASU-O System.

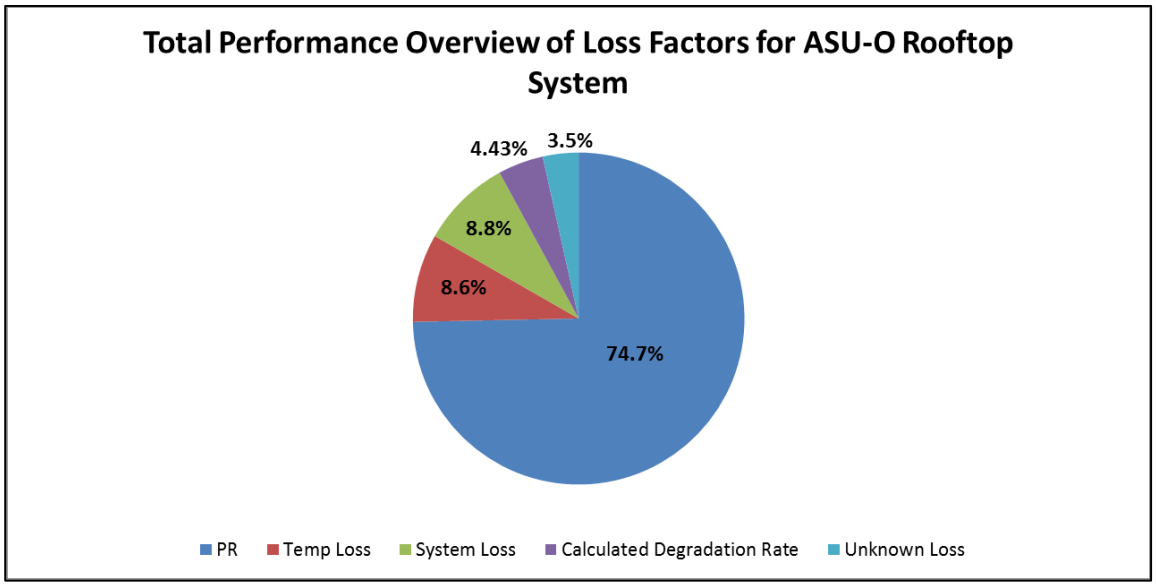

Fig. 64. Performance Overview of Loss Factors for ASU-O Rooftop PV System in the Phoenix-Metro Area of the Hot-Dry Climate of Arizona.

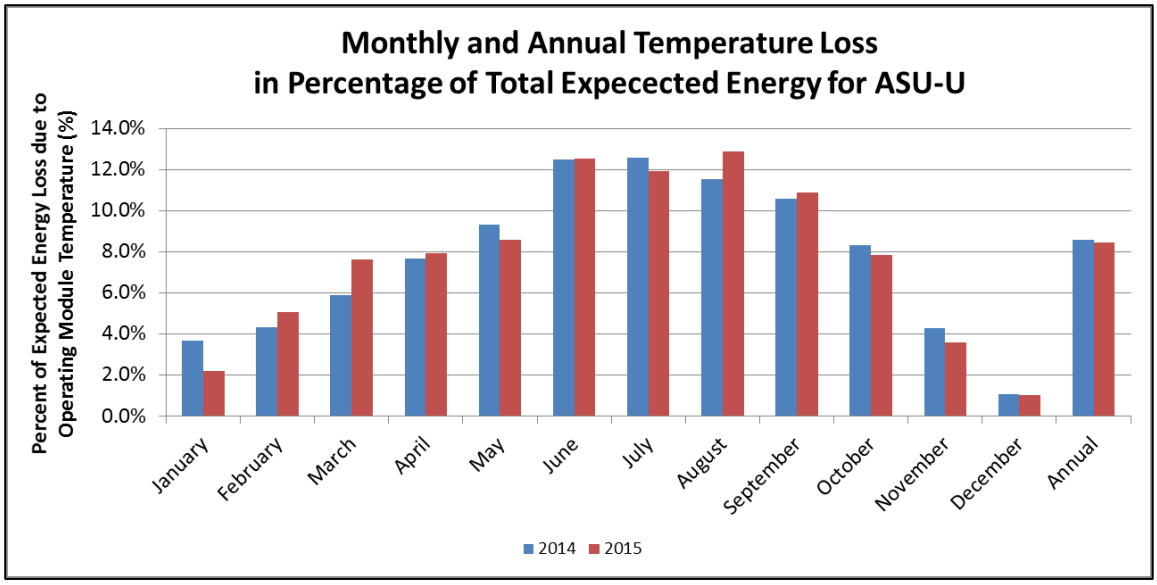

Fig. 65. Percent of Expected Energy Production Lost to Thermal Losses Based on Monthly and Yearly Basis for ASU-U System.

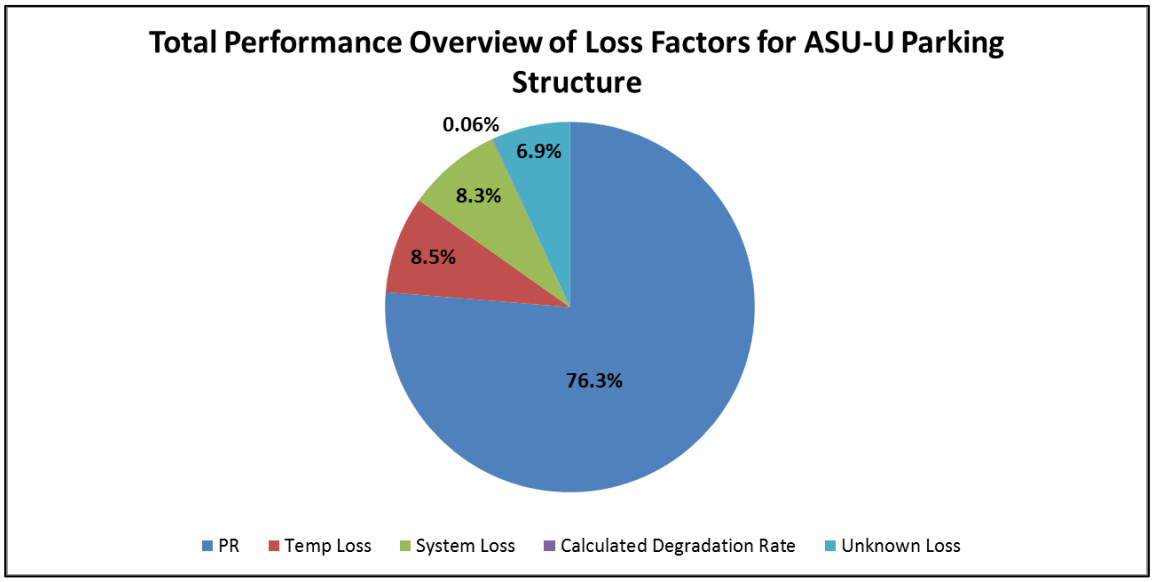

Fig. 66. Performance Overview of Loss Factors for ASU-U Parking Structure PV System in the Phoenix-Metro Area of the Hot-Dry Climate of Arizona.

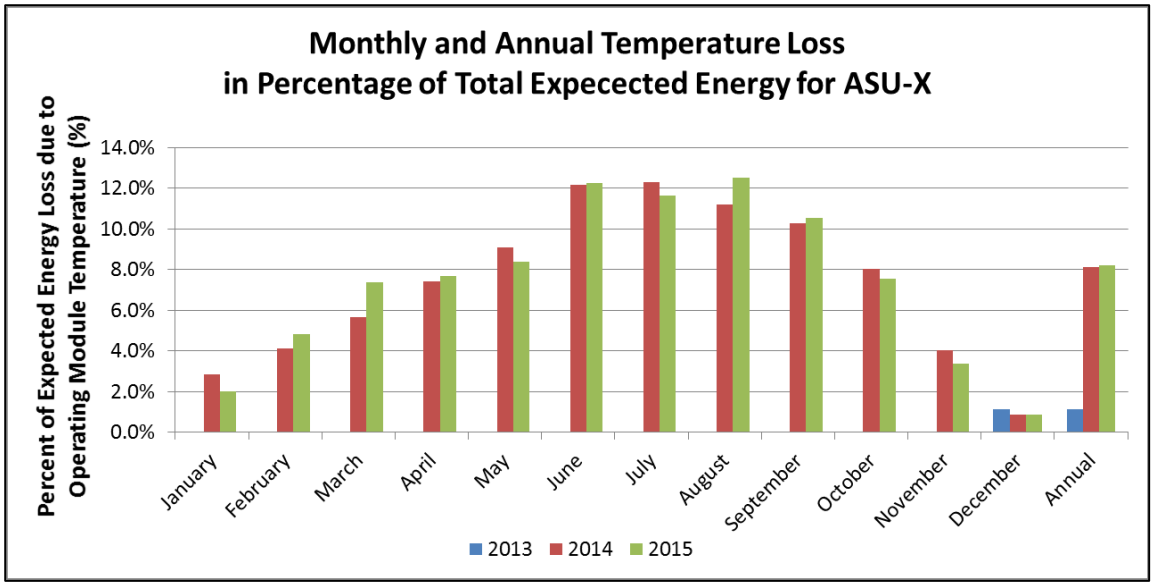

Fig. 67. Percent of Expected Energy Production Lost to Thermal Losses Based on Monthly and Yearly Basis for ASU-X System.

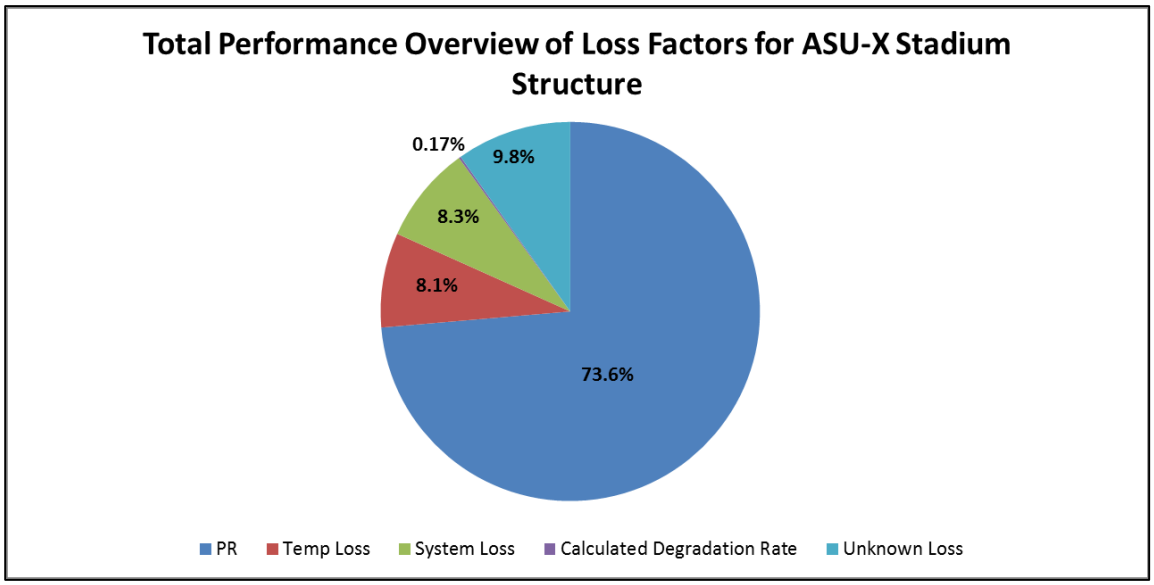

Fig. 68. Performance Overview of Loss Factors for ASU-X Stadium Structure PV System in the Phoenix-Metro Area of the Hot-Dry Climate of Arizona.

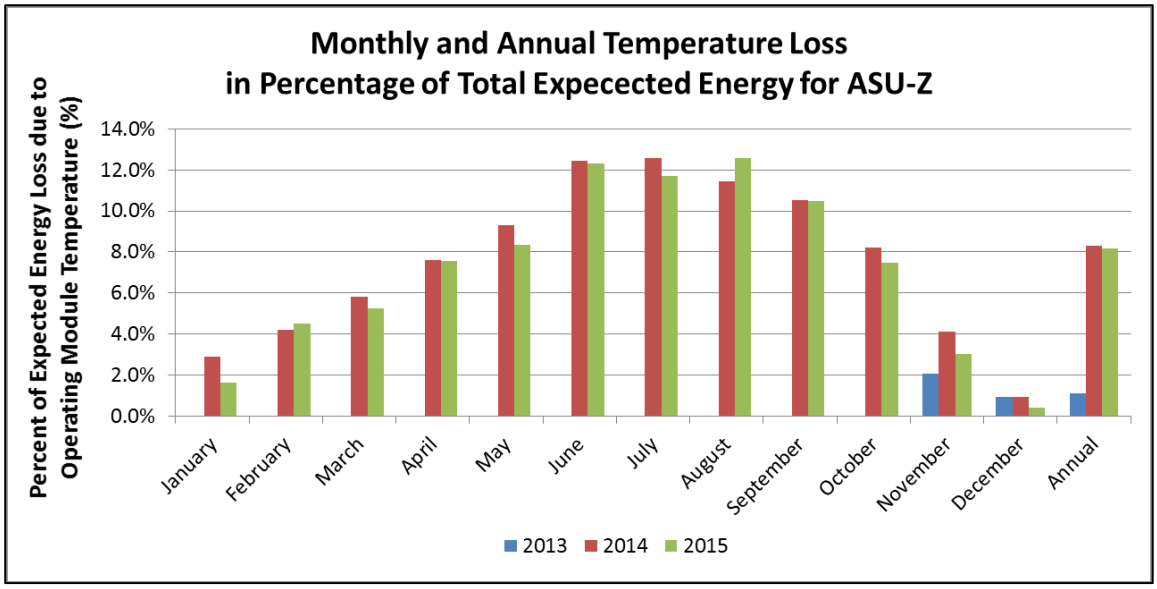

Fig. 69. Percent of Expected Energy Production Lost to Thermal Losses Based on Monthly and Yearly Basis for ASU-Z System.

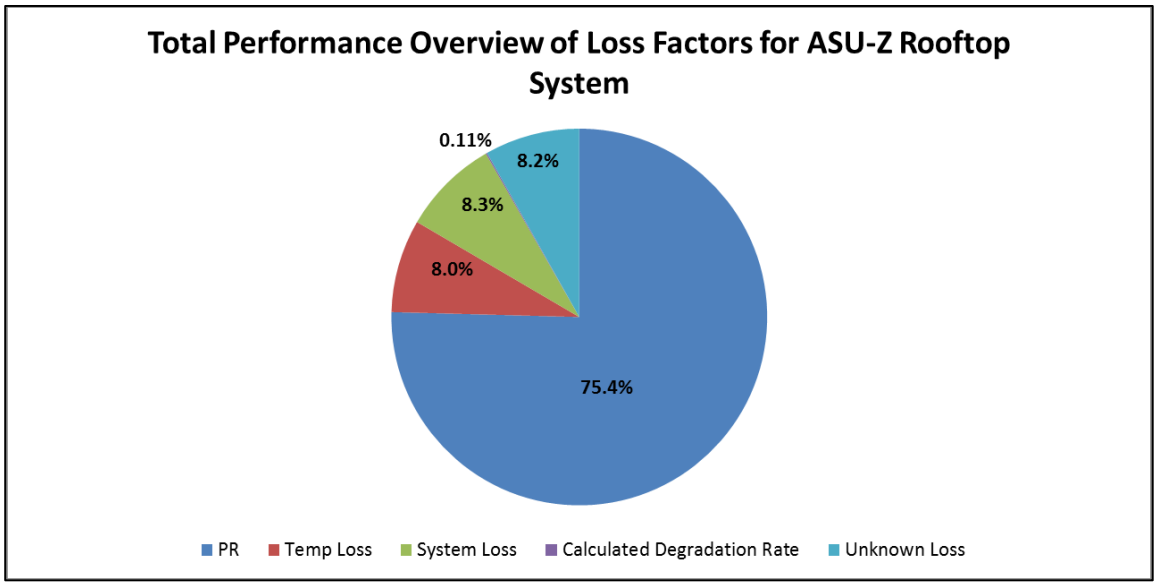

Fig. 70. Performance Overview of Loss Factors for ASU-Z Rooftop System PV System in the Phoenix-Metro Area of the Hot-Dry Climate of Arizona.

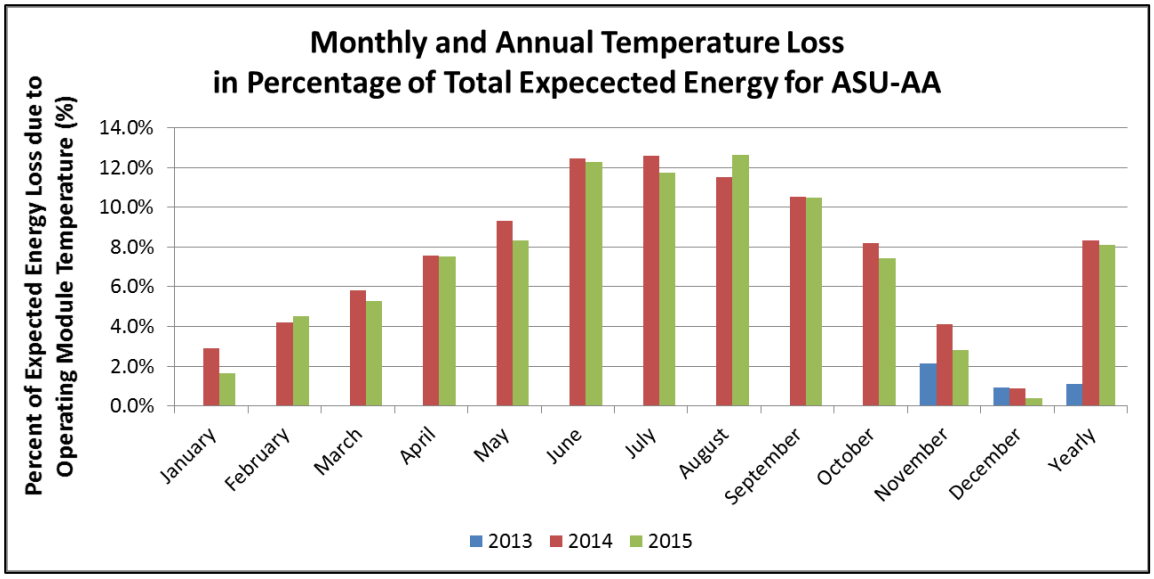

Fig. 71. Percent of Expected Energy Production Lost to Thermal Losses Based on Monthly and Yearly Basis for ASU-AA System.

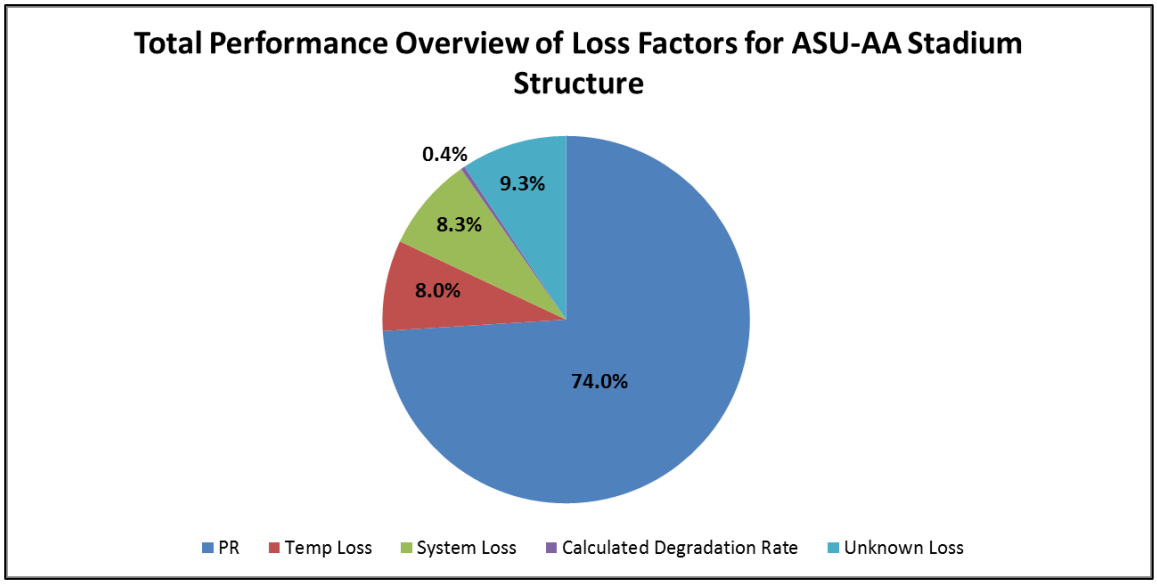

Fig. 72. Performance Overview of Loss Factors for ASU-AA Stadium Structure PV System in the Phoenix-Metro Area of the Hot-Dry Climate of Arizona.

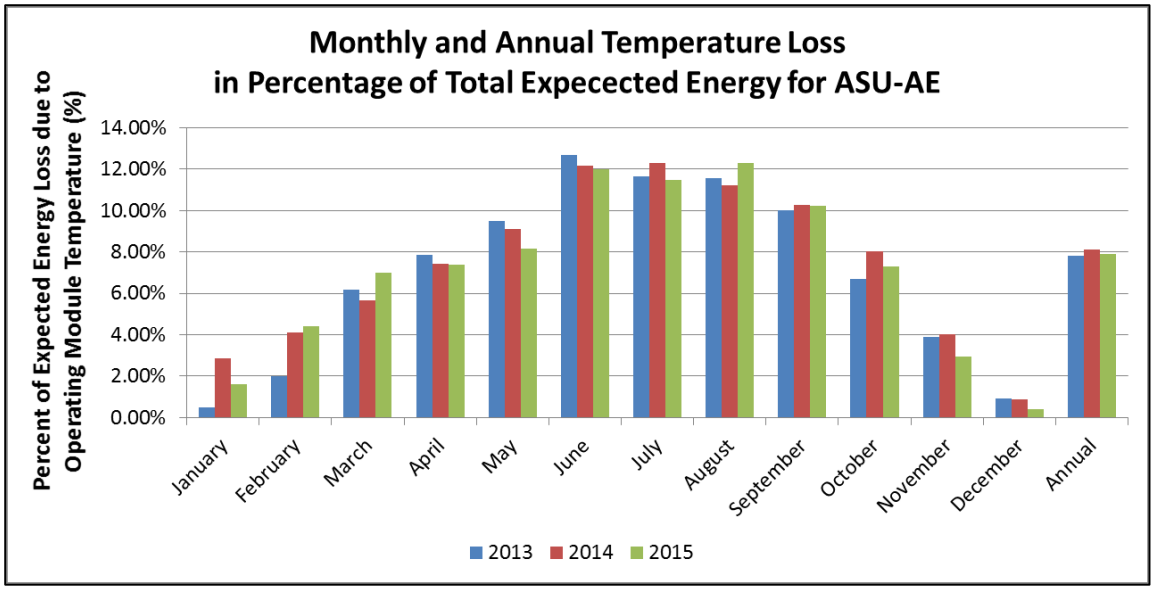

Fig. 73. Percent of Expected Energy Production Lost to Thermal Losses Based on Monthly and Yearly Basis for ASU-AE System.

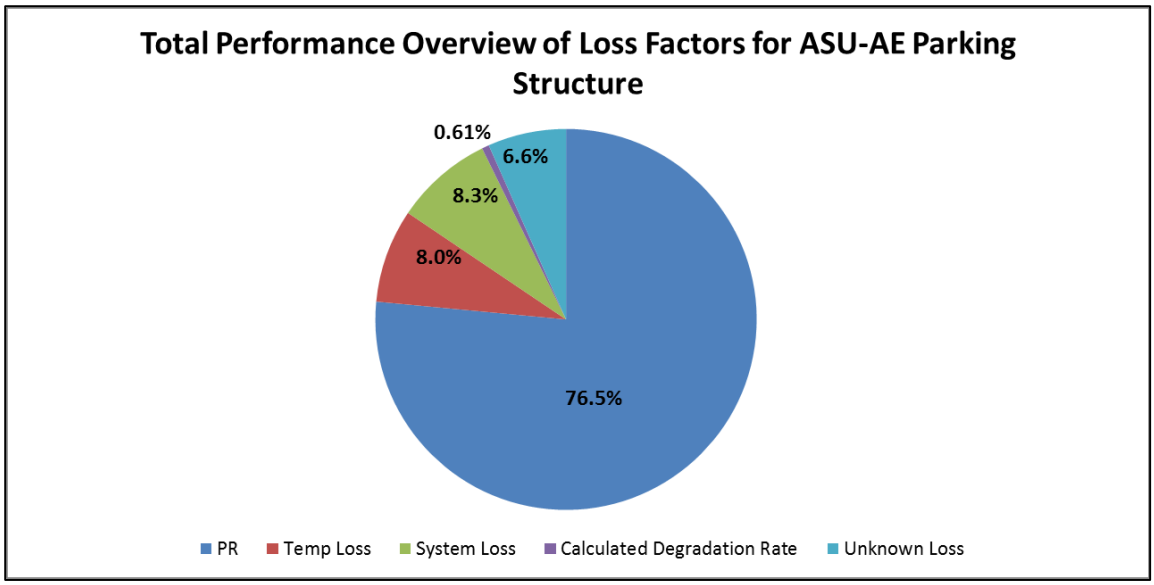

Fig. 74. Performance Overview of Loss Factors for ASU-AE Parking Structure PV System in the Phoenix-Metro Area of the Hot-Dry Climate of Arizona.